2010-12-13

# Axon Death Prevented: Wld$^S$ and Other Neuroprotective Molecules: A Dissertation

Michelle A. Avery
*University of Massachusetts Medical School*

# AXON DEATH PREVENTED: $WLD^S$ AND OTHER NEUROPROTECTIVE MOLECULES

A Dissertation Presented
By

Michelle A. Avery

Submitted to the faculty of the
University of Massachusetts Graduate School of Biomedical Sciences, Worcester
in partial fulfillment of the requirements for the degree of

DOCTOR OF PHILOSOPHY

December 13th, 2010

Program in Neuroscience

AXON DEATH PREVENTED: $WLD^S$ AND OTHER NEUROPROTECTIVE MOLECULES

A Dissertation Presented

By

Michelle A. Avery

The signatures of the Dissertation Defense Committee signifies completion and approval as to style and content of the Dissertation

Marc Freeman, Thesis Advisor

Eric Baehrecke, Member of Committee

Vivian Budnik, Member of Committee

Zuoshang Xu, Member of Committee

Michael Coleman, Member of Committee

The signature of the Chair of the Committee signifies that the written dissertation meets the requirements of the Dissertation committee

Michael Francis, Chair of Committee

The signature of the Dean of the Graduate School of Biomedical Sciences signifies that the student has met all graduation requirements of the school.

Anthony Carruthers, Ph.D.,
Dean of the Graduate School of Biomedical Sciences

Program in Neuroscience
December 13th, 2010

## Dedication

This work is dedicated to my family: Paul Avery (father), Jill Avery (mother), Ryan Avery (brother), Bob Avery (grandfather), and Ruth Avery (grandmother) for all their support throughout my education and allowing me to believe I can do whatever I set my mind to.

**Acknowledgements**

First and foremost, I would like to thank my thesis advisor, Marc Freeman, for all of his guidance throughout my graduate career. He has the ability to make an unexpected result seem like the best thing since sliced bread, and no one can ever leave his office feeling defeated. Marc has truly made me the scientist I am today, knowing how to analyze results, plan future experiments, write meaningful papers, and give excellent seminars. I would also like to thank all of my thesis committee members: Michael Francis, Vivian Budnik, Eric Baehrecke, Zuoshang Xu, and Tzumin Lee. They all helped guide my experiments by asking about aspects of my work, and providing alternate theories that I could set out to test. Next, I would like to thank all of the Freeman lab members, past and present: Meg Beach, Rebecca Bernardos, Johnna Doherty, Nicki Fox, Yuly Fuentes, Rachel Hackett, Kim Kerr, Sam Licciardo, Mary Logan, Tsai-Yi Lu, Jen MacDonald, Allie Muthukumar, Sanghamitra Mylarapu, Lukas Neukomm, Jeanette Osterloh, Edith Plada, Tim Rooney, Amy Sheehan, Tobi Stork, Ozge Tasdemir, and Jen Ziegenfuss. Although lab meetings can sometimes get heated, all members provided great input that shaped my experiments and methods of quantification. I would especially like to thank Nicki Fox, Kim Kerr, Lukas Neukomm, and Tim Rooney who helped in editing my thesis. Finally, I wish to thank all my friends and family, especially my dance partners, Jared Vigneault and Jay O'Leary, for keeping me sane throughout the graduate school process.

## Abstract

A common feature of many neuropathies is axon degeneration. While the reasons for degeneration differ greatly, the process of degeneration itself is similar in most cases. Axon degeneration after axotomy is termed 'Wallerian degeneration,' whereby injured axons rapidly fragment and disappear after a short period of latency (Waller, 1850). Wallerian degeneration was thought to be a passive process until the discovery of the *Wallerian degeneration slow* (*Wld*$^S$) mouse mutant. In these mice, axons survive and function for weeks after nerve transection. Furthermore, when the full-length protein is inserted into mouse models of disease with an axon degeneration phenotype (such as progressive motor neuronopathy), Wld$^S$ is able to delay disease onset (for a review, see Coleman, 2005). *Wld*$^S$ has been cloned and was found to be a fusion event of two neighboring genes: *Ube4b*, which encodes an ubiquitinating enzyme, and *NMNAT-1* (nicotinamide mononucleotide adenylyltransferase-1), which encodes a key factor in NAD (nicotinamide adenine dinucleotide) biosynthesis, joined by a 54 nucleotide linker span (Mack et al., 2001).

To address the role of Wld$^S$ domains in axon protection and to characterize the subcellular localization of Wld$^S$ in neurons, our lab developed a novel method to study Wallerian degeneration in *Drosophila in vivo* (MacDonald et al., 2006). Using this method, we have discovered that mouse Wld$^S$ can also protect *Drosophila* axons for weeks after acute injury, indicating that the molecular mechanisms of Wallerian degeneration are well conserved between

mouse and *Drosophila*. This observation allows us to use an easily manipulated genetic model to move the Wld$^S$ field forward; we can readily identify what Wld$^S$ domains give the greatest protection after injury and where in the neuron protection occurs. In chapter two of this thesis, I identify the minimal domains of Wld$^S$ that are needed for protection of severed *Drosophila* axons: the first 16 amino acids of Ube4b fused to Nmnat1. Although Nmnat1 and Wld$^S$ are nuclear proteins, we find evidence of a non-nuclear role in axonal protection in that a mitochondrial protein, Nmnat3, protects axons as well as Wld$^S$.

In chapter 3, I further explore a role for mitochondria in Wld$^S$-mediated severed axon protection and find the first cell biological changes seen in a Wld$^S$-expressing neuron. The mitochondria of Wld$^S$- and Nmnat3-expressing neurons are more motile before injury. We find this motility is necessary for protection as suppressing the motility with *miro* heterozygous alleles suppresses Wld$^S$-mediated axon protection. We also find that Wld$^S$- and Nmnat3- expressing neurons show a decrease in calcium fluorescent reporter, gCaMP3, signal after axotomy. We propose a model whereby Wld$^S$, through production of NAD in the mitochondria, leads to an increase in calcium buffering capacity, which would decrease the amount of calcium in the cytosol, allowing for more motile mitochondria. In the case of injury, the high calcium signal is buffered more quickly and so cannot signal for the axon to die.

Finally, in chapter 4 of my thesis, I identify a gene in an EMS-based forward genetic screen which can suppress Wallerian degeneration. This mutant

is a loss of function, which, for the first time, definitively demonstrates that Wallerian degeneration is an active process. The mammalian homologue of the gene encodes a mitochondrial protein, which in light of the rest of the work in this thesis, highlights the importance of mitochondria in neuronal health and disease.

In conclusion, the work presented in this thesis highlights a role for mitochondria in both $Wld^S$-mediated axon protection and Wallerian degeneration itself. I identified the first cell biological changes seen in $Wld^S$-expressing neurons and show that at least one of these is necessary for its protection of severed axons. I also helped find the first Wallerian degeneration loss-of-function mutant, showing Wallerian degeneration is an active process, mediated by a molecularly distinct axonal degeneration pathway. The future of the axon degeneration field should focus on the mitochondria as a potential therapeutic target.

## Table of contents

## List of Figures

## List of third party copyrighted material

| Figure Number | Publisher | License Number |
|---|---|---|
| Figure 1-1 | National Academy of Sciences | N/A |
| Figures 1-3 and 1-4 | Elsevier | 2552030712249 |

The following figures were reproduced from journals: no permission required

| Figure Number | Publisher |
|---|---|
| All Chapter 2 Figures | The Rockefellar University Press |

## List of frequently used abbreviations

**ATP- Adenosine triphosphate**

**$Ca^{2+}$- Calcium**

**CMT2a- Charcot-Marie Tooth Disease Type 2A**

**DRG- Dorsal root ganglion**

**EGTA- Ethylene glycol tetraacetic acid**

**EMS- Ethyl methane sulfonate**

**GFP- Green fluorescent protein**

**MARCM- Mosaic analysis with a repressible cell marker**

**MCU- Mitochondrial calcium uniporter**

**Miro- Mitochondrial Rho GTPase**

**NAD- Nicotinamide adenine dinucleotide**

**NADS- Nicotinamide adenine dinucleotide synthase**

**Nmnat- Nicotinamide mononucleotide adenylyltransferase**

**ORN- Olfactory receptor neuron**

**PTP- Permeability transition pore**

**RFP- Red fluorescent protein**

**RNAi- RNA interference**

**SCA- Spinocerebellar ataxia**

**shRNA- Short hairpin RNA**

**UPS- Ubiquitin proteasome system**

**VCP- Valosin-containing protein**

**$Wld^S$- Wallerian degeneration slow**

## Preface

All work described in this thesis was done at UMass Medical School in the laboratory of Marc Freeman. In chapter 2, Amy Sheehan helped with cloning various constructs. In chapter 3, Tim Rooney helped with various dissections and images. In chapter 4, Rachel Hackett, Mary Logan, Jen MacDonald, Jeannette Osterloh, and Jen Ziegenfuss all contributed to the EMS screen. Finally, in chapter 4, Jeannette Osterloh did the complementation crosses to uncover the location of 3 EMS alleles. Stefan Zuchner, Ph.D., (University of Miami) conducted the deep sequencing on the EMS alleles.

# CHAPTER I:

# Introduction

**Wallerian Degeneration: an overview**

Neurodegenerative disorders are caused by many factors, but most result in axon degeneration through a process which is not well-characterized at a molecular level. In 1850, Augustus Waller observed that when an axon was severed, it rapidly fragmented after a short period of latency, and was eventually cleared from the site of injury (Waller, 1850). This process, termed 'Wallerian degeneration', was long thought to be a passive process of an axon wasting away due to a lack of nutrient supply from the cell body. However, the thought that Wallerian degeneration was passive was changed upon the finding of spontaneous mouse mutant *Wallerian degeneration slow* (*Wld*$^S$) (Lunn et al., 1989). In these mice, axons survived and functioned for weeks after transection, suggesting that Wallerian degeneration is in fact an active process that can be inhibited (Lunn et al., 1989).

As degeneration following transection can be inhibited by *Wld*$^S$, the possibility arose that similar forms of axon degeneration, seen in other neurodegenerative diseases, may also be inhibited in *Wld*$^S$ mice. To address this question, *Wld*$^S$ mice were crossed with various mouse models of neurodegenerative disease. Interestingly, *Wld*$^S$ was found to delay the onset of several neurological diseases such as Parkinson's (Sajadi et al., 2004), gracile axonal dystrophy (Mi et al., 2005), progressive motor neuropathy (Ferri et al., 2003), and amyotrophic lateral sclerosis (Fischer et al., 2005). *Wld*$^S$-expressing neurons were also found to be

resistant to neurotoxic chemicals like vincristine (Wang et al., 2001) and taxol (Wang et al., 2002). The ability of *Wld*$^S$ to protect against such varied forms of axon degeneration led to the belief that the molecular mechanisms of degeneration were much more similar than originally thought. Thus, understanding how the Wld$^S$ protein protects axons is imperative for an overall understanding of how axon degeneration occurs.

To begin to understand axon degeneration, it was of utmost importance to identify the mutation that caused the *Wld*$^S$ phenotype in mice. The *Wld* locus was mapped to the 4$^{th}$ chromosome, and was found to be a spontaneous tandem triplication resulting in an in-frame fusion protein (**Figure 1-1**) (Conforti et al., 2000). The chimeric protein consists of the first 70 amino acids of Ube4b, an E4 ligase, and the full-length Nmnat1, a key enzyme in the NAD+ synthesis pathway, joined by an 18 amino acid linker sequence (Mack et al., 2001).

The unique 18 amino acid linker domain enabled researchers to develop an antibody to specifically recognize Wld$^S$, which revealed that Wld$^S$ localized to the nucleus of neurons (Mack et al., 2001). This result was unexpected since axon transection removes the cell body from Wld$^S$-protected axons. It is possible that low levels of axonal Wld$^S$ may be present below detection level; however, the prevailing thought is that a signal must be constitutively sent from the nucleus to the axon to prevent degeneration when the axon is cut. The identity of the signal and how it keeps the axon alive remains a mystery, but the nature of the domains of Wld$^S$ has given rise to several hypotheses as to how Wld$^S$ is acting.

Based on the information above and several other findings, four main hypotheses have been proposed to explain the neuroprotective actions of $Wld^S$ (Mack et al., 2001; Gilley and Coleman, 2010). (1) $Wld^S$ has a dominant-negative effect on the ubiquitin proteasome system through its N70 domain. (2) The Nmnat1 domain produces an excess of NAD+, which could protect axons by providing them with excess energy to delay degeneration or by promoting NAD+-dependent gene transcription. (3) $Wld^S$ affects gene regulation through a yet unknown mechanism. (4) $Wld^S$ compensates in the axon for the lack of an endogenous survival signal from the nucleus. It is possible that the protection of $Wld^S$ is due to a combination of one or more of the proposed hypotheses explained in detail below; none are mutually exclusive.

**(1) $Wld^S$ N70 Ube4b Domain and the Ubiquitin Proteasome System**

The ubiquitin proteasome system (UPS) is a quality control mechanism through which the cell can tag misfolded proteins for degradation and is also used for fine-tuning temporal resolution for proteins whose activity needs to be turned off quickly. The UPS has also been implicated in neurodegeneration. The addition of proteasome inhibitors prior to axon injury profoundly delays Wallerian degeneration both *in vitro* and *in vivo* (Zhai et al., 2003). The requirement for the inhibitor prior to injury, coupled with the knowledge that these inhibitors work very quickly, implies that the proteasome is involved in early stages of Wallerian degeneration. Additionally the earliest observed step in

Wallerian degeneration, microtubule destabilization, is delayed when the proteasome is inhibited (Zhai et al., 2003). Proteasome inhibitors cannot protect against microtubule destabilizing agents such as vincristine and colchine (Zhai et al., 2003), suggesting again that the proteasome acts upstream of microtubule destabilization. Before a protein bound for degradation reaches the proteasome, it is first tagged with ubiquitin. Therefore, protein ubiquitination is another step that could be involved in axon degeneration.

The first domain of the *Wld*$^{S}$ gene encodes for the 70 N-terminal amino acids of Ube4b, a member of the E4 class of ubiquitin chain assembly factors. This portion of Ube4b, called N70, is insufficient for substrate ubiquitination, but is necessary for binding its substrates targeted for ubiquitination. Therefore, it is thought that part of Wld$^{S}$ protection occurs through a dominant negative effect on the UPS, as Ube4b can bind proteins, but fails to process them for degradation. N70 may protect axons from degeneration by binding substrates destined for the proteasome whose degradation would normally initiate the cascade of degeneration events. Because Wld$^{S}$ cannot ubiquitinate substrates, the proteasome would no longer recognize the molecules for degradation, thereby saving the axon from this catastrophic event. Ube4b, however, may also be important in neuronal integrity.

Ube4b is expressed in cardiac muscles during development; however, in the adult it is abundant in neurons (Kaneko-Oshikawa et al., 2005). Adult mice heterozygous for Ube4b show striking axonal dystrophy and degeneration

phenotypes, which suggest indeed a role for Ube4b in neuronal integrity (Kaneko-Oshikawa et al., 2005). Ube4b also interacts with and mediates the polyubiquitination of ataxin-3, the protein involved in the neurodegenerative disease spinocerebellar ataxia 3 (SCA-3) (Matsumo et al., 2004). In SCA-3, ataxin-3 has an expanded polyglutamine repeat, resulting in protein aggregates and eventual neuronal death. Upon overexpression of Ube4b, the degeneration phenotype of a *Drosophila* model of SCA-3 was suppressed (Matsumo et al., 2004). This evidence suggests that Ube4b function has a vital role in the maintenance of healthy neurons. In fact, when the N70 portion of Ube4b was expressed in dorsal root ganglion (DRG) cultures, transected axons showed a slight delay in degeneration, though it was not as strong of a protection as full-length $Wld^S$ (Conforti et al., 2007).

Since the N70 Ube4b domain alone was found to confer some protection, it was important to find the substrates that bind the N70 domain of $Wld^S$. Aside from ataxin-3, Ube4b also binds to valosin-containing protein (VCP) (Matsumo et al., 2004). More specifically, VCP binds the N-terminal 16 amino acids of Ube4b and $Wld^S$ (N16) (Laser et al., 2006). VCP is a member of the AAA+ class of ATPases that has been shown to have critical roles in the ubiquitin proteasome system (for a review, see Halawani and Latterich, 2006). VCP also seems to play a role in neurodegeneration. The *Drosophila* homologue of VCP, Ter94, has been shown to be upregulated in late stages of polyglutamine disease models (Higashiyama et al., 2002). Overexpression of Ter94 induces eye degeneration

in otherwise wild-type flies, and a knockout of Ter94 suppresses eye degeneration in a polyglutamine disease model (Higashiyama et al., 2002). Because of its high homology to VCP, TER94 would be predicted to bind $Wld^S$ as well, shown in chapter 2 of this thesis. The exact mechanism by which VCP interaction with $Wld^S$ may lead to protection is unclear, but studies have shown that $Wld^S$ relocates VCP in the nucleus from a disperse arrangement to distinct nuclear foci (Laser et al., 2006). Also, ubiquitin epitopes accumulate in the foci where $Wld^S$ and VCP are located (Laser et al., 2006). Additionally, $Wld^S$ lacking the N16 portion that binds VCP is unable to protect *in vivo* (Coleman, personal communication), suggesting that the VCP binding event is critical for protection. However, the possibility that other protective molecules bind to N16 cannot be ruled out. Since it seems that Ter94 has an active role in promoting degeneration, one could imagine that its relocalization in the nucleus may inhibit its normal function, thereby inhibiting degeneration. Other evidence has shown that some proteins are activated by mono-ubiquitination and that an E4 enzyme (like Ube4b) is responsible for inactivating these proteins by adding a poly-ubiquitin chain (for a review, see Hoppe, 2005). Therefore, another model may be that the Ube4b domain and VCP act together to bind the proteins normally inactivated by ubiquitination in neurodegeneration, but because the Ube4b domain is unable to ubiquitinate the substrates, these substrates remain active.

**(2) $Wld^S$ Nmnat1 Domain and NAD+ Synthesis**

The third domain of the $Wld^S$ gene encodes the full-length Nmnat1 protein. Nmnat1 catalyzes the linking of NMN+ or NaMN+ with ATP to produce NAD+ or NaAD+, respectively. NAD+ is an important energy molecule in the cell, thus one proposed hypothesis is that $Wld^S$ is simply providing the axon with excess energy that prolongs its survival. There is evidence both supporting and contradicting this claim.

The Nmnat1 activity in $Wld^S$ mice is four times higher than that of wild-type mice (Mack et al., 2001). In DRG cultures, overexpression by transfection of Nmnat1 can protect axons against transection and vincristine exposure as well as $Wld^S$. This protection is due to NAD+ synthesis, as inhibiting the enzyme activity of Nmnat1 blocks its ability to protect axons (Araki et al., 2004). Furthermore, simply adding NAD+ or its precursor NAm can protect DRG neurites after transection, although the protection is not as robust as overexpressing Nmnat1 (Araki et al., 2004, Wang et al., 2005). Finally, addition of several substrates/enzymes involved in the salvage NAD+ pathway delays degeneration in DRG cultures (Sasaki et al., 2006). However, the steady-state NAD+ levels are not altered in the uninjured $Wld^S$ mouse (Mack et al., 2001), arguing that an increase in overall NAD+ levels is not the mechanism by which $Wld^S$ protects axons.

The *in vitro* evidence that suggests Nmnat1 alone is responsible for $Wld^S$ protection is not supported by what is found *in vivo*. Besides the fact that NAD+ levels are not increased in the uninjured $Wld^S$ mice, overexpression of Nmnat1 *in*

*vivo* (at levels comparable to that found in the $Wld^S$ mice) does not confer any protection against nerve transection (Conforti et al., 2007). When DRG neurons from these Nmnat1 overexpression mice are cultured and transected, still no protection occurs. Lentiviral delivery of Nmnat1 *in vitro* offers some protection against transection, but the protection is not at the same level as $Wld^S$ (Conforti et al., 2007). Unexpectedly, Conforti, et al. found that enzymatically inactive Nmnat1 provided the same amount of protection as Nmnat1 with enzymatic activity *in vitro*, arguing that NAD+ synthesis is not required for protection, and NAD+ alone added to the DRG culture had no protective effect (2007). The conflicting *in vivo* and *in vitro* evidence may be a result of differences in expression of Nmnat1, but the results overall call for an extensive *in vivo* study.

**(3) $Wld^S$ Gene regulation via NAD+ or an Unknown Mechanism**

To account for the fact that NAD+ levels do not increase in the cell body or axon of $Wld^S$-expressing mice, it has been proposed that NAD+ may be acting in a more localized manner in the nucleus. As stated before, $Wld^S$ is localized to the nucleus, so it follows that perhaps the Nmnat1 domain is functioning to increase NAD+ levels in the nucleus. NAD+ has known nuclear targets that affect gene transcription. Therefore, $Wld^S$ may regulate important genes through the Nmnat1 domain. Again, there are studies both supporting and contradicting this claim.

Further supporting the thought that NAD+ may be exerting its protective

effects by regulating genes is the fact that in the experiments where protection was seen, exogenous NAD+ had to be added at least 24 hours before transection to see a protective effect (Araki et al., 2004, Sasaki et al., 2006). Certain NAD+-dependent molecules exist in the nucleus. One class of molecules is the poly-ADP ribose polymerases, PARPs, which are important for DNA damage response and repair. However, when an inhibitor of PARP was added to cultured DRG neurons, NAD+ was still able to protect (Araki et al., 2004). Another class of NAD+-dependent molecules is the sirtuins, which are protein deacetylases that have been implicated in transcriptional regulation during stress responses and cell differentiation. When a SIRT1 inhibitor (sirtinol) was added to DRG cultures, exogenous NAD+ was no longer able to protect against nerve transection (Araki et al., 2004). An enhancer of SIRT1, resveratrol, was able to protect axons as well as NAD+. Furthermore, an siRNA directed against SIRT1, but not siRNAs directed against the other 6 mammalian sirtuins, blocked NAD+ protection of severed axons (Araki et al., 2004). This suggests that SIRT1, a sirtuin that targets histone proteins and transcription factors such as p53, forkhead, and NF-$\kappa$B, may regulate $Wld^S$-mediated protection through Nmnat1 production of NAD+ in the nucleus. Wang, et al., however, looked at neurons from a SIRT1 knock out mouse, and found no difference in the protective effects of $Wld^S$ on transected neurons (2005). Also, they found that neither sirtinol nor resveratrol had an effect on $Wld^S$, Nmnat1, or NAD+ protection. Another lab found that resveratrol had no protective effects on DRG cultures (Conforti et al.,

2007). These conflicting data once again point to the importance of studying claims *in vivo*.

It is entirely possible that $Wld^S$ is affecting the transcription of other genes through NAD+-independent mechanisms. In fact, some genes have been shown to be up or down-regulated in the $Wld^S$ mouse that are not known targets of sirtuins, though study on one such gene pulled out of a microarray did not show neuroprotection (Gillingwater et al., 2006).

**(4) $Wld^S$ compensates for an endogenous survival signal**

Since axon degeneration occurs in many instances where axonal transport is blocked, not just after transection, it was proposed that a survival signal is constantly delivered to a healthy axon that allows the axon to remain intact. Once the delivery of this molecule is compromised, either through transection or blockade, the axon will degenerate. In the case of $Wld^S$, something within $Wld^S$ is able to compensate for the loss of a survival signal and prolong the life of an axon.

Gilley and Coleman (2010) treated neurons with cyclohexamide or emetine to block protein synthesis and found that the axons showed signs of blebbing and fragmentation without affecting the cell body, strengthening the hypothesis that after the degradation of a putative survival signal, an axon dies. Moreover, $Wld^S$ was able to protect neurons treated with cyclohexamide or emetine from degeneration, indicating that $Wld^S$ is able to compensate for the

loss of a survival signal. Since full-length Nmnat1 is present in $Wld^S$, Gilley and Coleman chose to look at Nmnat as a possible survival signal. 3 different Nmnats exist in the mouse: Nmnat1 is nuclear, Nmnat2 is cytoplasmic, and Nmnat3 is mitochondrial. Nmnat2 is the only Nmnat highly expressed in neurons (Yan et al., 2009). When neurons are treated with short hairpin RNA (shRNA) for either Nmnat1, 2 or 3, only Nmnat2 shRNA reduces the number of healthy neurites present, and $Wld^S$ is able to inhibit the loss of healthy neurites (Gilley and Coleman, 2010). Finally, when looking at the turnover rates of the Nmnats, it is found that Nmnat2 has the shortest half-life, and the timing of its degradation coincides with degeneration of an axon and could account for the latent period seen after axotomy (Gilley and Coleman, 2010). Therefore, it was proposed that Nmnat2 is an endogenous survival signal delivered to the axon, and that the Nmnat1 in $Wld^S$ can compensate for loss of Nmnat2 in axons. This hypothesis assumes that the site of $Wld^S$ action is outside of the nucleus, as will be discussed below.

While this model is very intriguing, Wallerian degeneration is likely much more complicated than just the loss of a single survival signal present in the axon. Many proteins in the axon likely have a similar half-life to that of Nmnat2, which needs further investigation. Also, it is compelling that Nmnat2 can protect axons after degeneration (Gilley and Coleman, 2010; Yan et al., 2009). However, the protection only occurs when Nmnat2 is expressed at extremely high levels in culture, which may result in mislocalization of the protein.

Furthermore, there is no *in vivo* evidence of Nmnat2 protecting severed axons. Finally, in chapter 2 and 3 of this thesis, I will show that Nmnat2 is unable to protect *in vivo* in *Drosophila* 3 or 5 days after axotomy, even at the levels of Gal4 overexpression. The lack of protection in *Drosophila* cannot be due to the short half-life of mouse Nmnat2. Nmnat2, when co-expressed with $Wld^S$ in *Drosophila*, is still present in the axon at 5 days after axotomy, whereas in the mouse, Nmnat2 still degrades in the presence of $Wld^S$ (Gilley and Coleman, 2010). These data argue that either there is a different mechanism or survival signal in *Drosophila*, or Nmnat2 is not the whole story in mammals.

**$Wld^S$ is not restricted to the nucleus**

Because of the strong nuclear localization, many researchers assumed that the nucleus was the site of $Wld^S$ action. However, new insights into $Wld^S$ are beginning to support a site of action outside of the nucleus. Beirowski et al. found that when $Wld^S$ was removed from the nucleus by mutating the nuclear localization signal in Nmnat1, the cytoplasmic $Wld^S$ protected at a level that was higher than normal $Wld^S$ (2009). Synapses and axon structure were intact for much longer periods of time, and the cytoplasmic $Wld^S$ was even able to protect in older mice, which is not observed in normal $Wld^S$. They also found that this mutant $Wld^S$ fractionated mostly with mitochondria, providing a new and exciting site of action outside of the nucleus. Around the same time of this study, another group found that when Nmnat1 alone was targeted to the cytoplasm, it protected

at levels better than Wld$^S$, both *in vitro* and *in vivo* (Sasaki et al., 2009). *In vivo* protection of Nmnat1 in mammals had not been observed until this study. In chapter 2, I will show that mammalian Nmnat1 can protect *Drosophila* axons, but that the protection is never as strong as Wld$^S$. Perhaps due to the overexpression of the Gal4 system, some of the Nmnat1 is localized outside of the nucleus, which accounts for the partial protection. Immunohistochemistry of Nmnat1 in *Drosophila* axons shows that mammalian Nmnat1 is nuclear, however, the possibility exists that Nmnat1 is below detection level out in the axon. In fact, in a mammalian fractionation study, Nmnat1 exists in fractions other than just the nuclear one (Yahata et al., 2009).

Due to the increase in protection when detectable amounts of Wld$^S$ or Nmnat1 were in the cytoplasm, both the above mentioned studies highlighted the fact that although researchers had not yet been able to detect Wld$^S$ out in the axon with immunohistochemistry, a role for Wld$^S$ outside of the nucleus could not be excluded. In fact, Yahata et al. recently published evidence of Wld$^S$ predominantly in the nuclear and mitochondrial fractions of brain homogenate from Wld$^S$ mice (2009). They further fractionated the mitochondria, and found Wld$^S$ in the inner membrane and matrix. Interestingly, they found that Nmnat3 was also localized to the same suborganellar space as Wld$^S$. When Nmnat3 was overexpressed *in vivo*, it protected as well as Wld$^S$. This was the first endogenous Nmnat that when overexpressed *in vivo* protects axons. All of the mounting evidence points to a role for Wld$^S$ outside of the nucleus, and most

likely in the mitochondria.

**Mitochondria and calcium**

The discovery of $Wld^S$ in the mitochondria begs the question of whether the site of $Wld^S$ action is in the mitochondria and, if so, how $Wld^S$ could act in the mitochondria to prevent axon degeneration. But first, why are mitochondria important to the axon? The answer to this question lies in the ability of mitochondria to buffer calcium, a major signaling molecule in cells that can quickly lead to cell death if the amount of calcium becomes too high. It was first reported by Vasington and Murphy as well as DeLuca and Engstrom in 1961 that isolated mitochondria were able to uptake large amounts of calcium (reviewed in Carafoli, 2010). The calcium is taken up into mitochondria through what has been called the mitochondrial calcium uniporter (MCU), a highly selective ion channel made up of unknown proteins. Recent papers have proposed that LetM1 and MICU1 are necessary for mitochondrial calcium uptake and suggest either protein may be a part of the uniporter (Kirchok et al., 2004; Jiang et al., 2009; Perocchi et al, 2010). The low affinity of the MCU for calcium, however, lead to the belief that mitochondria were probably not a calcium sink *in vivo*. This viewpoint was challenged upon the discovery of localized pools of high amounts of calcium that could compensate for the low affinity of the MCU for calcium (Gunter et al., 1998). Also, advances in fluorescence technology and the ability to compartmentalize fluorescent calcium sensors have confirmed that

mitochondria do, indeed, uptake large amounts of calcium *in vivo* (Celsi et al., 2009).

Although the endoplasmic reticulum can also uptake calcium, mitochondria are thought to be the main calcium buffers, as they are highly motile and can respond to high amounts of calcium (Carafoli, 2010). Calcium uptake by mitochondria depends on the mitochondrial membrane potential; mitochondria cannot clear calcium from the cytoplasm if the membrane potential has collapsed (Babcock et al., 1997). Once inside the mitochondria, calcium can activate three key metabolic enzymes that lead to an increase in ATP production (Celsi et al., 2009). The calcium, in the presence of phosphate, is then precipitated into an insoluble phosphate salt, which serves to quench and buffer the calcium signal (Carafoli, 2010).

**Mitochondria movement is determined by $Ca^{2+}$**

We now know that mitochondria are able to uptake large amounts of calcium in the cell and it has been observed that mitochondria accumulate at sites of increased calcium (MacAskill et al., 2009). How do they reach local pools of calcium and when they get there, how do they sense the change in calcium? The answer to both of these questions is in part, mitochondria Rho-GTPase (Miro). Miro is an atypical Rho GTPase, which is bound to the outer mitochondrial membrane. In *miro* mutants, *Drosophila* larvae exhibit locomotor deficits, the neuromuscular junction shows abnormal organization, and the

mitochondria are clustered in the cell body with few, if any, in the axon (Guo et al., 2005). Further studies have shown that *miro* is also involved in mitochondrial movement in mammalian cells, as knockdown results in a reduction of mitochondria movement (Saotome et al., 2008; Wang and Schwarz, 2009; MacAskill et al., 2009). Overexpression of Miro in mammalian cells results in an increase in mitochondria movement (Saotome et al., 2008), but in *Drosophila* neurons, overexpression results in a dominant-negative phenotype of less mitochondrial movement (Russo et al., 2009). It was also noted that a heterozygous null of *miro* in *Drosophila* motorneurons results in a decrease in mitochondria movement, so it seems *Drosophila* motorneurons are highly sensitive to Miro levels (Russo et al., 2009). Miro's role in the movement of mitochondria consists of two parts: (1) sensing calcium, and (2) binding adaptor molecules and kinesin.

Miro contains 2 EF hand motifs, which are well-characterized calcium-binding domains. When a calcium-mobilizing hormone is added to cells, mitochondria movement is inhibited (Saotome et al., 2008). If the EF hands are mutated, the mitochondria no longer stop in the presence of calcium (Saotome et al., 2008). This finding has been repeated by two other groups with different methods to raise intracellular calcium levels (MacAskill et al., 2009; Wang and Schwarz, 2009). Mammalian cells that express a constitutively active version of Miro or overexpress wild-type Miro are more sensitive to calcium, consistent with Miro being a calcium sensor (Saotome et al., 2008).

The second function of Miro is to bind kinesins and adaptors to move the mitochondria along the microtubules, and is thought to be calcium-sensitive as well, providing a mechanism for how mitochondria can stop in the presence of calcium. Miro binds Milton, an adaptor molecule, in a calcium-independent manner (Wang and Schwarz, 2009; MacAskill et al., 2009). Mutations of *milton* show a very similar phenotype to those of *miro*, with a greatly reduced number of mitochondria present in axons (Glater et al., 2006). After Miro binds Milton, Milton then binds kinesin heavy chain in a calcium-independent manner, and promotes kinesin localization on mitochondria (Glater et al., 2006). Again, mutants of the kinesin heavy chain, *KIF5C*, result in a similar phenotype to that of *miro* and *milton* (Pilling et al., 2006). The involvement of calcium is less clear-cut. There are two conflicting results. Wang and Schwarz report that Miro can actually bind the motor domain of kinesin itself in the presence of only high amounts of calcium (2009). The thought is this direct binding of Miro to KIF5C without Milton causes the kinesin to fall off the microtubule track, in effect stopping the mitochondria. The MacAskill et al. group similarly reported that Miro can directly bind kinesin, however, this interaction occurred in low calcium environments (2009). Upon calcium binding to Miro in higher calcium environments, Miro dissociated from kinesin, giving the same effect of mitochondria stopping. Whichever is the mechanism, it is clear that mitochondria require Miro for movement, and the calcium-sensing EF domains to localize the mitochondria to areas of high calcium, which are in need of calcium buffering and

energy from the mitochondria.

### $Ca^{2+}$ dysregulation and cell death

The ability of mitochondria to respond to and buffer large amounts of calcium is incredibly important to the cell. When mitochondria become overloaded with calcium, the mitochondrial permeability transition pore (PTP) can open leading to apoptosis (Celsi et al., 2009). The calcium overload leads to a collapse in mitochondria membrane potential, allowing the PTP to open and release toxic signals. In neurons, calcium entry into the cell occurs during activity, and it is known that too much activity can lead to excitotoxic death, a mechanism known to involve calcium overload in mitochondria (Celsi et al., 2009). Interestingly, treating cells with taurine increases the amount of calcium that mitochondria can sequester in the presence of glutamate, an excitatory neurotransmitter. This treatment of taurine can actually weakly protect neurons from excitotoxicity, indicating that the ability of mitochondria to uptake large amounts of calcium is critical to the health of the neuron (Idrissi et al., 2008).

To put this in the context of Wallerian degeneration, two *in vitro* studies, and one *in vivo* study have shown the importance of calcium signaling after injury in causing degeneration. Ziv and Spira, and George et al. both reported the presence of high amounts of calcium in an axon after axotomy (1995). Addition of EGTA (ethylene glycol tetraacetic acid), a calcium chelator, to the media prevented axon degeneration after axotomy for one week, whereas wild-type

axons are degenerated in 48-60 hours (George et al., 1995). George et al. also found that if the extracellular calcium was below 200µm, the axon would not degenerate, indicating that extracellular calcium is an initiating factor in axon degeneration. Also, when a calcium ionophore was added to the media, spontaneous degeneration occurred, axon degeneration after axotomy occurred more quickly, and both effects were blocked with the addition of EGTA (George et al., 1995). Recently, these results were duplicated in an *in vivo* model (Knoferle et al., 2010). Calcium fluorescence was observed in a rat optic nerve *in vivo* after crush. Calcium levels increased rapidly within 30 seconds after crush, and the signal slowly declined. The increase in calcium was prevented with calcium channel blockers, indicating again that the calcium that enters the axon is extracellular. Upon the addition of calcium inhibitors, the axonal integrity remained intact, akin to uncrushed nerved, and reciprocally with the addition of calcium ionophores, axonal integrity declined at a rate faster than wild-type crush (Knoferle et al., 2010).

Although it still has yet to be confirmed that calcium overload in mitochondria after axotomy is what initiates degeneration, the data available suggest such a model. Therefore, one could imagine that if mitochondrial calcium buffering capacity were increased, perhaps axon degeneration would not occur. Since $Wld^S$ is localized in the mitochondria, it is perfectly poised to affect the calcium buffering capacity, a model which will be discussed in chapter 3 of my thesis.

**The *Drosophila* Olfactory System and Wallerian Degeneration**

The *Drosophila* olfactory system is highly characterized, and is a great model system for Wallerian degeneration. Odorant receptors (ORs) are encoded by 57 genes and each olfactory neuron expresses one or two odorant receptors (Vosshall et al., 2000). Neurons expressing a specific OR converge on one or two spatially distinct glomeruli in the antennal lobe (**Figure 1-2**) (Vosshall et al., 2000). The location of the cell bodies in the antennal segments or maxillary palps and the location of their respective glomeruli are replicable from animal to animal. Thus, researchers have been able to construct a map of the *Drosophila* olfactory system using OR promoters expressing Gal4 and a UAS-GFP (green fluorescent protein) (Vosshall et al., 2000, Cuoto et al., 2005). The OR promoter-Gal4 lines are extremely useful to the lab, as we can express different domains of $Wld^S$ under the UAS promoter in a specific, predictable subset of neurons. We can also express GFP in the same subset of neurons to visualize the axons before and after injury. This will enable us to be able to count numbers of remaining intact axons after injury is induced.

To confirm that Wallerian degeneration occurs in *Drosophila* axons, we labeled a subset of olfactory receptor neurons with GFP, surgically ablated the third antennal segment, and dissected the brain at various time points to view the axons. At about five hours post-ablation, the axons began to fragment, and by day five, the axons were mostly cleared (**Figure 1-3**) (MacDonald et al., 2006).

This is consistent with observations of Wallerian degeneration in mammals; there is a short latent period after axotomy after which axons undergo rapid fragmentation. Since axon degeneration was very similar to what has been observed in mammals, we decided to test if $Wld^S$ could suppress axon degeneration in *Drosophila*.

$Wld^S$ was driven in a subset of ORNs with the Gal4-UAS system. In $Wld^S$-expressing flies, axons were still present and unfragmented at day five, the time point in which wild-type axons were mostly gone (**Figure 1-4)** (MacDonald, et al., 2006). The $Wld^S$-protected axons were present out to 50 days post-ablation, showing a similar and even more robust protection than in mammals, thereby validating the use of the *Drosophila* model in studying mechanisms of $Wld^S$.

**Significance of the work in this thesis**

Although little is known about axon degeneration, the discovery of the *Wld*$^S$ mouse supports the notion that axon degeneration is an active process that is very similar in a wide range of diseases, such as Parkinson's, progressive motor neuronopathy, and multiple sclerosis. In order to better understand disease and open the doors to therapy options, it is imperative to study the molecular mechanisms of $Wld^S$ and axon degeneration. With our lab's development of a novel method to study axon degeneration after acute nerve transection in *Drosophila*, along with the many genetic tools available for this organism, we are poised to make advances in the molecular understanding of

axon degeneration and Wld$^S$-mediated protection.

In the second chapter of my thesis, I outline a detailed structure-function analysis of Wld$^S$. I define the minimal domains of Wld$^S$ necessary and sufficient for axon protection in *Drosophila*, which are N16 fused to Nmnat1. I also find that VCP/TER94 is essential for full protection of axons. Finally, I test if other mammalian Nmnats can protect axons, and find that Nmnat1 has an intermediate level of protection, Nmnat2 cannot protect, and Nmnat3 can protect as well as Wld$^S$ 5 days after axotomy.

In the third chapter of my thesis, I extend the finding that Nmnat3 can protect as well as Wld$^S$ out to 50 days post axotomy and find no differences between the two proteins in the level of axon protection. Because of their protective function and mitochondrial localization, I explore the differences in Wld$^S$- or Nmnat3-expressing mitochondria. I find that when either of these strongly neuroprotective molecules are present, mitochondria motility is increased. Upon suppressing this increase in movement with *Miro* heterozygous mutants or Miro overexpression, I find that I can suppress Wld$^S$ protective ability, indicating that the increase in mitochondrial motility is necessary for protection. Finally, I find that after injury, highly neuroprotective molecules strongly suppress calcium increase in the axon. Both the increase in motility of mitochondria and the decrease in injury-induced calcium are the first biological changes demonstrated in a Wld$^S$-expressing neuron.

In the fourth chapter of my thesis, I describe a forward genetic screen

taken on by many students and technicians in the laboratory to try to uncover genes involved in axon degeneration. $Wld^S$, while a great tool for studying degeneration, still does not answer whether axon degeneration is an active process because of its gain-of-function nature. In the screen, we hope to definitively demonstrate that axon degeneration is an active process, and in this chapter I will describe one such mutant.

In conclusion, my work has uncovered a model by which $Wld^S$ functions through mitochondria to increase calcium buffering capacity, thereby rescuing axons from calcium-induced death. Although the action of $Wld^S$ does not point to the actual mechanism or pathway of axon degeneration, the forward genetic screen we have conducted does. I have also been instrumental in pushing forward the screen to uncover axon degeneration genes, and have found at least one likely mitochondrial gene to definitively show axon degeneration is an active process. Thus, this work highlights the importance of mitochondria to the axon during degeneration, and future studies should focus on the mitochondria to find the axonal death pathway.

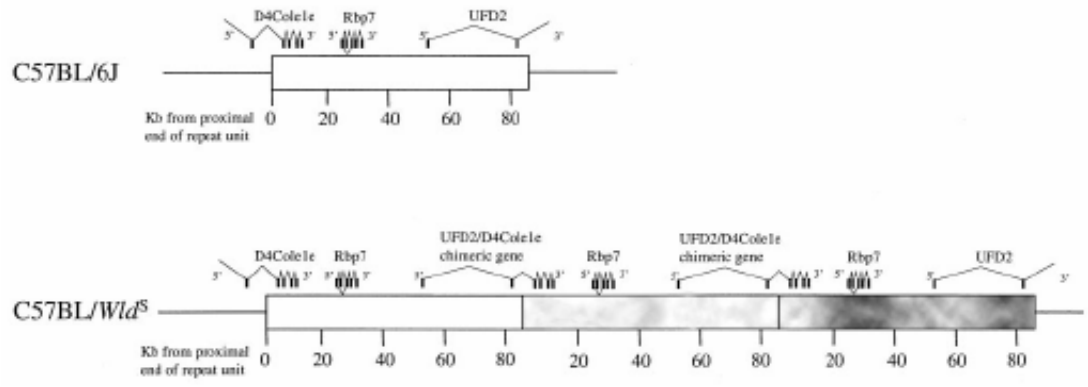
D4Cole1e
Rbp7
UFD2
C57BL/6J
Kb from proximal end of repeat unit
0
20
40
60
80
D4Cole1e
Rbp7
UFD2/D4Cole1e chimeric gene
Rbp7
UFD2/D4Cole1e chimeric gene
Rbp7
UFD2
C57BL/Wld^S
Kb from proximal end of repeat unit
0
20
40
60
80
20
40
60
80
20
40
60
80

**Fig 1-1**

**Figure 1-1 (Conforti, et al. 2000).** Schematic diagram of the $Wld^S$ locus (top) and the triplication event that occurred (bottom) in the *Wld*$^S$ mouse. Ufd2 (Ube4b) fused to D4Cole1e (Nmnat1) in the triplication, but both full-length normal genes are still present. Rbp7 was triplicated in full, resulting in an overexpression.

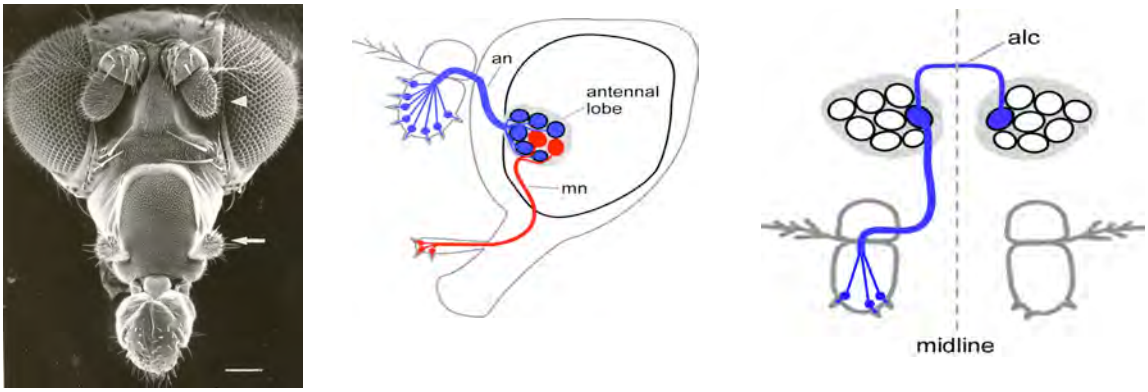


**Fig 1-2**

**Figure 1-2. The *Drosophila* Olfactory system.** (A) 2 pairs of sensory organs exist in the adult fly: the antennae (arrowhead) and maxillary palps (arrow). (B) Sagittal diagram of the adult fly head. Antennal nerves (an) or maxillary nerves (mn) project from the exterior structures and converge on spatially distinct glomeruli in the antennal lobe. (C) Frontal view of the antennae and antennal lobes. The projection pattern of neurons expressing the same olfactory receptor projects both ipsa- and contralaterally. The glomeruli are connected by the antennal lobe commissure (alc).

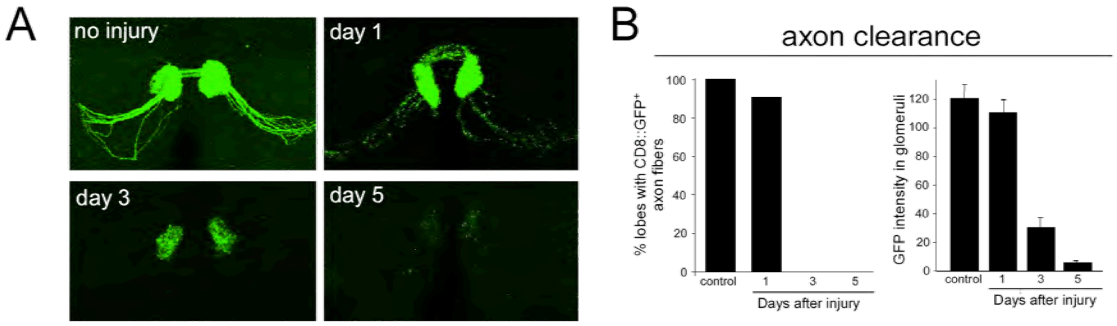
A
no injury
day 1
day 3
day 5
B
axon clearance
% lobes with CD8::GFP+ axon fibers
100
80
60
40
20
0
control
1
3
5
Days after injury
GFP intensity in glomeruli
120
100
80
60
40
20
0
control
1
3
5
Days after injury

**Fig 1-3**

**Figure 1-3. Wallerian degeneration occurs in *Drosophila* (MacDonald et al., 2006).** (A) Axons are fragmented 1 day post-ablation and mostly cleared by day 5 post-ablation. OR-22a axons are labeled with GFP (UAS-mcd8::GFP/+; OR22aGal4/+). (B) Quantification of axon clearance. 3 days post-injury no axonal fibers are detected, and GFP intensity decreases post-ablation.

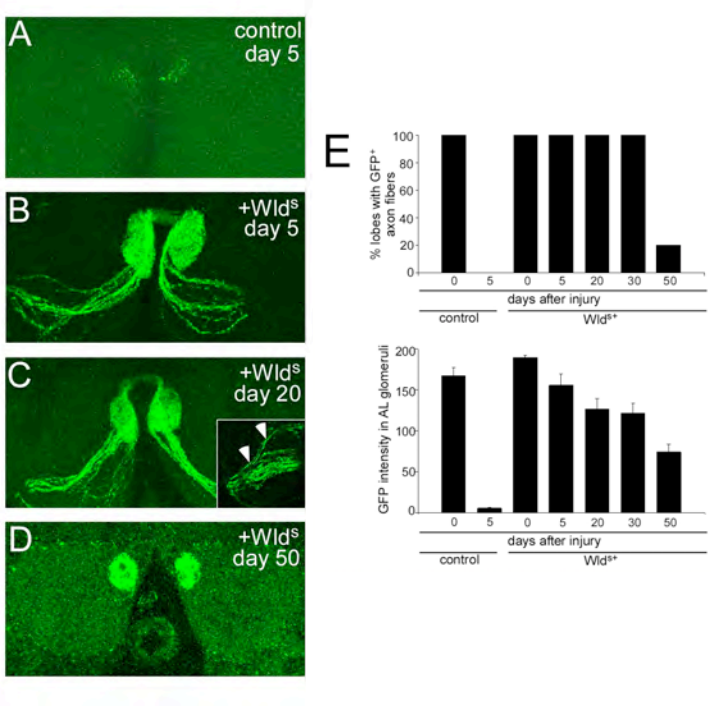
A
control
day 5
B
+Wld$^S$
day 5
C
+Wld$^S$
day 20
D
+Wld$^S$
day 50
E
% lobes with GFP$^+$ axon fibers
100
80
60
40
20
0
0
5
0
5
20
30
50
days after injury
control
Wld$^{S+}$
GFP intensity in AL glomeruli
200
150
100
50
0
0
5
0
5
20
30
50
days after injury
control
Wld$^{S+}$

**Fig 1-4**

**Figure 1-4. Wld$^S$ can protect severed *Drosophila* axons (MacDonald et al., 2006).** (A) Control flies 5 days post-ablation have very little GFP-positive axonal material remaining in the antennal lobe (UAS-mcd8::GFP/+; OR22aGal4/+). (B) Wld$^S$-expressing flies have intact axons 5 days post-ablation, (C) axons are still seen at day 20, and (D) GFP-positive material is still present at 50 days post-ablation (UAS-mcd8::GFP/+; OR22aGal4/UAS-Wld$^S$). (E) Quantification of axonal presence in the antennal lobes (top) and GFP intensity in the glomeruli (bottom). Wld$^S$-expressing flies show 100% axon presence out to 30 days post ablation and show a very minimal decline in GFP intensity out to 50 days post-ablation. This is in sharp contrast to wild-type where no axons are present 5 days post-ablation, and the glomeruli GFP intensity is near zero at 5 days post-ablation.

# Chapter II:

# $Wld^S$ requires Nmnat1 enzymatic activity and N16-VCP interactions to suppress Wallerian degeneration

The following work is reprinted from the Journal of Cell Biology article of the same name published as:

Avery, M.A., Sheehan, A.E., Kerr, K.S., Wang, J., and Freeman, M.R. J Cell Bio, 23 February 2009: Vol. 184. No. 4, pp 501-513.

**Abstract**

Slow Wallerian degeneration ($Wld^S$) encodes a chimeric Ube4b/nicotinamide mononucleotide adenylyl transferase 1 (Nmnat1) fusion protein that potently suppresses Wallerian degeneration, but the mechanistic action of WldS remains controversial. In this study, we characterize $Wld^S$-mediated axon protection in vivo using *Drosophila melanogaster*. We show that Nmnat1 can protect severed axons from autodestruction but at levels significantly lower than $Wld^S$, and enzyme- dead versions of Nmnat1 and $Wld^S$ exhibit severely reduced axon-protective function. Interestingly, a 16–amino acid N-terminal domain of $Wld^S$ (termed N16) accounts for the differences in axon-sparing activity between $Wld^S$ and Nmnat1, and N16-dependent enhancement of Nmnat1-protective activity in Wld requires the N16-binding protein valosin-containing protein (VCP)/TER94. Thus, $Wld^S$-mediated suppression of Wallerian degeneration results from VCP–N16 interactions and Nmnat1 activity converging in vivo. Surprisingly, mouse Nmnat3, a mitochondrial Nmnat enzyme that localizes to the cytoplasm in *Drosophila* cells, protects severed axons at levels indistinguishable from WldS. Thus, nuclear Nmnat activity does not appear to be essential for WldS-like axon protection.

## Introduction

Axons represent the key cellular outgrowth that permits connectivity between distant neurons or neurons and their non- neuronal targets (e.g., muscles). Axons can be extremely long, traversing great distances, and in most neurons, the axonal compartment composes the majority of the cellular volume. Because of the significant length and volume of the axon, its stabilization represents a major and ongoing challenge for neuronal cell types.

Wallerian degeneration serves as an extremely useful context in which to study molecular and cellular mechanisms that mediate axon integrity. Acute axotomy induces large-scale axon degeneration after a defined latent phase that bears striking resemblance to axon degeneration during developmental pruning (Luo and O'Leary, 2005) and in neurodegenerative disease (Coleman, 2005). Wallerian degeneration was long thought to represent a passive wasting away of the distal portion of the severed axons (Waller, 1850) caused by a lack of nutrients from the cell body, but a revolution in our understanding of axon biology came with the discovery of the spontaneous C57BL/slow Wallerian degeneration ($Wld^S$) mutant mouse. Amazingly, severed $Wld^S$ mutant axons survived for weeks after axotomy (Lunn et al., 1989; Glass et al., 1993). This observation indicated that the $Wld^S$ mutation somehow suppressed axon autodestruction and suggested for the first time that Wallerian degeneration might be an active process of axon autodestruction akin to apoptotic cell death (Coleman and Perry, 2002; Raff et al., 2002). Subsequent analysis of the $Wld^S$ mutant has provided

intriguing insights into the molecular relationships between axon degeneration in developmental, injury, and disease contexts. For example, the $Wld^S$ mutation can suppress axon degeneration induced by chemical toxicity (Wang et al., 2001), nerve crush (Beirowski et al., 2005), and mouse models of neurodegenerative disease (Ferri et al., 2003; Coleman, 2005), suggesting that the underlying programs that drive axon autodestruction in these distinct degenerative contexts share common molecular features. However, $Wld^S$ does not suppress axon degeneration during developmental axon pruning in *Drosophila melanogaster* or mammals (Hoopfer et al., 2006), arguing that $Wld^S$-independent molecular programs drive axon degeneration in developmental settings.

The $Wld^S$ mutation was recently found to result in the fusion of two genes, the $NAD^+$ biosynthetic molecule nicotinamide mononucleotide adenylyl transferase 1 (nmnat1) and Ube4b, an E4 ubiquitin ligase (Conforti et al., 2000; Mack et al., 2001). The protein encoded by this locus, termed $Wld^S$ (Fig. 2-1 A), is composed of the N-terminal 70 amino acids of Ube4b (termed N70), a unique 18–amino acid domain generated during the gene fusion event (termed W18), and the full-length sequence of mouse nmnat1. Expression of this protein in mouse neurons fully recapitulates the $Wld^S$ mutant phenotype (Mack et al., 2001) and can even protect severed axons from autodestruction in distant species like *Drosophila* (Hoopfer et al., 2006; MacDonald et al., 2006).

Three main models have been proposed to explain $Wld^S$-mediated axon protection. The first argues that Ube4b may have a dominant-negative effect on

the ubiquitin proteasome (UPS) pathway. Although the N70 portion of Ube4b does not have ubiquitination activity on its own, it contains domains capable of binding Ube4b substrates, implying that N70 may bind key substrates in vivo, fail to target them for degradation, and, in turn, somehow stabilize severed axons. Consistent with this model, the UPS pathway has been shown to be essential in promoting axon autodestruction during Wallerian degeneration (Zhai et al., 2003) and developmental axon pruning (Watts et al., 2003), but a direct functional link between $Wld^S$ and the UPS pathway is lacking. A second hypothesis is that Nmnat1, a NAD+ biosynthetic enzyme, acts to produce excess NAD+ in the axon after injury and thereby stabilize the axon. Two groups reported that application of NAD+ or its precursors to neuronal cultures partially suppressed axon degeneration in vitro (Araki et al., 2004; Wang et al., 2005); however, a third study found no enhancement of survival of severed axons from primary neuronal cultures with NAD+ application (Conforti et al., 2007). Moreover, transgenic mice expressing Nmnat1 in neurons failed to phenocopy $Wld^S$ (Conforti et al., 2007). Finally, a third model proposes that Nmnat1 acts in the nucleus before injury through Sirt1, a member of the sirtuin family of NAD+-binding histone deacetylases, to change patterns of neuronal gene expression before injury, which protects severed axons after axotomy (Araki et al., 2004). Araki et al. (2004) provided in vitro data in support of this model showing that siRNAs directed toward sirt1 could partially suppress the neuroprotective effects of bath-

applied NAD+; however, a null allele of sirt1 failed to suppress the ability of $Wld^S$ to protect severed axons in vivo (Wang et al., 2005).

The aforementioned models remain open possibilities but have not been tested incisively in vivo. In this study, we explore the in vivo mechanistic action of $Wld^S$ in *Drosophila*. We find that $Wld^S$-mediated protection requires two activities: Nmnat1 enzymatic function and the N-terminal 16 amino acids of N70 (termed N16). We show that N16 associates with TER94, the fly orthologue of the mouse N16-binding molecule valosin-containing protein (VCP; Laser et al., 2006), and that VCP is essential for $Wld^S$-like levels of axon protection. Thus, the converging activity of domains derived from both Ube4b and Nmnat1 are essential for WldS-like levels of axon protection in vivo. Surprisingly, we find that Nmnat3, a mouse mitochondrial Nmnat that localizes throughout the cytoplasm in *Drosophila* cells (but not to the nucleus), can protect severed axons as well as $Wld^S$. Thus, nuclear localization of Nmnat activity is not essential for robust axon protection, and these data raise the intriguing possibility that N16–VCP/Ter94 interactions may function to relocalize Nmnat1 outside of the nucleus, perhaps to mitochondria, where it exerts its neuroprotective effects.

## Results

### Constructs generated for in vivo functional dissection of $Wld^S$

The adult *Drosophila* olfactory system offers an excellent opportunity to study Wallerian degeneration and $Wld^S$ function in a well-controlled in vivo

setting: odorant receptor (OR)–Gal4 driver lines can be used to reproducibly label specific subsets of axons with membrane-tethered GFP (mCD8-GFP); nonlethal surgical ablation of antennae or maxillary palps induces Wallerian degeneration of olfactory receptor neuron (ORN) axons; severed axon degeneration can be monitored in the intact brain for months after injury; and neuroprotective molecules like $Wld^S$ can be expressed in these axons at standardized levels to quantitatively compare neuroprotective activity (MacDonald et al., 2006). In this study, we use this system to define the functional domains in $Wld^S$ that are essential for protection of severed axons in vivo.

We constructed several transgenic *Drosophila* lines carrying variants of the $Wld^S$ molecule (**Fig. 2-1 A**): (a) upstream activating sequence (UAS)–nmnat1, full-length mouse nmnat1; (b) UAS-$nmnat1^{dead}$, full-length mouse nmnat1 with an H24A substitution, which has been previously shown to allow folding of Nmnat and binding of its substrate but largely to abolish substrate conversion to NAD+ (Saridakis et al., 2001); (c) UAS- $Wld^{S\text{-}\Delta N16}$, $Wld^S$ with a deletion of the first 16 amino acids (termed N16), which was previously shown to bind VCP (Laser et al., 2006); (d) UAS-N16::nmnat1, a fusion of N16 to full-length Nmnat1; and (e) UAS-$Wld^{S\text{-}dead}$, full-length $Wld^S$ with an H24A substitution in the Nmnat1 portion of the molecule. To determine the subcellular localization of $Wld^S$ and the aforementioned variants, we also generated C-terminally Myc epitope–tagged versions of $Wld^S$, $Wld^S$-dead, and Nmnat1 (UAS- $Wld^S$::Myc,

UAS-Wld$^{S\text{-}dead}$::Myc, and UAS-Nmnat1::Myc). When expressed in *Drosophila*, antennal lobe projection neurons in the central brain of all of these molecules localized exclusively to the nucleus (**Fig. 2-1, B–G**), indicating that the H24A mutations that abolish NAD+ biosynthetic activity do not alter the subcellular localization of Wld$^{S}$. We further note the conspicuous absence of Wld$^{S}$+ nuclear puncta in *Drosophila* neurons (**Fig. 2-1, B** and **C**) and S2 cells (see **Fig. 2-5, A** and **B**) that have been observed when Wld$^{S}$ is expressed in mammalian cell lines (Laser et al., 2006). Thus, Wld$^{S}$ localizes to the nucleus in *Drosophila* neurons, and these data argue that the presence of Wld$^{S}$+ nuclear puncta is not essential for Wld$^{S}$ to exert its neuroprotective effects.

Multiple transgenic lines were established for each construct, and at least three lines bearing independently isolated transgene insertions were assayed for protein expression levels (**Fig. 2-2**) and functional protection (see following section). The efficiency of protein expression from each transgene was assayed by crossing individual UAS lines to the panneuronal driver elav-Gal4, preparing protein extracts from head, and assaying protein levels with $\alpha$-Nmnat1 antibodies on Western blots. All Wld$^{S}$ variants carry full-length Nmnat1, and thus, this antibody should recognize each with equal affinity. In some cases, each of the three transgenic lines for a given construct expressed very similar levels of protein (e.g., N16::Nmnat1 and Wld$^{S\text{-}_{\Delta}N16}$); for others, the total expression level of each protein varied among transgenic lines (e.g., Wld$^{S}$, Nmnat1, Nmnat1$^{dead}$, and Wld$^{S\text{-}dead}$). Despite this fact, the in vivo axon-protective function of each molecule

was in most cases strikingly similar among transgenic lines carrying different insertions of the same transgene (see following section).

**Wallerian degeneration is potently suppressed by Wld$^S$ and partially blocked by Nmnat1, and axonal protection requires Nmnat1 enzymatic activity**

To compare the protective effects of the aforementioned transgenes, we crossed each to the ORN-specific driver OR22a-Gal4, severed ORN axons, and determined the number of remaining intact axonal fibers present at 5, 10, 15, 20, and 30 d after injury (**Fig. 2-S1**). Each neuroprotective molecule showed a unique pattern of protection, but this was indistinguishable among the other transgenic lines carrying the same transgene (**Fig. 2-S2**), and therefore, axon protection data were pooled for each transgene (**Fig. 2-3**).

We first asked whether Nmnat1 could protect severed axons in vivo at a level similar to Wld$^S$ and whether Nmnat1 enzymatic activity was essential for axonal protection. Previously, we reported that mouse Wld$^S$ could robustly suppress Wallerian degeneration in *Drosophila* for at least 20 d after injury (MacDonald et al., 2006). We have now confirmed and extended this finding to 30 d after injury, with the majority (77%) of Wld$^S$-expressing axons remaining intact for this period (**Fig. 2-3**). Interestingly, we found that expression of mouse Nmnat1 in ORNs also partially suppressed Wallerian degeneration; however, Nmnat1 was significantly less effective than Wld$^S$ at protecting severed axons.

For example, the majority of severed axons in animals expressing $Wld^S$ remained intact even 30 d after injury (77%), whereas a minority of axons expressing Nmnat1 (32%) remained intact at this time point. Thus, Nmnat1 is indeed a neuroprotective molecule in vivo and likely represents an important component of the severed axon-protecting activity of $Wld^S$. However, the fact that Nmnat1 provided significantly reduced protection of severed axons compared with $Wld^S$ argues that N70 and/or W18 enhances the neuroprotective nature of Nmnat1 in important ways to provide $Wld^S$-like levels of axon protection.

Next, we assayed the ability of enzyme-dead variants of $Wld^S$ and Nmnat1 to protect severed axons. Strikingly, blocking the enzymatic activity of Nmnat1 with an H24A mutation almost completely eliminated the ability of Nmnat1 to protect severed axons. In $Nmnat1^{dead}$-expressing animals, 100% of all axons had undergone Wallerian degeneration within 10 d after injury (**Fig. 2-3**). Thus, Nmnat1-dependent axon protection requires the NAD+ biosynthetic activity of Nmnat1. Consistent with a role for Nmnat1 enzymatic activity in promoting $Wld^S$-dependent axon protection, we found that $Wld^{S\text{-}dead}$ also exhibited strongly reduced neuroprotection: in $Wld^{S\text{-}dead}$-expressing animals, 92% of axons had degenerated within 15 d after injury (**Fig. 2-3**). Interestingly, and in contrast to $Nmnat1^{dead}$, $Wld^{S\text{-}dead}$ exhibited intermediate levels of protection until 10 d after injury, indicating that $Wld^{S\text{-}dead}$ retains a moderate level of axon-sparing activity despite having reduced Nmnat1 enzymatic activity. These data provide further strong evidence that N70 or W18 domains of $Wld^S$ are important for $Wld^S$-

dependent protection of severed axons and indicate that Nmnat1 enzymatic activity is essential for sustained $Wld^S$-dependent protection of axons.

The N16 domain of $Wld^S$ is essential for maximal axon protection and accounts for differences in neuroprotection observed between $Wld^S$ and Nmnat1.

Which portion of N70 or W18 is responsible for the increased neuroprotection of $Wld^S$ relative to that observed with Nmnat1? Previous biochemical experiments identified N16 as a binding site for association of $Wld^S$ with VCP (Laser et al., 2006). We sought to determine the functional requirements for the N16 domain in $Wld^S$-mediated protection of severed axons in vivo. Therefore, we generated two transgenic constructs, $Wld^{S\text{-}_{\Delta}N16}$ (harboring a specific deletion of the N16 domain) and N16::Nmnat1 (in which only the N16 domain is directly fused to the N terminus of Nmnat1; **Fig. 2-1 A**) and assayed axon-protective effects. In striking contrast to the protection observed with $Wld^S$, $Wld^{S\text{-}_{\Delta}N16}$ provided significantly reduced protection of severed axons, with 25% and 35% of axons degenerating by day 10 and day 20 after injury, respectively (**Fig. 2-4**). $Wld^{S\text{-}_{\Delta}N16}$- mediated protection was indistinguishable from that afforded by Nmnat1, suggesting that N16 is the key domain responsible for the increased protection we observed in axons expressing $Wld^S$ compared with Nmnat1. Reciprocally, N16::Nmnat1 expression in axons provided significantly increased protection of severed axons relative to Nmnat1 alone, with >90% of axons surviving as long as 20 d after injury (**Fig. 2-4**). Therefore, N16::Nmnat1–mediated protection of severed axons was indistinguishable from the protection

provided by Wld$^S$. In summary, we find that N16 is essential for Wld$^S$-like neuroprotective activity and is sufficient when tethered to Nmnat1 to provide Wld$^S$-like levels of severed axon protection in vivo. Together, the aforementioned data indicate that Wld$^S$-mediated axon protection results from two synergizing activities: (1) Nmnat1 enzymatic activity and (2) N16-dependent protein–protein interactions.

**VCP/TER94 binds to N16 and is essential for WldS-like neuroprotection**

The only protein known to physically interact with Wld$^S$ is VCP, and it does so through the N16 domain (Laser et al., 2006), but its role in Wld$^S$-mediated axon protection remains unclear. To determine whether *Drosophila* VCP, known as TER94 (Pinter et al., 1998), associates with mouse Wld$^S$, we transfected *Drosophila* S2 cells with Wld$^S$::Myc and performed coimmunoprecipitation experiments with $\alpha$-Myc antibodies. We found that Wld$^S$::Myc was stably expressed in *Drosophila* S2 cells and localized primarily to the nucleus (**Fig. 2-5, A** and **B**). Two isoforms of TER94 are present in *Drosophila*, one of 50 kD (isoform A) and a second of 97 kD (isoform B). We found that S2 cells normally express the 50-kD isoform and lower levels of the 97-kD isoform. Immunoprecipitations with $\alpha$-Myc antibodies from Wld$^S$::Myc–transfected S2 cells led to robust co- purification of the 97-kD isoform (which is >80% identical to mouse VCP; **Fig. 2-5 C**), indicating that Wld$^S$::Myc can associate with TER94. Whether Wld$^S$::Myc associates with the 50-kD isoform of TER94 remains unclear

because this protein runs at the same size as the mouse IgG heavy chain used for $Wld^S$::Myc pull-downs. Thus, TER94, like VCP in mammals, can physically associate with $Wld^S$ in *Drosophila*.

Next, we sought to determine whether loss of TER94 function could suppress the ability of $Wld^S$ to protect severed axons. Because deletion of N16 from $Wld^S$ suppresses the axon-protective function of $Wld^S$ to levels equivalent to Nmnat1 (**Fig. 2-4**), we predicted that blocking TER94 function in $Wld^S$-expressing neurons should phenocopy the protective effects of Nmnat1 and $Wld^{S\text{-}_{\Delta}N16}$. We first assayed whether null alleles of TER94 could dominantly suppress the ability of $Wld^S$ to protect severed axons, but $Wld^S$-expressing animals lacking a single copy of TER94 showed the normally high levels of axon protection we observe in $Wld^S$-expressing axons (unpublished data). We were unable to assay TER94 function in $Wld^S$-mediated axon protection in a null TER94 background because animals homozygous for strong loss of function alleles of TER94 are homozygous lethal (Ruden et al., 2000). Therefore, we turned to RNAi methods to knock down TER94 function specifically in $Wld^S$-expressing axons. Strikingly, we found that knocking down TER94 in $Wld^S$-expressing axons with UAS-$TER94^{RNAi}$ suppressed the axon-protective function of $Wld^S$ to levels indistinguishable from Nmnat1 and $Wld^{S\text{-}_{\Delta}N16}$ (**Fig. 2-5 D**). Uninjured age-matched controls for $Wld^S$/$TER94^{RNAi}$ and $TER94^{RNAi}$ animals were indistinguishable from day 0 controls, and thus, the axon loss observed in $Wld^S$/$TER94^{RNAi}$ animals was dependent on axotomy. We note that RNAi for TER94 alone did result in a slight

but significant reduction in the number of axons present in uninjured animals in the absence of $Wld^S$ (**Fig. 2-5 D**), suggesting that $TER94^{RNAi}$ can induce low level axon degeneration. However, the vast majority of axons in these animals were intact before injury and in age-matched controls, indicating that $TER94^{RNAi}$ treatment does not cause widespread degeneration of axons on its own. In summary, we conclude that TER94 is autonomously required in $Wld^S$-expressing neurons in vivo for $Wld^S$ to maximally protect severed axons from autodestruction. Furthermore, we propose that the key neuroprotective portion of the N70/W18 domain of $Wld^S$ is N16 and that its neuroprotective effects are mediated by a TER94/VCP-dependent mechanism.

A major cellular role for TER94/VCP is targeting proteins for refolding, or destruction as part of the UPS degradation pathway. TER94/VCP sits at a pivotal point in the cascade, having the ability to direct refolding or degradation of substrates based on its binding partners. When associated with ubiquitinated proteins, VCP can either bind Npl4 and Ufd2 and target proteins for proteasomal degradation or bind Ufd1 and Plap and release refolded proteins into the cytoplasm (for review see Halawani and Latterich, 2006). In an attempt to identify additional molecules that interact with TER94/VCP to modulate axon autodestruction or $Wld^S$-mediated neuroprotection, we assayed the requirements of the following *Drosophila* genes in Wallerian degeneration and $Wld^S$ function: *CG4673*, encoding the *Drosophila* orthologue of *npl4*; *ufd2*; *ufd1-like*; and *plap*, encoding the *Drosophila* orthologue of *Ufd3*. For each molecule, we used UAS-

regulated RNAi constructs to knock down their function in neurons and assayed the ability of these molecules to (a) induce spontaneous axon degeneration, (b) suppress axon autodestruction 15 d after injury, and (c) suppress the ability of $Wld^S$ to protect severed axons. We found that knockdown of each of these genes failed to dramatically suppress normal axon development, axon stability, degeneration after axotomy, or the ability of $Wld^S$ to protect severed axons (**Fig. 2-S3**). These data argue that additional components of the TER94/VCP complex are not involved in Wallerian degeneration or $Wld^S$-mediated protection of severed axons.

**A lack of evidence for a requirement for Sir2 function in $Wld^S$-mediated axon protection**

Sirt1, a member of the mammalian family of Sir2-like NAD+- binding histone deacetylases (the sirtuins), has been implicated in NAD+-mediated axon protection through a lentiviral-expressing siRNA study in mammalian tissue culture. Specifically, siRNA knockdown of Sirt1, but not the six other mammalian sirtuins (Sirt2–7), partially suppressed the ability of NAD+ application to protect axons in dorsal root ganglion explant cultures (Araki et al., 2004). Surprisingly, in a subsequent study in which a sirt1-null mutation was crossed into the $Wld^S$ background, loss of sirt1 failed to suppress the ability of $Wld^S$ to protect severed axons in vivo (Wang et al., 2005), calling into question the role of Sirt1 in executing $Wld^S$ function. Importantly, it remains an open possibility that the

remaining mammalian sirtuins (Sirt2–7) might functionally compensate for Sirt1 in this context, and thus, the functional requirements for mammalian sirtuins in $Wld^S$ function remain unclear.

In *Drosophila*, there is a single gene that bears strong sequence similarity to the mammalian sirtuins, *Sir2*; *Sir2* is 55.9% identical to the Sirt1 at the amino acid level. The simplicity of the *Drosophila* sirtuin family offers the opportunity to directly reassess the requirements for sirtuins in $Wld^S$ function in vivo. We first assayed the requirements for *Drosophila* Sir2 in $Wld^S$- mediated protection of severed axons using a UAS-regulated RNAi construct targeted to Sir2. We found that expression of $Sir2^{RNAi}$ in axons did not induce spontaneous degeneration and that ORN axons appeared to develop normally (unpublished data). Axotomized $Sir2^{RNAi}$-expressing axons exhibited normal axon degeneration, arguing that Sir2 function is not required for Wallerian degeneration (**Fig. 2-6 A**). Moreover, expression of $Sir2^{RNAi}$ in $Wld^S$-expressing axons did not suppress the ability of $Wld^S$ to protect severed axons (**Fig. 2-6 A**). Next, we confirmed our observation with $Sir2^{RNAi}$ genetically by crossing $Wld^S$ into a *Sir2*-null mutant background. Loss of function alleles of *Sir2* are not available; however, removal of the *Sir2* gene can be accomplished using a heteroallelic combination of the two partially overlapping deletions in $sir2^{5.2\ 6}$ and $sir2^{4.5}$ mutants (Newman et al., 2002). As with our $Sir2^{RNAi}$ experiments, we found that deletion of the *Sir2* gene in a $Wld^S$ background failed to suppress the ability of $Wld^S$ to protect severed axons from degeneration (**Fig. 2-6 B**). These data argue strongly that $Wld^S$ does

not require the NAD+-binding histone deacetylase Sir2 to protect severed axons from autodestruction.

**Wallerian degeneration is strongly suppressed by mouse mitochondrial Nmnat3, but NAD+ synthase (NADS), membrane-tethered Wld$^S$, and cytoplasmic Nmnat2 fail to protect severed axons**

Do all NAD+ biosynthetic enzymes protect axons from auto-destruction? The *Drosophila* genome encodes one additional NAD+ biosynthetic enzyme called *NADS* that by primary sequence is not related to *Nmnat* and in yeast localizes throughout the cell (Suda et al., 2003). We generated transgenic flies carrying a UAS-NADS construct, drove expression in ORN axons as described in the first section of Results, and assayed axon-protective function 5 d after injury (**Fig. 2-7 A**). Surprisingly, NADS provided no protection of axons. To determine whether NADS might require VCP/TER94 interactions through N16 for detectable axon-protective activity, we also generated flies bearing an N16::NADS fusion protein but found that this molecule also completely failed to suppress axon autodestruction (**Fig. 2-7 A**).

Wld$^S$ is normally localized in the nucleus, but can Wld$^S$ protect severed axons from degeneration if it is forced to localize elsewhere in the cell? We used two approaches to address this question. First, we generated a membrane-tethered version of Wld$^S$. In brief, we fused the extracellular and transmembrane domains of the mouse CD8 surface receptor (Lee and Luo, 2001) to the N-

terminus of $Wld^S$ (termed mCD8::$Wld^S$) and drove the expression of this molecule in $22a^+$ axons. We found that adult ORNs stably expressed high levels of mCD8::$Wld^S$ in the axonal compartment (**Fig. 2-7 B**). However, we found that mCD8::$Wld^S$ completely failed to suppress the degeneration of severed axons; 10 d after axotomy, 100% of mCD8::$Wld^{S+}$ axons degenerated and were cleared from the central nervous system (**Fig. 2-7 C**). Thus, tethering $Wld^S$ to the cell surface in vivo is sufficient to block the ability of $Wld^S$ to protect severed axons.

As a second approach, we assayed the protective function of mammalian Nmnat molecules that show unique patterns of subcellular localization. In mammals, there are three genes encoding Nmnat molecules: Nmnat1, which, as described in the first section of Results, localizes to the nucleus; Nmnat2, which is cytoplasmic; and Nmnat3, which localizes primarily to mitochondria (Sasaki et al., 2006). Nmnat2 localized to the cytoplasm in *Drosophila* S2 cells (**Fig. 2-7 E**) but completely failed to suppress axon degeneration (**Fig. 2-7 D**). In striking contrast, Nmnat3, which also appeared to localize largely to the cytoplasm in S2 cells (**Fig. 2-7 E**), provided levels of axon protection that were indistinguishable from those afforded by $Wld^S$ (**Fig. 2-7 D**).

In summary, these data indicate that only a subset of NAD+ biosynthetic enzymes can provide significant protection of severed axons, that membrane-tethered $Wld^S$ is not sufficient to protect axons, and that Nmnat3, an enzyme that localizes primarily to mitochondria in mammalian cells, provides $Wld^S$-like levels of axon protection. Thus, nuclear localization appears to be nonessential for

Wld$^S$-like axon protection, and Nmnat3 and Wld$^S$ appear to have unique activities or localizations relative to Nmnat2 and mCD8::Wld$^S$ that allow for robust axon-protective function in vivo.

## Discussion

### The enzymatic activity of Nmnat1 is a critical feature of Wld$^S$

Whether Nmnat1 and its enzymatic product NAD+ underlie the protective activity of Wld$^S$ has remained a point of great controversy. Two studies found that transfection of nmnat1 into dorsal root ganglia neurons or direct application of NAD+ or its biosynthetic precursors to dorsal root ganglia cultures was sufficient to prolong the survival of severed axons in vitro (Araki et al., 2004; Wang et al., 2005). In contrast, a subsequent study reported a lack of protection of axons by direct expression of Nmnat1 in neurons or application of NAD+ in vitro, and transgenic mice expressing Nmnat1 failed to exhibit significant increased axon protection in vivo (Conforti et al., 2007). We find that expression of Nmnat1 in *Drosophila* axons provides significant levels of protection for severed axons, with the majority of axons surviving for longer than 2 wk. Thus, Nmnat1 is indeed strongly neuroprotective on its own, although the levels of protection provided by Nmnat1 are significantly reduced compared with Wld$^S$. This observation argues that Nmnat1 is a critical component of Wld$^S$ but indicates that the protection afforded by Wld$^S$ and Nmnat1 is not equivalent. As discussed in the following section, we propose that the increased efficiency of protection provided by Wld$^S$

maps to the N16 domain of $Wld^S$, which interacts with VCP/TER94. Why doesn't Nmnat1 protect severed axons in transgenic mice? We can think of at least two explanations for the difference observed between mice and flies with respect to in vivo axon protection by Nmnat1. First, we express Nmnat1 in *Drosophila* using the Gal4/UAS binary expression system, which can drive very high levels of expression in ORN neurons. It is possible that we have increased the relative amount of Nmnat1 in neurons to a point exceeding that necessary for Nmnat1-dependent protection of severed axons, whereas expression levels of Nmnat1 in mouse sciatic nerve using the β-actin promoter (Conforti et al., 2007) remain below this critical threshold. Second, the axons of *Drosophila* ORNs are much shorter than mammalian axons in the sciatic nerve and may thus be more easily protected relative to lengthy mammalian axons.

The protection of severed axons by Nmnat1 critically depends on its enzymatic activity. To generate an Nmnat1 molecule that fails to synthesize NAD+, we engineered an H24A substitution in Nmnat1. Based on analysis of the crystal structure of Methanobacterium thermoautotrophicum NMNAT, the corresponding histidine (H19) resides in the binding site for ATP. Mutational analysis of the importance of this histidine with an H19A substitution demonstrated that mutation of this residue reduced NAD+ biosynthetic activity to <1%, did not significantly affect protein folding (determined by solving the crystal structure of the H19A mutant version), and led to the copurification of NMNAT with its substrate nicotinamide mononucleotide trapped in the active site rather

than its product NAD+, which copurifies with wild-type NMNAT (Saridakis et al., 2001). This suggests a failure of NMNAT to convert nicotinamide mononucleotide to NAD+. We find that an H24A substitution in Nmnat1 completely suppresses the neuroprotective effects of Nmnat1, with close to 100% of the axons from Nmnat1$^{dead}$-expressing neurons degenerating within 5 d after injury. Wld$^{S\text{-}dead}$, harboring the same H24A mutation in Nmnat1, also shows dramatically reduced efficacy in the protection of severed axons. Together, these data demonstrate a requirement for Nmnat1 enzymatic activity in Wld$^{S}$-mediated protection of severed axons in vivo. In turn, along with the aforementioned studies, they suggest that the effects of Nmnat1 are mediated by its biosynthetic products. NAD+ is certainly the best-known product of Nmnat1 enzymatic activity and likely plays a key role in axon protection; however, we note that we cannot exclude the formal possibility that in the context of axon protection, Nmnat1 may generate additional biosynthetic products beyond NAD+ that might be neuroprotective.

Interestingly, recent work on *Drosophila* Nmnat (dNmnat) has revealed a role for dNmnat1 in the suppression of activity- or spinocerebellar ataxia 1 (Sca1)–induced degeneration in the visual system (Zhai et al., 2006, 2008). Surprisingly, the dNmnat-dependent protection of neurons in the visual system is independent of its enzymatic activity, and dNmnat appears capable of acting as a chaperone-like molecule in an enzymatic activity–independent manner (Zhai et al., 2008). Is this chaperone-like activity contributing to Wld$^{S}$-dependent neuroprotection? Although this remains an open possibility, we suspect it is not a

major contributing force in the mechanistic action of $Wld^S$ in severed axons for two reasons. First, $Wld^S$ and Nmnat1 both require their enzymatic activity to protect severed axons in vivo, whereas dNmnat can protect against Sca1-induced neurodegeneration in the absence of enzyme function. Second, dNmnat is induced in response to the formation of Sca1 aggregates and localizes to sites of protein aggregation, whereas $Wld^S$ and Nmnat1 show no such localization. A more thorough delineation of the mechanistic action of $Wld^S$, Nmnat1, and dNmnat will be essential to resolve these issues.

**N70 contributes to $Wld^S$ neuroprotective function through interactions with VCP/TER94**

How N70 or W18 could contribute to $Wld^S$ function has remained enigmatic. The portion of Ube4b found in $Wld^S$, N70, lacks the U box found in Ube4b that is essential for E4 ubiquitination activity (Hatakeyama et al., 2001; Hatakeyama and Nakayama, 2003) and thus does not have ubiquitin-conjugating activity on its own. However, a deletion study of Ube4b has shown that this N-terminal domain is indeed essential for Ube4b ubiquitination activity (Mahoney et al., 2002). Although specific domains necessary for ubiquitination activity of mouse Ube4b have not been identified in N70, the first 16 amino acids of N70 (termed N16) have recently been shown to bind VCP/p97 (Laser et al., 2006). Through N16, $Wld^S$ can redistribute VCP into the nucleus (Dai and Li, 2001). VCP, in turn, could result in the association of $Wld^S$ with a variety of cellular

proteins because VCP is capable of binding an array of oligonucleotide-ubiquitinated proteins or misfolded proteins and can act to drive their polyubiquitination and proteasomal degradation or, alternatively, deubiquitination and release of refolded proteins into the cytoplasm (for review see Halawani and Latterich, 2006). Consistent with a VCP-dependent recruitment of polyubiquitinated proteins to $Wld^S$, $\alpha$-ubiquitin immunoreactivity appears to be enriched with $Wld^S$ in the nucleus in vitro (Laser et al., 2006).

The aforementioned data provide an exciting link between $Wld^S$ and VCP/polyubiquitin, but a requirement for $Wld^S$–VCP interactions or N16 in vivo in protecting severed axons has not been demonstrated. In this study, we have shown that (a) deletion of the VCP-binding domain N16 from $Wld^S$ reduces the axon-protective ability of $Wld^S$ to levels indistinguishable from Nmnat1; (b) tethering N16 to Nmnat1 is sufficient to provide levels of axon protection equivalent to those observed with $Wld^S$; (c) $Wld^S$ associates with *Drosophila* TER94, the fly orthologue of VCP; and (d) knocking down TER94 function in $Wld^S$-expressing neurons suppresses the axon-protective effects of $Wld^S$ to levels indistinguishable from those observed with Nmnat1. Together, these data argue strongly for a role for N16– VCP interactions and VCP function in mediating the ability of $Wld^S$ to protect severed axons.

How do N16–VCP interactions help $Wld^S$ protect axons? A simple model is that N16–VCP interactions function to redistribute nuclear Nmnat1 activity in the cell to a compartment in which its axon-protective effect is maximal. As

discussed in the following section, an interesting possibility is that this redistribution mimics the localization of Nmnat3 (a mitochondrial Nmnat), which appears to protect *Drosophila* axons in vivo at a level indistinguishable from $Wld^S$. Alternatively, N16 may bring Nmnat1 together with VCP-associating proteins that mediate protective effects. For example, perhaps VCP/TER94 binds an unidentified ubiquitinated protein that promotes axon destruction. Because $Wld^S$ redistributes VCP/TER94 to the nucleus, this molecule would in turn be titrated out of axons. This effect, combined with the NAD+ biosynthetic capacity of Nmnat1, which is partially neuroprotective on its own, could combine for robust protection of axons. Alternatively, VCP/TER94 may bring a polyubiquitinated NAD+-sensitive molecule into close proximity with Nmnat1, which in turn promotes robust axon protection. Identified VCP-binding proteins that mediate refolding versus degradative outputs of the VCP complex may not be involved in protecting the axons of $Wld^S$-expressing neurons. We assayed the ability of several VCP-interacting molecules that are essential to promote proteasomal degradation of polyubiquitinated proteins (Ufd2 and Npl4/CG4673) or refolding and cytoplasmic release of misfolded proteins (Ufd1-like and Plap). Knockdown of these molecules in neurons failed to induce widespread spontaneous axon degeneration, suppress axon degeneration after axotomy, or reduce the ability of $Wld^S$ to protect severed axons. Although we cannot exclude the possibility that RNAi knockdown of these molecules was incomplete, these data begin to argue that VCP/TER94 interactions with N16 do not require these molecules for the

execution of Wld$^S$-mediated axon protection. Further work aimed at defining the site of action of Wld$^S$ and identifying molecules interacting with Wld$^S$–VCP/TER94 complexes in vivo will be essential to clarify these issues.

Finally, we note that we have defined the minimal domains essential for Wld$^S$-like levels of neuroprotection as N16::Nmnat1. W18 is not normally a domain found in any mouse protein, being generated by the spontaneous fusion event in Wld$^S$ mice, but a role for this domain in axon protection remained an open possibility. The deletion of amino acids 17–70 of N70 and W18 in the N16::Nmnat1 construct demonstrates that these domains are dispensable for Wld$^S$-mediated axon protection.

**Severed axon autodestruction: the role of nuclear WldS, NAD+, and Nmnat activity**

The strong localization of Wld$^S$ to the nucleus in mice and *Drosophila* provides a compelling argument for a nuclear role for Wld$^S$ in protecting severed axons. Impressively, even expression of high levels of Wld$^S$ in fly neurons with the Gal4/UAS binary system failed to result in detectable axonal localization of Wld$^S$::Myc in vivo. Despite its clear localization to the nucleus, it has remained unclear whether nuclear localization is essential for Wld$^S$ to protect severed axons or whether its presence in the nucleus points to an underlying role in modifying gene expression patterns and thereby axon stability. A role for the NAD+-binding histone deacetylase Sirt1 in Wld$^S$-mediated axon protection seems

increasingly unlikely; previous work has shown that crossing null alleles of Sirt1 into the $Wld^S$ background fails to suppress the ability of $Wld^S$ to protect axons (Wang et al., 2005), and we show that loss of the *Drosophila* orthologue of *Sirt1*, *Sir2*, does not affect the ability of $Wld^S$ to protect severed axons in vivo. Interestingly, we found that tethering $Wld^S$ to the membrane by fusing it with mCD8 completely suppressed the ability of $Wld^S$ to protect severed axons; therefore, the presence of membrane-tethered (likely) monomers of $Wld^S$ is insufficient for any level of axon protection, suggesting that localization or free solubility of $Wld^S$ is important to its function.

Are changes in NAD+ production responsible for the axon-protective effects of $Wld^S$? To further explore the role of NAD+ biosynthesis in suppressing axon autodestruction, we assayed the ability of various *Drosophila* and mammalian NAD+ biosynthetic enzymes to block Wallerian degeneration. Surprisingly, of the four NAD+ biosynthetic molecules we tested, only two, Nmnat1 and Nmnat3, protected severed axons from autodestruction. Nmnat2, which localizes to the cytoplasm in mammalian and *Drosophila* cells, exhibited no protective effect. Likewise, NADS, an NAD+ biosynthetic molecule that generates NAD+ from a different pool of precursors than Nmnat (Rongvaux et al., 2003), failed to protect severed axons from degeneration. In striking contrast, Nmnat3, which localizes to mitochondria in mammals and throughout the cytoplasm in *Drosophila* cells, provided robust protection of axons at levels indistinguishable from those afforded by $Wld^S$ 5 d after injury. These observations raise several

important points: (a) not all NAD+ biosynthetic enzymes are capable of suppressing Wallerian degeneration, which argues that Nmnat1 and Nmnat3 are somehow unique in localization, protein–protein interactions, or enzymatic activity, which results in axon-protective activity; (b) the fact that multiple NAD+ biosynthetic enzymes protect severed axons may indicate that changes in NAD+ are a key factor in suppression of Wallerian degeneration; (c) Nmnat3 is not expected to bind VCP/TER94 but can protect axons at levels equivalent to $Wld^S$; thus, N16–VCP interactions do not appear to be essential for $Wld^S$-like neuroprotection by Nmnat molecules; and (d) Nmnat3 localizes outside the nucleus in *Drosophila* and mammals, arguing that nuclear localization of Nmnat activity is not essential for robust axon protection. Interestingly, it was recently found that Nmnat1 and Nmnat3 can also suppress degeneration induced by rotenone, an activator of mitochondrial oxidative stress (Press and Milbrandt, 2008). This observation, coupled with the robust protection of axons we observe with Nmnat3, may point to a role for $Wld^S$/Nmnat activity in mitochondria for axon protection. In the future, it will be critical to define the site of action of $Wld^S$ and Nmnat3 and determine whether they are protecting axons by similar mechanisms.

The $Wld^S$ mutation protects axons through gain of function mechanisms. Is $Wld^S$ telling us that axons initiate an active axon autodestruction pathway akin to cell death, as has been previously speculated (Coleman and Perry, 2002; Raff et al., 2002), or is $Wld^S$ an aberration that fortuitously blocks Wallerian

degeneration? Based on work in other invertebrates, we favor the notion that axons in mice, *Drosophila*, and many other species indeed initiate an active process of autodestruction after axotomy. A considerable literature exists supporting the ability of severed axons in both vertebrates and invertebrates to exhibit long-term survival (Bittner, 1991). A striking example comes from two species of crickets, Teleogryllus commodus and Gryllus bimaculatus. In these animals, behavioral rhythmicity is governed by a small number of pigment-dispersing factor–positive neurons whose cell bodies reside in the optic lobes. The removal of cell bodies fails to induce degeneration of severed pigment-dispersing factor–positive axons, which can survive for up to 90 d after axotomy, and, impressively, behaviors subject to circadian control remain robust, indicating that severed surviving axonal stumps remain functionally intact for many weeks after axotomy (Stengl, 1995). Why some axons spontaneously degenerate after injury whereas others do not is unknown, but defining the molecular pathways that account for these striking differences in the axonal survival and precisely how $Wld^S$ impinges upon these pathways will be an extremely important future goal to further our understanding of the basic cellular mechanisms by which neurons maintain the functional integrity of axons. Our findings point to the importance of defining molecules downstream of $Wld^S$, perhaps outside the nucleus, that interact with VCP or NAD+, and we suggest that these will be key modulators of Wallerian degeneration.

## Materials and Methods

### *Drosophila* stocks and transgenics

The following stocks were used: OR22a-Gal4 (a gift from J. Carlson, Yale University, New Haven, CT); pUAST-mCD8–GFP, GH146-Gal4, and elav- Gal4 (a gift from T. Lee, University of Massachusetts Medical School, Worcester, MA); Sir24.5 and Sir25.26 (a gift from S. Smolik, Oregon Health and Science University, Portland, Oregon); UAS-Ter94RNAi, UAS-CG4673RNAi, UAS-CG9934RNAi, UAS-PlapRNAi, and UAS-Ufd1–likeRNAi (Vienna *Drosophila* RNAi Center); and UAS-Sir2-RNAi (National Institute of Genetics Stock Center).

pUAST-Wld$^{S}$::myc was created by PCR amplifying a 1.1-kb fragment from pUAST-Wld$^{S}$ and fusing six tandem Myc tags onto the C terminus of Wld$^{S}$ using the primers 5 -GATCAGATCTCAAAACATGGAGGAGCT- GAGCGCTGAC-3 and 5 -ATAATCCGCGGCAGAGTGGAATGGTTGT- GCTTG-3 and subsequently subcloning this fragment into pUAST with BglII and SacII.

pUAST-Nmnat1 was created by subcloning mouse nmnat1 (858 bp from *Mus musculus*) from pHSVPrPUC (a gift from Z. He, Harvard University, Cambridge, MA) into pBluescript-KS with BamHI and EcoRI. It was then subcloned from pBluescript-KS into pUAST with BamHI and XhoI cut sites and was subsequently subcloned into pUAST using BglII and XhoI cut sites. Nmnat1dead was subcloned in the same manner but carries the H24A mutation (a gift from Z. He).

pUAST-Wld$^{S\text{-}dead}$ was created by subcloning Wld$^{S}$ from pUAST (a gift from L. Luo, Stanford University, Stanford, CA) to pBluescript-KS using EcoRI and XbaI, and then a 245-bp C-terminal fragment including the H24A mutation was used to replace the corresponding region of nmnat1. The resulting 1.1-kb fragment (Wld$^{S\text{-}dead}$) was then subcloned from pBluescript-KS into pUAST.

pUAST-Wld$^{S\text{-}\Delta N16}$ was created by cloning amino acids 17–373 of Wld$^{S}$ into pUAST with BglII and XhoI and adding a 5 Met-encoding codon using the primers 5 -GATCAGATCTCAAAACAT- GCTTGCTGGTGGACAGACCTCCC-3 and 5 -TATACTCGAGTCACAGA- GTGGAATGGTTGTGCTTGGCC-3 .

pUAST-N16::nmnat1 was created by subcloning N16 into pUAST and subsequently amplifying an 850-bp fragment of *M. musculus nmnat1* using the primers 5 -GAATGCTAGCATGGACTCATCCAAGAAGACAGA- GGTGG-3 and 5 -TATACTCGAGTCACAGAGTGGAATGGTTGTGCTTG- GCC-3 and then subcloning this fragment into pUAST-N16 with NheI and XhoI.

pUAST-mCD8::Wld$^{S}$ was created by amplifying a 672-bp fragment encoding the extracellular and transmembrane domains of mCD8 from pUAST-mCD8::GFP (Lee and Luo, 2001) and subcloning it into pBluescript-KS using BglII and XbaI. The Wld$^{S}$ open reading frame was then subcloned into this plasmid using engineered BglII and XbaI sites to generate pBluescript-KS–mCD8::Wld$^{S}$. mCD8::Wld$^{S}$ was then subcloned into pUAST using BglII and XbaI to generate pUAST-mCD8::Wld$^{S}$.

pUAST-Nmnat1::myc was created by amplifying Nmnat1 from the pUAST vector

(as described for pUAST-Nmnat1) with the primers 5 -GGC-GAGATCTCAAAACATGGACTCATCCAAGAAGACAGAGGTGG-3 and 5 -TATTAATCCGCGGCAGAGTGGAATGGTTGTGCTTGG-3 and was subsequently cloned into the C-terminal myc pUAST vector with BglII and SacII.

pUAST-Nmnat2 was amplified from mouse cDNA clone BC098007 (Open Biosystems) using the primers 5 -AATTGATTGCGGCCGCAAAA-CATGACCGAGACCACAAAGACC-3 and 5 -AATTGTCTAGACTAGCCC-GAGGCGTTGATGTACAGC-3 and subsequently cloned into pUAST with NotI and XbaI.

pUAST-Nmnat2::myc was amplified from the same clone as Nmnat2 with the primers 5 -AATTGATTGCGGCCGCAAAACATGACC-GAGACCACAAAGACC-3 and 5 -ATTAATATTAGCGGCCGCGTGCCC-GAGGCGTTGATGTACAGCTGACTCTTGAG-3 and subsequently cloned into C-terminal myc pUAST vector with NotI.

pUAST-Nmnat3 was amplified from mouse cDNA clone BC092086 (Open Biosystems) using the primers 5 -ACTTATATGCGGCCGCAAAA-CATGAAGAACCGAATTCCCTGTGGTGC-3 and 5 -AGCAGTCTAGAC-TAGCCAGTCTTTCCTTTCCC-3 and was subsequently cloned into pUAST with NotI and XbaI.

pUAST-Nmnat3::myc was amplified from the same clone as Nmnat3 using the primers 5 -ACTTATATGCGGCCGCAAAACAT-GAAGAACCGAATTCCCTGTGGTGC-3 and 5 -TATAATTAGCGGCCGC-

GTGCCAGTCTTTCCTTTCCCTTTCCAGGAACCGTCATTGATG-3 and was subsequently cloned into C-terminal myc pUAST vector with NotI.

pUAST-NADS was amplified from cDNA clone LD11409 (Berkeley *Drosophila* Genome Project) using the primers 5 -GATCGAATTCCAAAA-CATGGGACGCAAGGTGACCGTAGCGG-3 and 5 -GATCCTCGAGC-TAGACGGGAATACCGGTGCGA-3 and was subsequently cloned into pUAST with EcoRI and XhoI.

pUAST-N16::NADS was amplified from the same clone as NADS with the primers 5 -GATCGAATTCCAAAACATG-GAAGAACTGAGCGCGGATGAAATTCGCCGCCGCCGCCTGGCGCG-CATGGGACGCAAGGTGACCGTAGCGG-3 and 5 -GATCCTCGAGC-TAGACGGGAATACCGGTGCGA-3 and subsequently cloned into pUAST with EcoRI and XhoI.

**Axon injury protocol**

Antennal ablations were performed on animals carrying OR22a-Gal4, UAS-mCD8::GFP, and the indicated constructs. 1 wk after eclosion, both third antennal segments were surgically ablated with tweezers, and the flies were kept at 25°C until dissection (5, 10, 15, 20, or 30 d), as indicated in Figs. 3–7 and Figs. S2 and S3. Uninjured flies were dissected 1 wk after eclosion unless denoted in legends as age matched. Adult heads were fixed with 4% formaldehyde (Sigma-Aldrich) in 1× PBS and 0.1% Triton X-100 (PTx; Sigma-

Aldrich) for 20 min before dissection and washed five times with PTx. Dissected brains were subsequently fixed in 4% formaldehyde in PTx for 10 min and washed five times with PTx and three times with 1× PBS/0.1% Triton X-100/1% BSA (PBT; Thermo Fisher Scientific). Brains were rocked for 30 min in PBT at room temperature, and primary antibodies were added in PBT and rocked overnight at 4°C. Brains were washed 10 times over 1.5 h with PBT, and secondary antibodies were added in PBT. Brains were rocked for 3 h in secondary antibody at room temperature and subsequently washed 10 times over 1.5 h with PBT. Brains were stored at 4°C in antifade reagent (Bio-Rad Laboratories). In the case of animals expressing GFP, no antibodies were used to enhance the GFP signal.

**Immunolabeling, confocal microscopy, and quantification of axon protection**

Standard methods were used for dissection, fixation, and antibody labeling of the *Drosophila* adult brain (MacDonald et al., 2006). Primary antibodies were used at the following dilutions: 1:1,000 for immunolabeling of mouse tissue with α-Myc (9E10; Covance), 1:500 for Western blot analysis of α-VCP (BD), and 1:250 for rabbit α-Nmnat1 (a gift from M. Cole- man, Babraham Institute, Cambridge, England, UK). Secondary antibodies (Cy3; Jackson ImmunoResearch Laboratories) for immunolabeling of tissues were used at 1:200. Specimens were mounted in a 1:1 mixture of antifade reagent and 75% glycerol. Confocal z stacks

of antennal lobes and S2 cells were collected on a confocal microscope (Axioskop2 LSM 5 Pascal; Carl Zeiss, Inc.) with a Plan Apochromat 63× NA 1.4 objective lens (Carl Zeiss, Inc.), which was also equipped with a transmitted light detector used for acquisition of differential interference contrast images of S2 cells. All confocal microscopy was performed at room temperature (21°C) using acquisition software (LSM 5 Pascal; Carl Zeiss, Inc.). Confocal images were compressed with ImageJ software (National Institutes of Health), and intact GFP+ axons were counted individually at the indicated time points. At least two lines (in most cases three to four) were assayed for each construct, results among lines carrying the same construct were indistinguishable from one another, and data were subsequently pooled.

**Immunoprecipitations from S2 cell extracts**

*Drosophila* S2 cells were counted and plated at 1 × 106 cells/ml, incubated overnight at 30°C, transfected with pUAST-Wld$^{S}$::myc and pAC- Gal4 according to the instructions in the Transfectene kit (QIAGEN), and incubated for 48 h. Protein G–Sepharose fast-flow beads (GE Healthcare) were washed in extraction buffer (150 mM NaCl, 1% Igepal CA630, 50 mM Tris, pH 7.5, and 1× EDTA-free complete protease inhibitor) and bound with $\alpha$-Myc antibody for 3 h at 4°C. Transfected and untransfected cells were isolated and centrifuged at 3,000 rpm for 5 min at 4°C. Cells were resuspended in extraction buffer and placed in ethanol/dry ice bath for 5 min, thawed in a cold ice bath, homogenized, and

centrifuged at 11,000 rpm for 10 min at 4°C. A fraction of the supernatant was reserved as input, and remaining samples were precleared with equilibrated protein G– Sepharose beads for 2 h at 4°C, added to α-myc–conjugated protein G– Sepharose beads, and incubated at 4°C overnight. The samples were then centrifuged at 2,000 rpm for 1 min. A portion of the supernatant was reserved as the flow-through sample, and the remaining supernatant was discarded; beads were washed five times with extraction buffer, and bound protein was eluted from beads with SDS-PAGE loading buffer.

**S2 cell transfection and immunolabeling**

*Drosophila* S2 cells were counted and plated at 1 × 106 cells/ml, incubated overnight at 30°C, and transfected with pUAST-Wld$^{S}$::myc and pAC-Gal4 according to the instructions in the Transfectene kit. Cells were then fixed in PEM (Pipes, EGTA, and MgCl2 buffer)/4% formaldehyde and washed with PBT. Primary antibody (α-myc) was added to the cells at 1:1,000, cells were washed, and secondary α-mouse anti- bodies were added at 1:200. Immunolabeling was then viewed with confocal microscopy.

**Online supplemental material**

Fig. S1 shows how the quantification of intact axons was counted. Fig. S2 compares the various transgenes of each construct to show that expression level variations did not affect the protection level. Fig. S3 shows RNAi experiments of

proteins thought to complex with VCP/Ter94, none of which appear to have a role in $Wld^S$-mediated protection. Online supplemental material is available at http://www.jcb.org/cgi/content/full/ jcb.200808042/DC1.

We wish to thank L. Conforti and M. Coleman for helpful discussions and sharing unpublished data. We thank Z. He and L. Luo for DNA constructs and J. Carlson and S. Smolik for *Drosophila* stocks. We thank all members of the Freeman laboratory and U. Homberg for helpful discussions.

This work was supported by National Institutes of Health (grants NS053538 and NS059991 to M.R. Freeman), the Christopher and Dana Reeves Foundation, and the Worcester Foundation for Biomedical Research. M.R. Freeman is an Alfred P. Sloan Research Fellow.

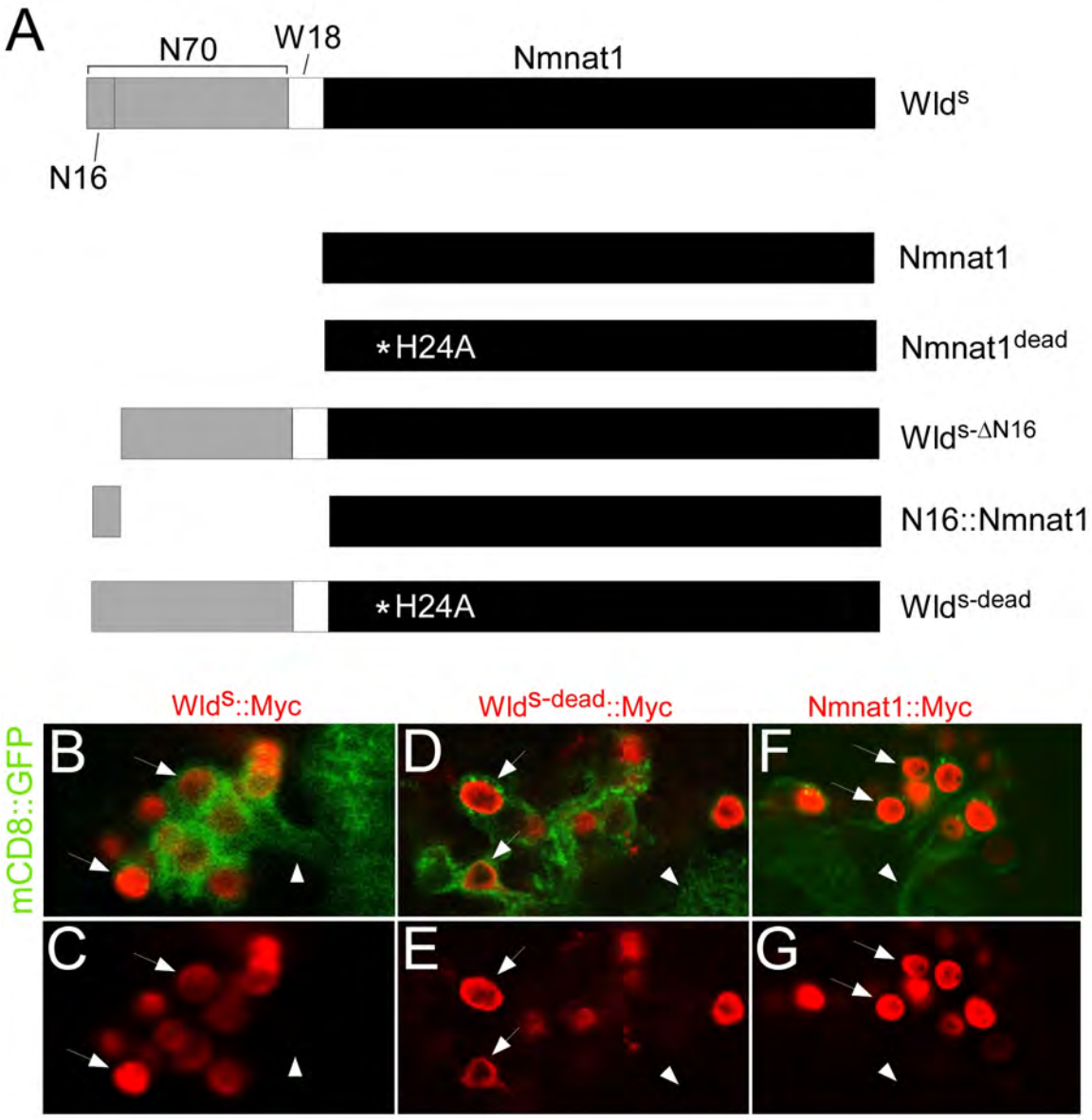
A
N70
W18
Nmnat1
N16
Wld^S
Nmnat1
*H24A
Nmnat1^dead
Wld^S-ΔN16
N16::Nmnat1
*H24A
Wld^S-dead
Wld^S::Myc
Wld^S-dead::Myc
Nmnat1::Myc
mCD8::GFP
B
D
F
C
E
G

**Figure 2-1**

**Figure 2-1. Constructs used to dissect Wld$^S$ functional domains and localization in *Drosophila* neurons.** (A) All constructs were generated from mouse Wld$^S$, which contains N70, the first 16 amino acids (N16) that encode the VCP-binding site, W18, an 18–amino acid linker, and full-length Nmnat1. Nmnat1$^{dead}$ harbors an H24A mutation; Wld$^{S\text{-}\Delta N16}$ lacks the N16 domain; N16::Nmnat1 is N16 tethered to the N terminus of Nmnat1; Wld$^{S\text{-}dead}$ is full-length Wld$^S$ with an H24A mutation in Nmnat1. See Materials and methods for details. (B–G) UAS-Wld$^S$::Myc (B and C), UAS-Wld$^{S\text{-}dead}$::Myc (D and E), and UAS-Nmnat1::myc (F and G) were expressed with UAS-mCD8::GFP in projection neurons using GH146-Gal4. The arrows point to nuclei, and the arrowheads point to axons. Bar, 12.14 µm.

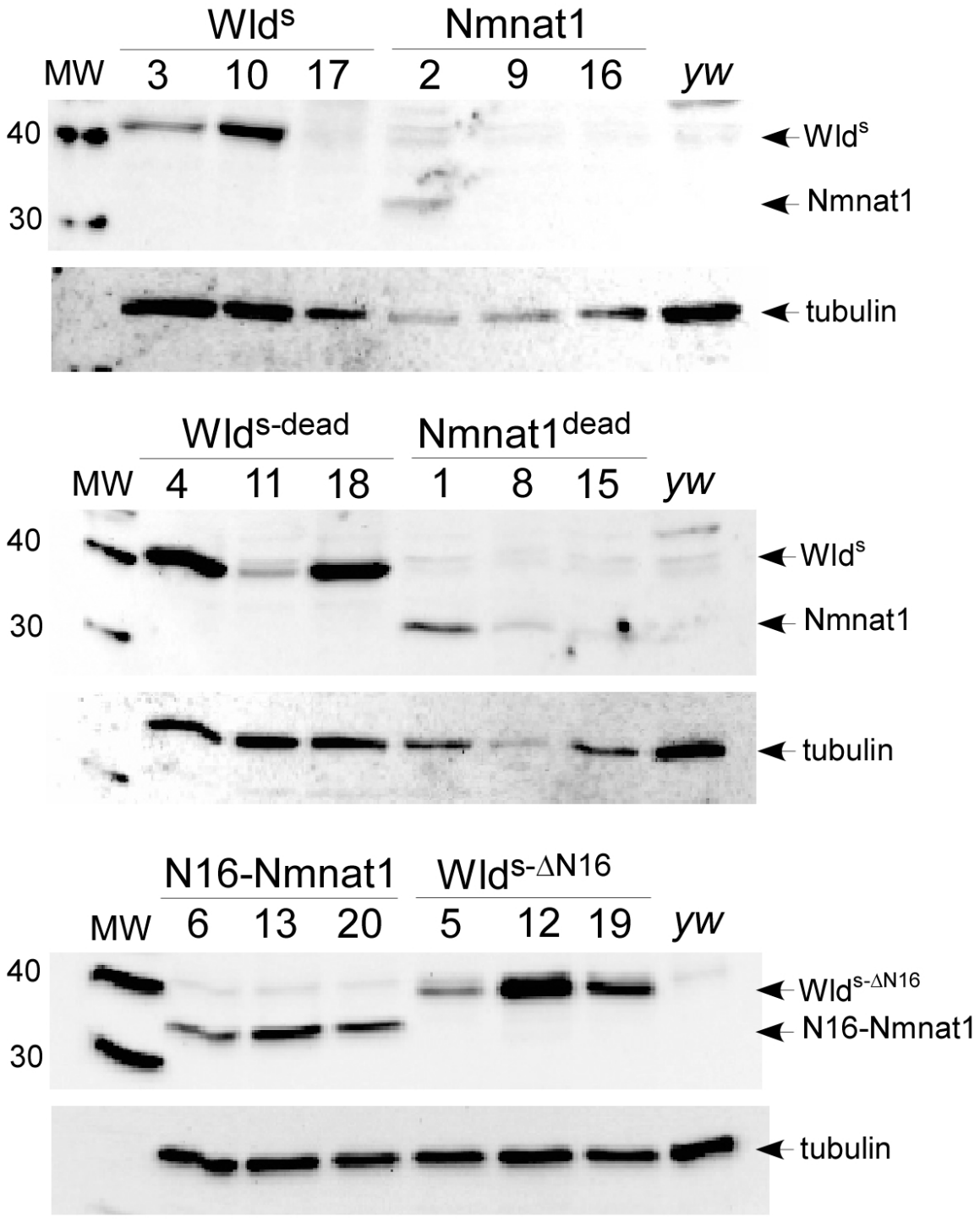
Wld^s
Nmnat1
MW
3
10
17
2
9
16
yw
40
30
Wld^s
Nmnat1
tubulin
Wld^s-dead
Nmnat1^dead
MW
4
11
18
1
8
15
yw
40
30
Wld^s
Nmnat1
tubulin
N16-Nmnat1
Wld^s-ΔN16
MW
6
13
20
5
12
19
yw
40
30
Wld^s-ΔN16
N16-Nmnat1
tubulin

**Figure 2-2**

**Figure 2-2. Wld$^S$ variant proteins are stably expressed in *Drosophila* neurons.** Three independent UAS-driven transgene insertion lines for each Wld$^S$ variant molecule were crossed to elav-Gal4, and protein extracts from heads were assayed for expression using $\alpha$-Nmnat1 antibodies. Multiple lines for each construct were found to express detectable levels of protein. The expression of each of these molecules in ORNs with OR22a-Gal4 did not lead to expression of proteins at levels detectable by Western blot analysis (not depicted). Molecular masses are shown in kilodaltons. MW, molecular weight.

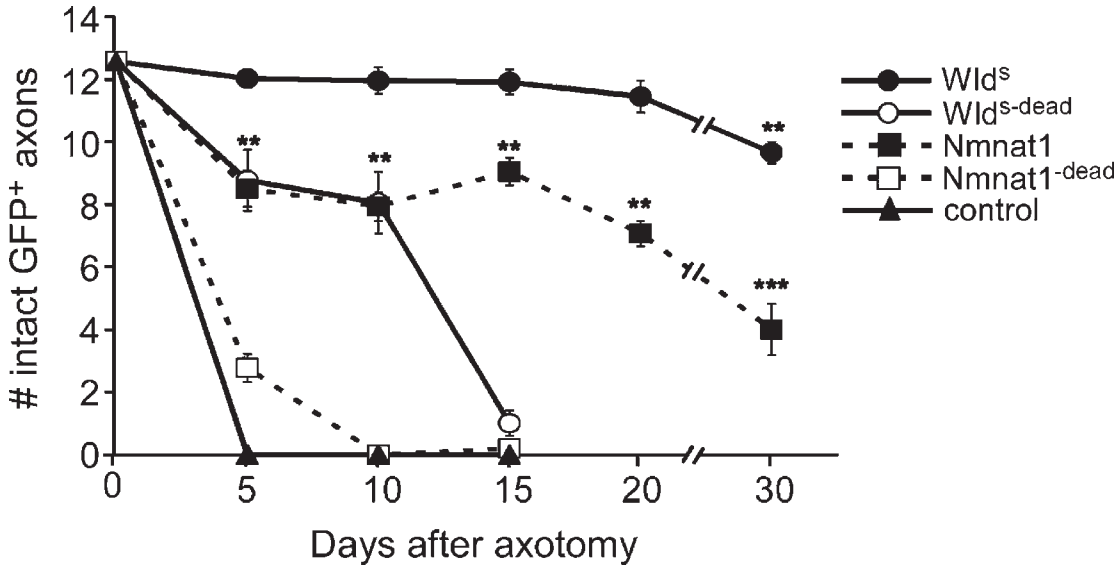
14
12
10
8
6
4
2
0
# intact GFP+ axons
0
5
10
15
20
30
Days after axotomy
**
**
**
**
**
***
Wlds
Wlds-dead
Nmnat1
Nmnat1-dead
control

**Figure 2-3**

**Figure 2-3. Wld$^S$ requires N70 and Nmnat1 biosynthetic activity for maximal protection of severed axons in vivo.** UAS-regulated versions of Wld$^S$ variants were expressed in OR22a+ ORNs with OR22a-Gal4, axons were severed, and the number of remaining intact GFP+ axons was scored at the time points indicated. Two to four independent insertion lines were tested for each UAS-regulated Wld$^S$ variant molecule (Fig. S1, available at http://www.jcb.org/cgi/content/full/jcb.200808042/DC1); n ≥ 10 for individual lines; data were subsequently pooled and are presented here. For Nmnat1, **, $P < 0.01$ and ***, $P < 0.001$ (Nmnat1 vs. Wld$^S$ at corresponding time points). For Wld$^S$, **, $P < 0.01$ (day 0 vs. day 30). Error bars represent SEM.

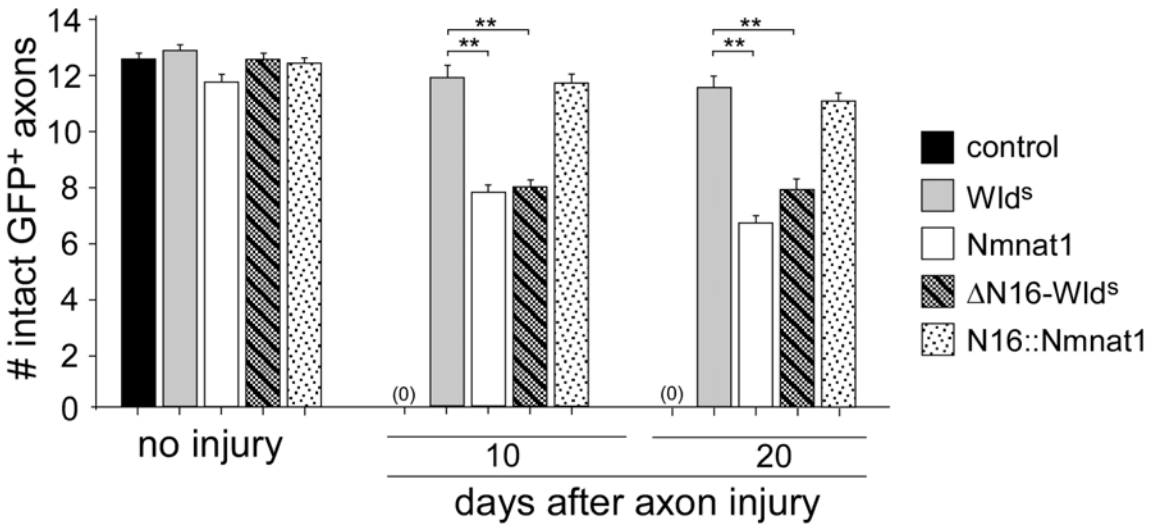
14
12
10
8
6
4
2
0
# intact GFP+ axons
**
**
**
**
(0)
(0)
no injury
10
20
days after axon injury
control
Wlds
Nmnat1
ΔN16-Wlds
N16::Nmnat1

**Figure 2-4**

**Figure 2-4. N16 is the key domain in the N terminus of Wld$^S$ that is essential for Wld$^S$-like axon protection.** Wld$^S$, Nmnat1, ΔN16-WldS, and N16::Nmnat1 were expressed in ORNs using OR22a-Gal4, axons were severed, and the number of remaining intact GFP+ severed axons were scored at the time points indicated. n ≥ 10 for all genotypes; **, P < 0.01. Error bars represent SEM.

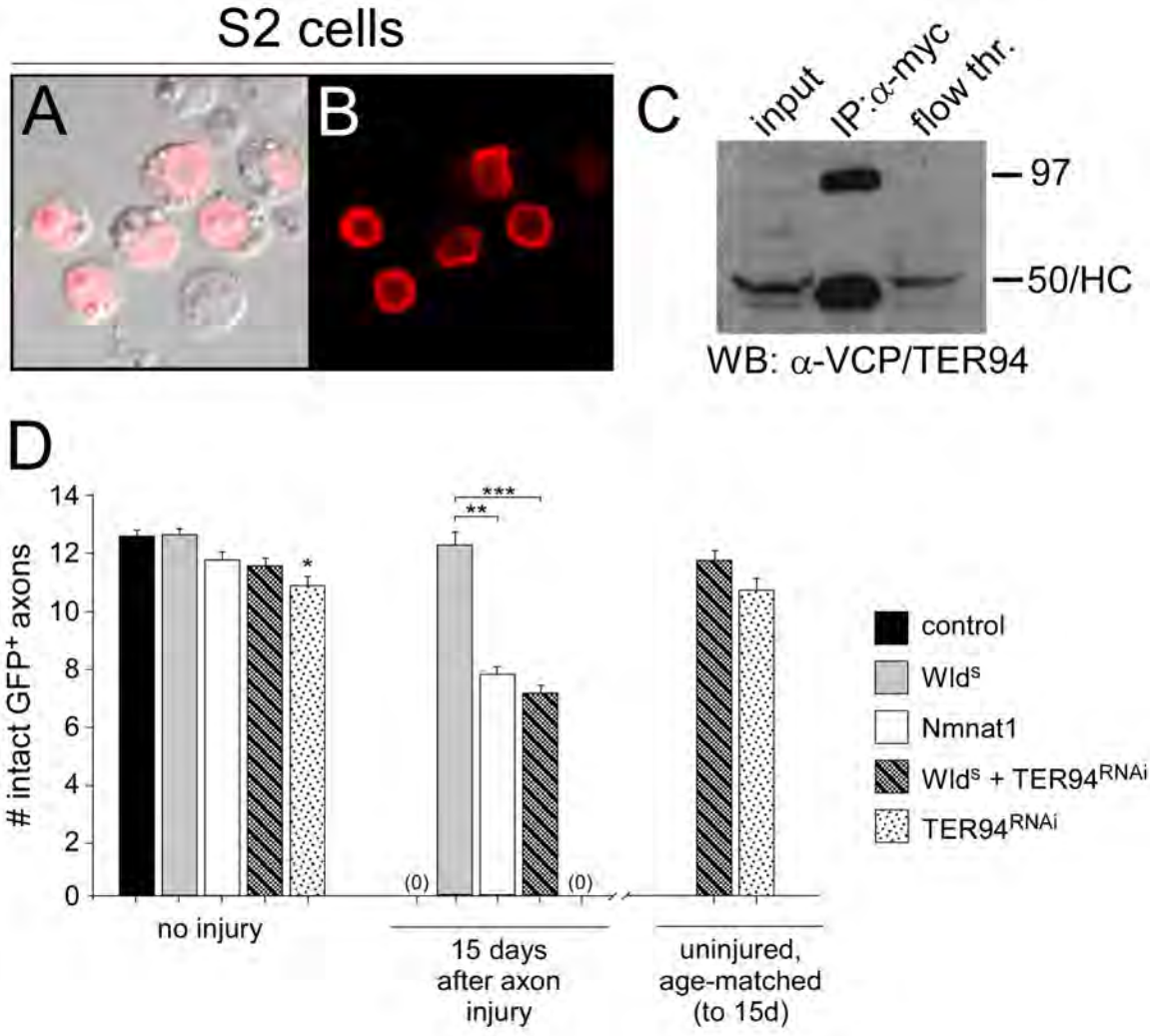
S2 cells
A
B
C
input
IP: α-myc
flow thr.
97
50/HC
WB: α-VCP/TER94
D
# intact GFP+ axons
14
12
10
8
6
4
2
0
*
**
***
(0)
(0)
no injury
15 days after axon injury
uninjured, age-matched (to 15d)
control
Wld^S
Nmnat1
Wld^S + TER94^RNAi
TER94^RNAi

**Figure 2-5**

**Figure 2-5. $Wld^S$ localizes to the nucleus in *Drosophila* S2 cells and associates with TER94, and TER94 is essential for $Wld^S$-like levels of axon protection.** (A and B) S2 cells were transfected with $Wld^S$::myc and stained with $\alpha$-Myc antibodies, and $\alpha$-Myc immunoreactivity localized to the nucleus. (C) Immunoprecipitation (IP) from $Wld^S$::Myc–transfected cell lysates with $\alpha$-Myc antibodies led to the purification of a 97-kD isoform of Ter94. HC, heavy chain from $\alpha$-Myc IgG; WB, Western blot. (D) UAS-Ter94RNAi was driven in OR22a+ ORNs in the presence or absence of $Wld^S$. n ≥ 10 for all genotypes; *, $P < 0.05$; **, $P < 0.01$; ***, $P < 0.001$. Error bars represent SEM. Bar, 13.56 µm.

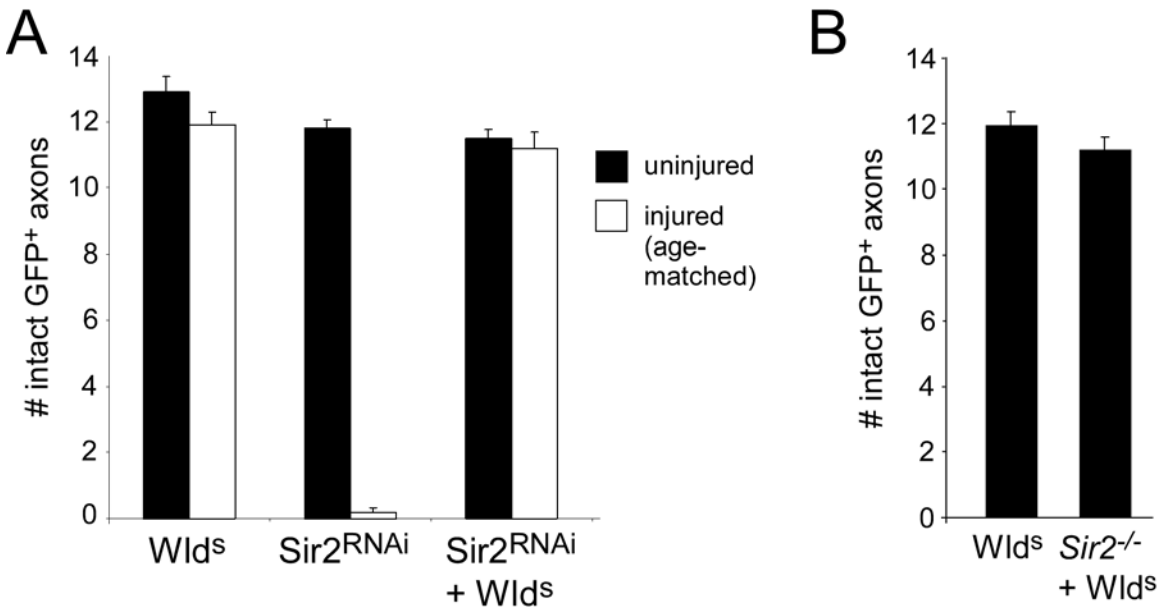
A
# intact GFP+ axons
14
12
10
8
6
4
2
0
uninjured
injured (age-matched)
Wlds
Sir2RNAi
Sir2RNAi + Wlds
B
# intact GFP+ axons
14
12
10
8
6
4
2
0
Wlds
Sir2-/- + Wlds

**Figure 2-6**

**Figure 2-6. Sir2 is not required for $Wld^S$-mediated protection of severed axons.** (A) UAS-$Sir2^{RNAi}$ was driven in OR22a+ ORNs with OR22a-Gal4 in the presence or absence of $Wld^S$, and axons were assayed 15 d after injury. (B) The requirements for Sir2 in $Wld^S$-mediated axon protection were assayed 15 d after injury in $Wld^S$-expressing axons and $Wld^S$ axons that lacked sir2 ($sir2^{4.5}/sir2^{5.26}$). WldS, n = 10; Sir2 -/- + $Wld^S$, n = 6. Error bars represent SEM.

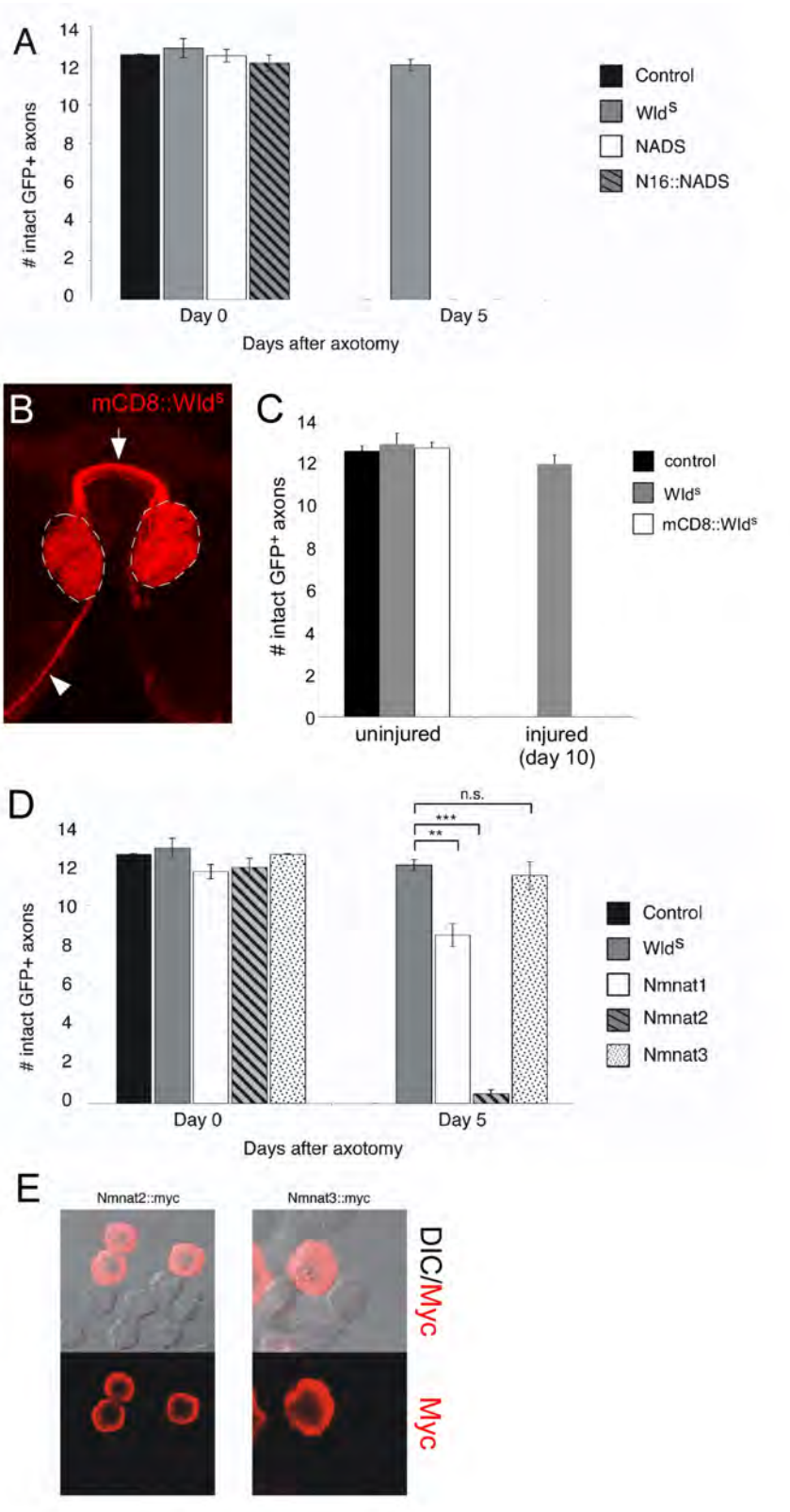
A
# intact GFP+ axons
14
12
10
8
6
4
2
0
Day 0
Day 5
Days after axotomy
Control
Wld^S
NADS
N16::NADS
B
mCD8::Wld^S
C
# intact GFP+ axons
uninjured
injured (day 10)
control
Wld^S
mCD8::Wld^S
D
n.s.
***
**
# intact GFP+ axons
Day 0
Day 5
Days after axotomy
Control
Wld^S
Nmnat1
Nmnat2
Nmnat3
E
Nmnat2::myc
Nmnat3::myc
DIC/Myc
Myc

## Figure 2-7

**Figure 2-7. Axon-protective function of NAD+- producing enzymes is specific to Nmnat1 and -3, and Nmnat3 protects as well as Wld$^S$.** (A) NADS and N16::NADS were expressed in ORNs using OR22a-Gal4, and axons were severed and analyzed for protection 5 d after axotomy. (B) Localization of mCD8::Wld$^S$ was assayed using $\alpha$-CD8 antibodies, and expression of mCD8::Wld$^S$ was driven in ORNs using the OR22a-Gal4 driver. Axons are indicated projecting to glomeruli (arrowhead) and across the midline (arrow), and OR22a+ ORN- innervated glomeruli are shown with dashed lines. (C) Membrane-tethered Wld$^S$ (mCD8::Wld$^S$) was assayed for axon-protective function 10 d after axotomy. n ≥ 10 for all genotypes. (D) Nmnat2 and -3 were driven by OR22a-Gal4 in ORNs to assay for protective function 5 d after axotomy. n ≥ 10 for all genotypes; **, P < 0.01; ***, P < 0.001. (E) S2 cells were transfected with Nmnat2::myc and Nmnat3::myc and stained with $\alpha$-myc. In both cases, $\alpha$-myc immunoreactivity was localized to the cytoplasm but not the nucleus. DIC, differential interference contrast. Error bars represent SEM. Bars: (B) 27.47 µm; (E) 14.71 µm.

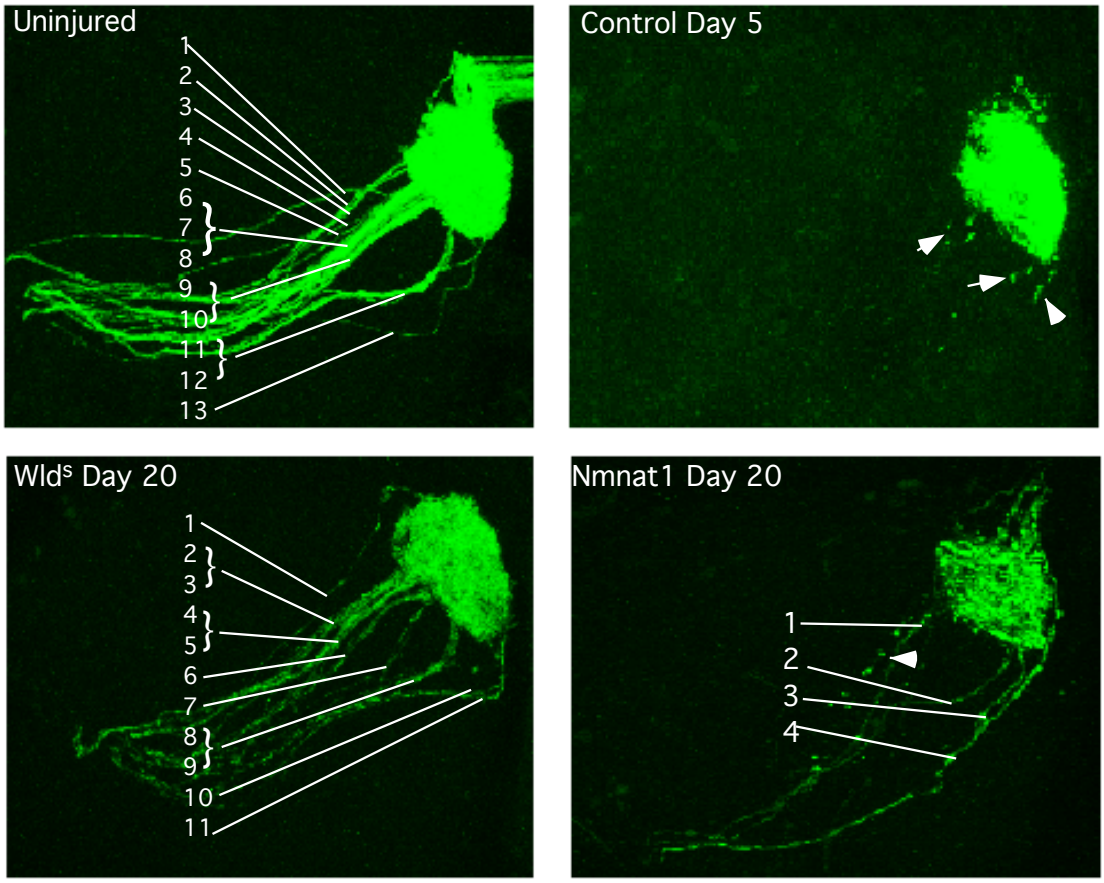
Uninjured
1
2
3
4
5
6
7
8
9
10
11
12
13
Control Day 5
Wld$^{s}$ Day 20
1
2
3
4
5
6
7
8
9
10
11
Nmnat1 Day 20
1
2
3
4

**Figure 2-S1**

**Figure 2-S1. Representative images of UAS-22a-Gal4, mcd8::GFP axons and glomeruli expressing either UAS-Wld$^S$, UAS-Nmnat1, or neither.** The uninjured lobe has 13 intact axons. By day 5 all control axons are degenerated (arrows). UAS-Wld$^S$-expressing lobe shows 11 intact axons 20 days after injury. In contrast, the UAS-Nmnat1-expressing lobe only shows 4 intact axons at this timepoint (arrow points to a fragmented axon).

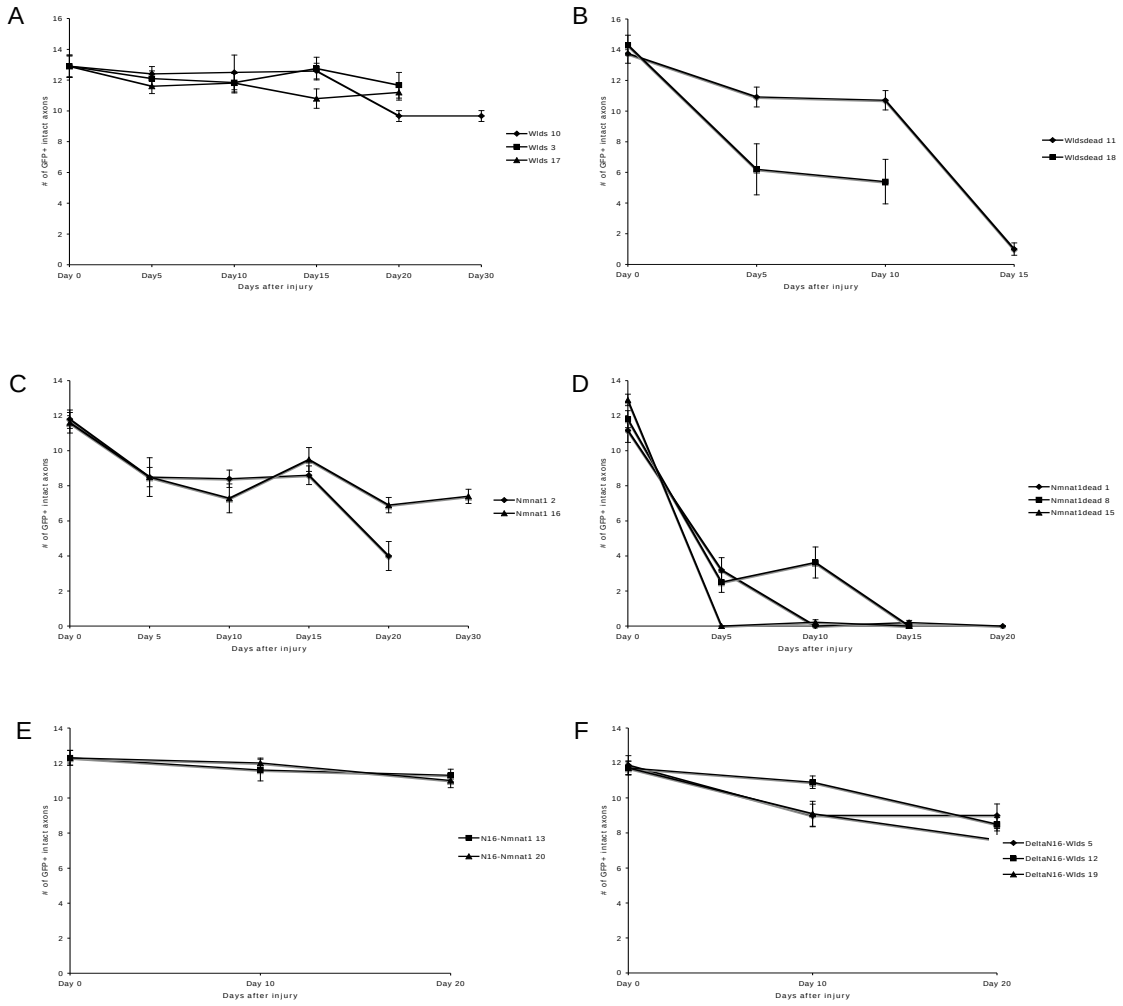
A
B
C
D
E
F
# of GFP+ intact axons
Days after injury
Day 0
Day5
Day10
Day15
Day20
Day30
Day 10
Day 15
Day 5
Wlds 10
Wlds 3
Wlds 17
Wldsdead 11
Wldsdead 18
Nmnat1 2
Nmnat1 16
Nmnat1dead 1
Nmnat1dead 8
Nmnat1dead 15
N16-Nmnat1 13
N16-Nmnat1 20
DeltaN16-Wlds 5
DeltaN16-Wlds 12
DeltaN16-Wlds 19

**Figure 2-S2**

**Figure 2-S2. Axonal protection afforded by WldS variant transgenes.** (A–F) UAS-regulated transgenes were driven in ORNs with OR22a-Gal4, axons were severed by antennal ablation, and the number of intact GFP+ axons was scored at the time points indicated. Transgene insertion line identifiers are indicated, and two to four insertion lines were assayed for each transgene. Note that not all x axes are the same among different lines (days after injury) because constructs that lost efficacy were not assayed at later time points. UAS-$Wld^{S}$ (A), UAS-$Wld^{S\text{-}dead}$ (B), UAS-Nmnat1 (C), UAS-$Nmnat1^{dead}$ (D), UAS- N16::Nmnat1 (E), and UAS-$Wld^{S_{\Delta}N16}$ (F) are shown. n > 10 for all genotypes for all time points. Error bars represent SEM.

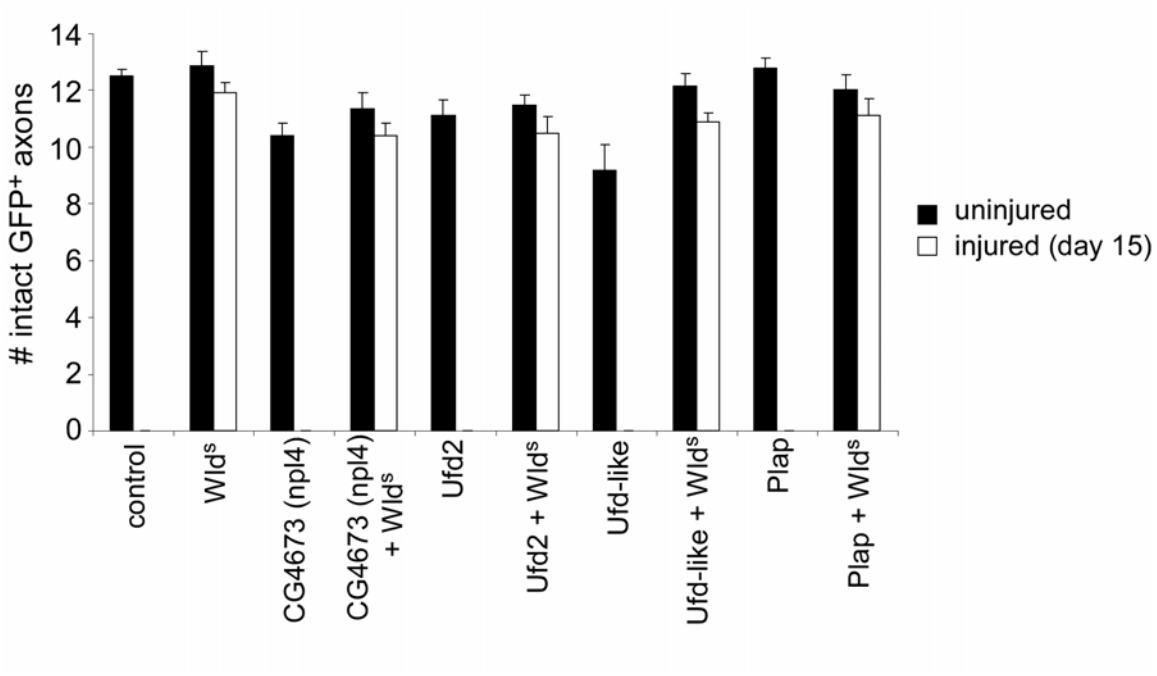
# intact GFP+ axons
14
12
10
8
6
4
2
0
control
Wlds
CG4673 (npl4)
CG4673 (npl4) + Wlds
Ufd2
Ufd2 + Wlds
Ufd-like
Ufd-like + Wlds
Plap
Plap + Wlds
uninjured
injured (day 15)

**Figure 2-S3**

**Figure 2-S3. RNAi knockdown of VCP/TER94 interacting molecules does not suppress axon degeneration or the ability of $Wld^S$ to protect severed axons.** The ability of Npl4, Ufd2, Ufd1-like, and Plap to modulate severed axon autodestruction or the neuroprotective effects of $Wld^S$ were assayed by expressing UAS-regulated RNAi transgenes targeting each with OR22a-Gal4, severing axons, and assaying protection 15 d after transection. RNAi knockdown of these genes had no effect on Wallerian degeneration, and the ability of $Wld^S$ to suppress axon autodestruction was not suppressed. n>10 for all genotypes; *, $P < 0.05$. Error bars represent SEM.

# Chapter III:

# $Wld^S$ requires increased mitochondrial motility and $Ca^{2+}$-buffering efficiency for severed axon protection

## Introduction

Neurodegenerative diseases have many different causes, however, the death of neurons is a common result. Recently, it has been found that many neurodegenerative diseases share mitochondria dysfunction as either a common byproduct or possibly even cause of disease (Celsi et al., 2009; Chen and Chan, 2009). It is of particular interest that $Wld^S$, a highly neuroprotective molecule, has been found to be localized to mitochondria (Yahata et al., 2009). When expressed in neurons, $Wld^S$ can cell-autonomously protect axons from physical injury, neurotoxicity, and some neurodegenerative diseases (Coleman, 2005). $Wld^S$ is a novel fusion protein consisting of: (1) the first 70 amino acids of Ube4b, an E4 ubiquitin ligase, (2) an 18 amino acid linker sequence and (3) full-length Nmnat1, a key enzyme in $NAD^+$ synthesis (Mack et al., 2001). Only the first 16 amino acids of Ube4b and full-length Nmnat1 are required for $Wld^S$-like protection (Avery et al., 2009). Although we know that N16 is required for $Wld^S$-like protection, its function is axon protection is unknown. It is possible that N16 serves to relocalize Nmnat1 to the mitochondria as Nmnat3, a mitochondrial protein, can protect as well as $Wld^S$ in both mammals and *Drosophila*. Other studies that have mislocalized Nmnat1 outside of the nucleus find its neuroprotective ability increases greatly (Avery et al., 2009; Yahata et al., 2009; Sasaki et al., 2009; Beirowski et al., 2009; Babetto et al., 2010).

Studying the mitochondria of $Wld^S$-expressing animals is of utmost importance to see if there are detectable biological changes which could account

for the differences seen in Wallerian degeneration between a wild-type and $Wld^S$ animal. In this study, we examine mitochondria as the potential site of $Wld^S$ action. We extend our finding that Nmnat3 can protect axons after axotomy as well as $Wld^S$ to 50 days after injury. We also report the first biological changes seen in neurons expressing $Wld^S$, and find key changes in mitochondrial biology: $Wld^S$ causes the number of stationary mitochondria to decrease; and the $Wld^S$ decreases the amount of $Ca^{2+}$ in the cell after axotomy. We find that suppressing the increase in mitochondrial movement can suppress $Wld^S$ protection of axons after injury. Finally, we propose that $Wld^S$, functioning through the mitochondria to increase $Ca^{2+}$ buffering, suppresses a degeneration signal after axotomy.

## Results

We have previously shown that expression of mouse Nmnat3, a reported mitochondrial protein, in *Drosophila* olfactory receptor neurons (ORNs) was able to protect severed axon from degeneration as well as $Wld^S$ 5 days after injury (Avery et al., 2009). It was also recently found that $Wld^S$ localizes to mitochondria, and that expression of Nmnat3 can protect severed axons in the mouse as well (Yahata et al., 2009 and T. Gillingwater, personal communication). This led us to further investigate the protective ability of Nmnat3.

First we wanted to confirm the localization of mouse Nmnat3 to mitochondria in *Drosophila*. UAS-Nmnat3::myc was driven by the olfactory receptor neuron (ORN) driver, 22aGal4, along with UAS-mito-GFP to label the

mitochondria. Nmnat3::myc was found to colocalized with mito-GFP in *Drosophila* ORNs (**Fig 3-1A**). Next, we wanted to extend the timepoints of our Wallerian degeneration assay to compare the protective ability $Wld^S$ and Nmnat3. To do so, UAS-Nmnat3 was driven by ORN-22aGal4. We found that Nmnat3 protective ability is similar to $Wld^S$ at 10, 20, and 50 days after ablation, with a strong protection at days 10 and 20 and a significant decrease in protection at day 50 (**Fig 3-1B**). It should be noted that two other Nmnat molecules, Nmnat1, which localizes to the nucleus of *Drosophila* neurons, and Nmnat2, which localizes to the cytoplasm of ORNs, is unable to protect severed axons from degeneration (**Fig 3-S1** and Avery et al., 2009). Thus, mitochondrial localization of Nmnat activity is critical for full axon protection from severed axon auto destruction.

Recent reports have stated that expression of Nmnat2 can protect axons *in vitro* from axotomy-induced degeneration (Yan et al., 2009 and Gilley and Coleman, 2010). However, this protection is much weaker than that of $Wld^S$, and is thought to be due to the short half-life of Nmnat2. To test the possibility that Nmnat2 is degraded at 5 post-axotomy and thereby accounting for the lack of protection seen in *Drosophila* ORNs, we drove UAS-Nmnat2::myc along with UAS-$Wld^S$ so that the axon would still be intact 5 days after axotomy. In all cases, Nmnat2::myc was present in the axon 5 days after axotomy (data not shown). Therefore, a shortened half-life cannot account for the lack of

protection, but instead, we postulate Nmnat2 is not in the right location for protection, the mitochondria.

The mitochondrial localization of both Nmnat3 and $Wld^S$ along with their impressive protection against Wallerian degeneration, led us to look at the mitochondria themselves for changes in size, number, and movement. For this, we turned to 3$^{rd}$ instar larval fillet preparations for live imaging. We created 5 minute movies using UAS-CD2::RFP or UAS-mCherry driven by Tdc2Gal4 to visualize the axons, and UAS-mito-GFP to label the mitochondria (**Fig 3-2A**). We then quantified the number, size, speed, direction, and movement of mitochondria (**Fig 3-2B, 3-S2,** and data not shown). Surprisingly, the only change observed in the mitochondria expressing $Wld^S$ was that the number of stationary mitochondria decreased greatly (**Fig 3-2C**). Figure 3-2B shows representative kymographs of control and $Wld^S$; the vertical lines represent stationary mitochondria, whereas diagonal lines are moving mitochondria. We also quantified the mitochondria movement when driving other molecules found to be neuroprotective in axon degeneration in our previous work (Avery et al., 2009). Strikingly, the number of stationary mitochondria correlated indirectly with the degree of protection against axon degeneration at 5 days after injury (**Fig 3-2B**); weakly protective molecules slightly decrease the number of stationary mitochondria, whereas highly protective molecules greatly decrease the number of stationary mitochondria. Thus, more mitochondria are moving in the presence of Nmnat-containing neuroprotective molecules. This observation is the first

biological change that has been seen *in vivo* in a $Wld^S$-expressing neuron prior to injury, and may be indicative of $Wld^S$ function.

To test if the increase in motile mitochondria is necessary for axon protection of $Wld^S$, we assayed mutants that would inhibit mitochondrial movement. Miro, an atypical Rho GTPase, is responsible for both antero- and retro- grade movement of mitochondria (Russo et al., 2009). It localizes to the outer membrane of mitochondria and either binds to the kinesin via an adaptor protein, Milton, or binds the kinesin heavy chain itself (Guo et al., 2005; Glater et al, 2006, MacAskill et al., 2009). While mutations in *Miro* render the axon almost completely devoid of mitochondria, heterozygous alleles as well as overexpression of Miro in *Drosophila* neurons causes a reduction in the number of moving mitochondria (Guo et al., 2005; Russo et al., 2009). Allelic loss of *Miro* does not affect the number of mitochondria in an axon, and the overexpression of Miro reduces the number of mitochondria present in axons; however this reduction of mitochondria does not have an effect on ORN viability (Russo et al., 2009; **Fig 3-S3**). To test whether Miro alleles and overexpression are able to suppress the decrease in stationary mitochondria seen in $Wld^S$-expressing flies, we again looked at open filet preparations of 3$^{rd}$ instar wandering larvae. Five minute movies were made of Tdc2Gal4 driving UAS-CD2-RFP or mCherry to mark the axons, UAS-mito-GFP to label the mitochondria, UAS-$Wld^S$, and one of the following: $Miro^{SD32}$/+, $Miro^{SD26}$/+, or UAS-myc::Miro/+. We also looked at the alleles and overexpression line without $Wld^S$. As previously reported, the

heterozygous alleles and overexpression line were able to increase the amount of stationary mitochondria (**Fig 3-S4**, Russo et al., 2009). Surprisingly, Miro alleles and overexpression line suppressed the decrease in stationary mitochondria seen in $Wld^S$-expressing (**Fig 3-3A**). Moreover, the number of stationary mitochondria in $Wld^S$-expressing flies with either Miro allele actually increased compared to wild-type (**Fig 3-3A**).

To test if suppressing the movement of mitochondria had an effect on axon protection, we again used our model of Wallerian degeneration in the adult ORNs. We drove UAS-mCD8::GFP with OR-22a-Gal4, along with $Wld^S$ and either of the *Miro* alleles or UAS-myc::Miro. Allelic loss of *Miro* and UAS-myc-Miro on their own do not affect uninjured axon integrity or degeneration after injury (**Fig. 3-S4**). $Miro^{SD32}$/+, $Miro^{SD26}$/+, and UAS-myc::Miro/+ also do not have an effect on uninjured axons expressing $Wld^S$ (**Fig 3-3B**). However, Miro heterozygous alleles and overexpression have a striking dominant suppression of $Wld^S$ protection at 5, 15, and 30 days after ablation (**Fig 3-3B**). It is also important to note that the axons surviving at those times points appear to have morphological defects, such as the presence of blebs, which are not seen in $Wld^S$ alone expressing flies after injury (**Fig 3-3C**). Therefore, an increase in mitochondrial movement is necessary for $Wld^S$ to protect severed axons after axotomy.

What does the increase in moving mitochondria mean? Mitochondria are known to be major $Ca^{2+}$ sinks in the cell. In order to buffer the $Ca^{2+}$, they need to

be able to sense changes in cytoplasmic $Ca^{2+}$. Miro has 2 EF hand domains that are known to be able to bind $Ca^{2+}$ (MacAskill et al., 2009). When Miro binds to $Ca^{2+}$, the mitochondria either dissociate from the kinesin or bind the motor domain of the kinesin directly, making it detach from microtubules (MacAskill et al., 2009; Wang and Schwarz, 2009). The effect in either case is the freezing of mitochondria at local pools of high $Ca^{2+}$. Such a high $Ca^{2+}$ sensitivity enables mitochondria to get to and remain in areas where an increase in energy production and $Ca^{2+}$ buffering is needed. Once the $Ca^{2+}$ has been buffered, the mitochondria can bind kinesin again, and move along the axon to find the next area of increased activity (Saotome et al., 2008; Wang and Schwarz, 2009; MacAskill et al., 2009). A simple model is that either $Wld^{S}$-expressing mitochondria are unable to sense $Ca^{2+}$ and thereby move more, or they can uptake the $Ca^{2+}$ more quickly and therefore, spend most of the time moving in the cell. Since we are interested in how $Wld^{S}$ functions to suppress axon degeneration, we decided to look at differences in the $Ca^{2+}$ wave after axon injury. To test whether $Wld^{S}$-expressing flies are either unable to sense $Ca^{2+}$ or can quench the signal faster, we looked at $Ca^{2+}$ waves after injury in wild-type and $Wld^{S}$-expressing open filet preparations of 3$^{rd}$ instar larvae. We used Tdc2-Gal4 driving UAS-MCD8::Cherry to visualize the axons and UAS-gCaMP3 to visualize the $Ca^{2+}$ wave after injury. A baseline movie of the gCaMP3 signal was taken before ablation, then a $cherry^{+}$ axon was laser-ablated, and the movie continued until well after the gCaMP3 signal abated. In wild-type animals, there

was a sharp peak of $Ca^{2+}$ directly after injury, which slowly comes back to baseline. Similar $Ca^{2+}$ curves have been seen in other species both *in vivo* and *in vitro* after axotomy, indicating that the $Ca^{2+}$ wave after injury is a conserved event (Ziv and Spira, 1995; George et al., 1995; Knoferle et al., 2010). Interestingly, in both distal and proximal segments, the peak gCaMP3 signal after injury in $Wld^S$-expressing flies was less intense and was cleared faster (**Fig 3-4A and 3-S5**). We also find that Nmnat3 has the same effect on injury-induced $Ca^{2+}$ as $Wld^S$, and that weakly neuroprotective molecules have an intermediate effect on the injury-induced $Ca^{2+}$ wave (**Fig 3-4B**). Once again, this correlates the axon protective function with the ability to dampen injury-induced $Ca^{2+}$ signal. If $Wld^S$-expressing flies were unable to sense $Ca^{2+}$, they would most likely have a longer-lasting signal than wild-type. As this is not the case, we hypothesize that $Wld^S$ mitochondria are able to uptake and buffer the $Ca^{2+}$ wave after injury more quickly than in wild-type.

## Conclusions

In this study, we show that Nmnat3 can protect at levels similar to that of $Wld^S$ in *Drosophila* olfactory neurons. At 10 and 20 days after axotomy, the number of GFP+ intact axons is similar to uninjured flies, and the protective ability of $Wld^S$ and Nmnat3 decreases similarly at 50 days after axotomy. We also show that Nmnat3, a mammalian protein, localizes to the mitochondria of *Drosophila* ORNs. With previous findings of $Wld^S$ in the mitochondria (Yahata et al., 2009; T.Gillingwater, personal communication), as well as our finding that the

protective phenotypes of $Wld^S$ and Nmnat3 are very similar, we propose that the site of action is in the mitochondria.

Through our study of mitochondria, we have described the first cell biological change seen in $Wld^S$-expressing axons prior to injury, showed that this change in mitochondrial movement is essential to $Wld^S$ protective function, and hypothesize that an increase in $Ca^{2+}$ buffering after injury is the mechanism of action. $Ca^{2+}$ buffering is known to be influenced by a negative mitochondrial membrane potential (Babcock et al., 1997), and increasing the negative potential increases mitochondrial $Ca^{2+}$ uptake capacity (Tanaka et al., 2009). The membrane potential is maintained through the pumping of protons out of the mitochondria and the activity of the electron transport chain. $Wld^S$ could aid in increasing the membrane potential by increasing $NAD^+$ inside the mitochondria, which could feed into the electron transport chain, making more ATP and decreasing the membrane potential. Interestingly, Yahata et al., 2009, recently published that Nmnat3 and $Wld^S$-expressing mitochondria show an increase in ATP production, supporting our model. Certainly, biochemical studies of $Ca^{2+}$ buffering capacity in $Wld^S$-expressing mitochondria would be key to solidify the model. An increase in $Ca^{2+}$ buffering and therefore a decrease of $Ca^{2+}$ in the cytoplasm would account for both the increase in mitochondrial movement and the decrease in $Ca^{2+}$ signal after axotomy. High $Ca^{2+}$ waves are responsible for apoptosis and necrosis, suggesting a common initiation signal for many types of death, although signaling cascades that follow can vary greatly (Celsi et al.,

2009). It becomes more likely then, that a $Ca^{2+}$ wave could be the initiating event in the Wallerian degeneration cascade. More importantly, mitochondria seem to be important when it comes to $Ca^{2+}$ overload; in apoptosis, factors are released due to high $Ca^{2+}$ in the mitochondria that lead to death, and in necrosis, the permeability transition pore is opened, most likely in response to high $Ca^{2+}$, again leading to cell death (Celsi et al., 2009). What remains downstream in Wallerian degeneration is still a mystery, but the fact that $Wld^S$ localizes to mitochondria and has an extremely important function there seems to point to the initiation factor being associated with mitochondria.

It is quite interesting that the initial peak of $Ca^{2+}$ after axotomy is reduced in $Wld^S$- and Nmnat3- expressing flies. One possibility is the ability of $Wld^S$-expressing mitochondria to uptake calcium is so quick, we simply do not see the highest peak on the microscope in between the time it takes to ablate the axon and set up the recording of the image. It is also possible that $Ca^{2+}$ is unable to enter the cell as efficiently in $Wld^S$- or Nmnat3- expressing flies. A marker for mitochondrial $Ca^{2+}$, such as mito-gCaMP3 would be helpful to address this question.

The mechanism of $Wld^S$ in mitochondria may precede deficits in mitochondria seen in certain disease models, such as Alzheimer's and Parkinson's, which would explain why $Wld^S$ has been ineffective in protecting these disease models. In these disease states, the electron transport chain is defective, leading to a compromised mitochondrial membrane potential, which

would presumably affect the calcium uptake capacity of those mitochondria. Since our model places $Wld^S$ upstream of the electron transport chain and mitochondrial potential, any deficits downstream would not allow $Wld^S$ to protect the axons. Thus, it is imperative that the role of mitochondria in neurodegeneration be fully elucidated to find potential therapeutic targets.

## Materials and Methods

### Injury protocol

Flies were anesthetized on $CO_2$ pads and their 3$^{rd}$ antennal segments removed. *Drosophila* were kept at 25°C for 5, 10, 15, 20, or 50 days post ablation. All uninjured flies were dissected one week post-eclosion unless noted as age matched.

### *Drosophila* stocks and transgenics

The following stocks were used: OR22a-Gal4 (B.Dickson, Vienna), pUAST-mcd8::GFP, p{UAS-mitoGFP.AP}2, p{UAS-mitoGFP.AP}3, p{Tdc2-Gal4.C}2, p{UAS-CD2-RFP} Bloomington), Miro$^{SD32}$/TM6, Miro$^{SD26}$/TM6 (Guo et al., 2005), p(UAS-Myc-Miro) (K. Zinsmaier, University of Arizona), UAS-gCaMP3 (L. Looger, JFRC), pUAST-Wld$^{S}$, pUAST-N16::Nmnat1, pUAST-Nmnat1, pUAST-Nmnat1$^{dead}$, pUAST-Wld$^{S\text{-}dead}$, pUAST-Nmnat3, pUAST-Nmnat2, and pUAST-ΔN16-Wld$^{S}$ (Avery et al., 2009)

*pUAST-Nmnat2::myc* was made by PCR amplifying amino acids 1-306 of mouse Nmnat2, cDNA clone BC098007 (Openbiosystems), with NotI sites at both ends, excluding the stop codon at 3' end. It was the cloned into pUAST-myc vector and checked for correct orientation.

*pUAST-Nmnat3::myc* was made by PCR amplifying amino acids 1-244 of mouse Nmnat3, cDNA clone BC092086 (Openbiosystems), with NotI sites at both ends, excluding the stop codon at 3' end. It was then cloned into the pUAST-myc vector and checked for correct orientation.

*pUAST-mcd8::mcherry* was made by PCR amplifying 726bp of mCherry PCR from pKR5-mCherry. EcoRI site was added to the 5', and XbaI added to 3' after stop codon and then it was cloned into the EcoRI/Xba site of pUAST.

**Immunolabeling and Confocal Microscopy**

Standard methods were used for dissection, fixation, and antibody labeling of the *Drosophila* adult brain (Voshall et al., 2000). Primary antibodies were used at the following dilutions: mouse anti-myc (9E10, Covance Innovative Antibodies) 1:1000. Secondary antibodies (Jackson Immunoresearch) were used at 1:200. Images were then mounted in Vectashield, and viewed with a Zeiss Imager M10 spinning disc confocal.

**Quantification**

For adult brain axotomy, Z stacks were compressed with ImageJ software, and intact GFP+ axons were counted. For live imaging, 4D movies were compressed to 2D along the Z axis. The number of GFP+ mitochondria were counted in the first frame of the movie, and stationary mitochondria were counted throughout

the timeframe. For gCaMP3 quantification, 4D movies were compressed to 2D, and average intensity from an uncut nerve was subtracted from the average intensity of a cut nerve (either distal or proximal) at each timepoint. We then subtracted from this number the average intensity from the 5 minute baseline movie.

**Live Imaging**

3rd instar wandering larvae were fillet-prepped in HL6 (MacLeod et, al., 2002), and glued to the live imaging chamber with Surgi-Lock 2oc (Healthypets.com). Starting near the ventral nerve cord, 3 sections of the nerves were imaged in the larva for 5 minutes each.

**Kymographs**

2D movies were aligned with Image J plugin “align slice”. The Image J plugin “multiple kymograph” was then used to create the kymograph.

**Laser ablation**

3rd instar wandering larvae were fillet-prepped in HL6 (MacLeod et al., 2002) and glued to a perfusion chamber (Warner Instruments, RC-30) with Surgi-Lock 2oc (Healthypets.com). A baseline movie ran for 5 minutes, then a small section of 1 nerve was laser ablated with a 435 wavelength laser at 70% power. Movies

were then collected every 5 minutes afterwards for a total of 20 minutes. Larvae were washed with HL6 in between each 5 minute movie.

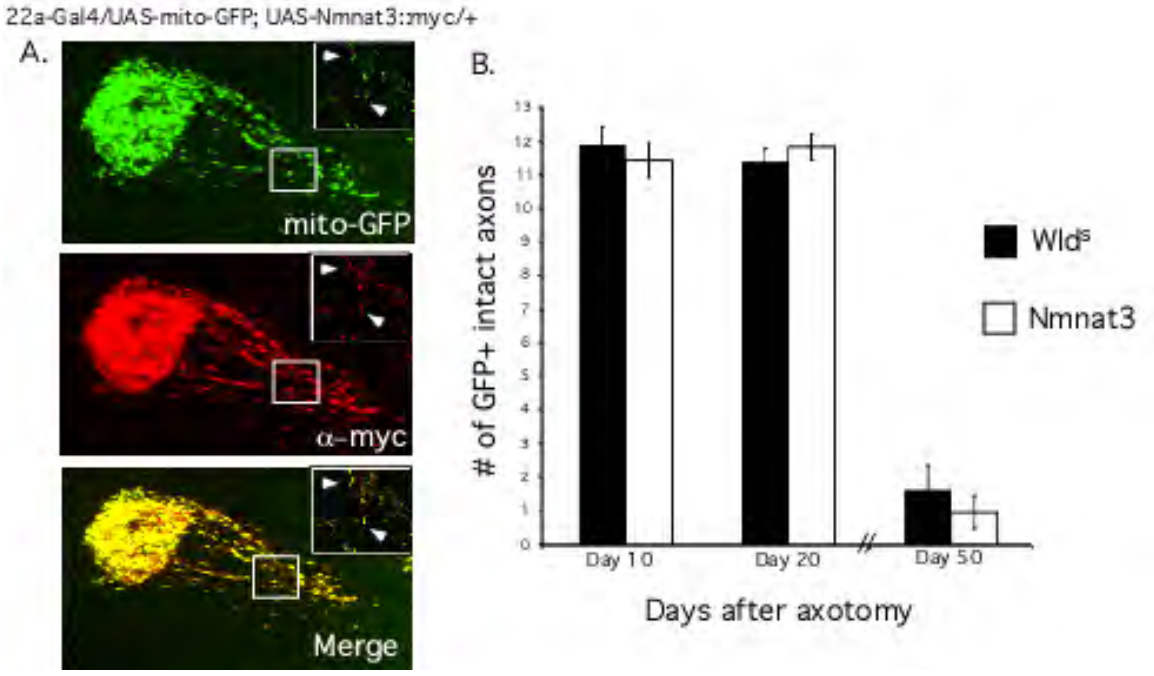
22a-Gal4/UAS-mito-GFP; UAS-Nmnat3:myc/+
A.
mito-GFP
α-myc
Merge
B.
# of GFP+ intact axons
Wld^S
Nmnat3
Day 10
Day 20
Day 50
Days after axotomy

**Fig 3-1**

**Fig 3-1. Nmnat3 is mitochondrial in *Drosophila* ORNs and protects as well as Wld$^S$.** (A) Mitochondrial GFP (top panel) colocalizes with Nmnat3 myc tag staining (middle panel). The merge is shown in the bottom panel. (B) At 10, 20, and 50 days post axotomy, the level of axon protection afforded by Nmnat3 is no different from that of Wld$^S$.

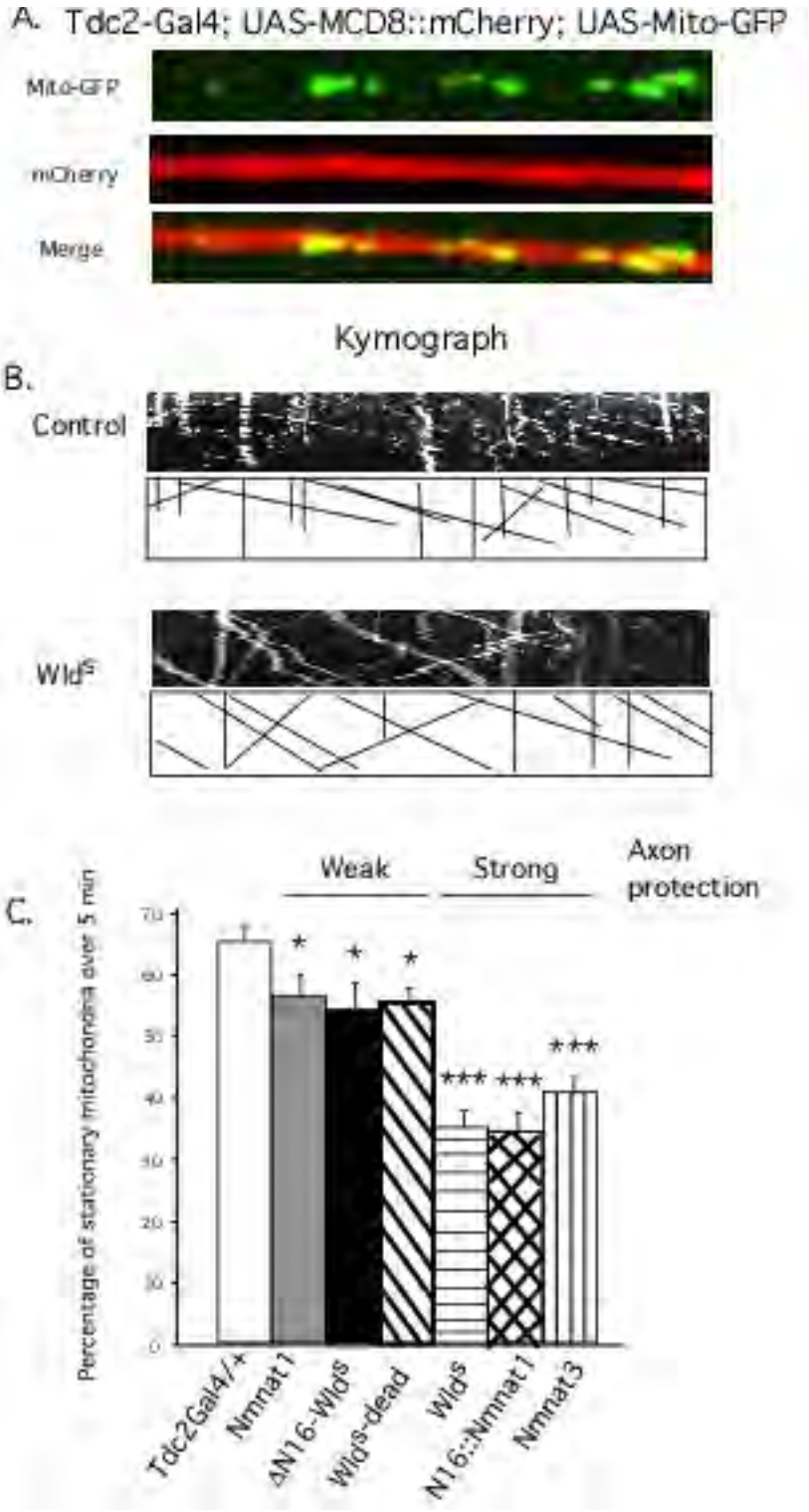
A. Tdc2-Gal4; UAS-MCD8::mCherry; UAS-Mito-GFP
Mito-GFP
mCherry
Merge
Kymograph
B.
Control
Wld^S
C.
Weak
Strong
Axon protection
Percentage of stationary mitochondria over 5 min
Tdc2Gal4/+
Nmnat1
ΔN16-Wld^S
Wld^S-dead
Wld^S
N16::Nmnat1
Nmnat3

**Fig. 3-2**

**Fig. 3-2. $Wld^S$ and other strongly neuroprotective molecules show a decrease in stationary mitochondria.** (A) Representative confocal image of mitochondria (mito-GFP, top panel) and $mCherry^+$ motorneurons (middle panel) used for imaging of mitochondrial movement. (B) Representative kymographs from control and $Wld^S$-expressing larvae. Straight lines denote stationary mitochondria; diagonal lines denote moving mitochondria. (C) Quantification of the number of stationary mitochondria per nerve per 5 minute period ($n>10$, * $p<.05$, *** $p<.001$).

Figure 3

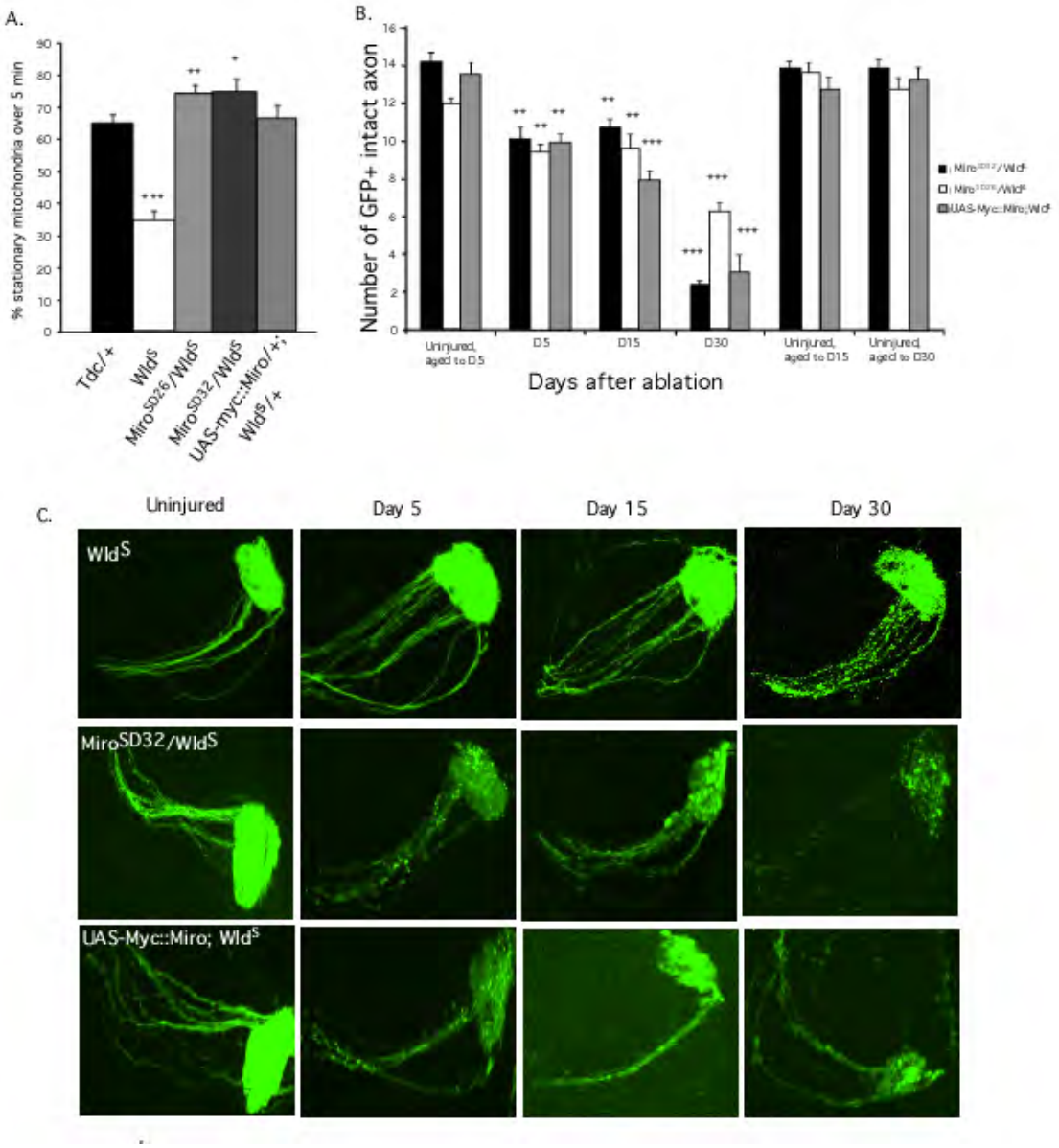


**Fig. 3-3**

**Fig. 3-3. Suppression of mitochondria movement suppresses $Wld^S$ protection of severed axons.** (A) Quantification of mitochondria movement in heterozygous *miro* alleles expressing $Wld^S$. *Miro* heterozygotes with $Wld^S$ and overexpression of Miro increase the number of stationary mitochondria in 3rd instar larvae compared to both control and $Wld^S$-expressing mitochondria. (B) Quantification of the effect of *miro* heterozygous alleles or overexpression of Miro on $Wld^S$-mediated axon protection. *Miro* reduces the efficacy of $Wld^S$ severed axon protection. (C) Representative images of $Wld^S$, $Miro^{SD32}/Wld^S$, and UAS-myc-Miro at 0, 5, 15, and 30 days post axotomy. Note the appearance of blebs on the axons with the *Miro* allele and the overall decrease in axon integrity compared to $Wld^S$ alone. ($n>10$, $^{**}p<.01$, $^{***}p<.001$)

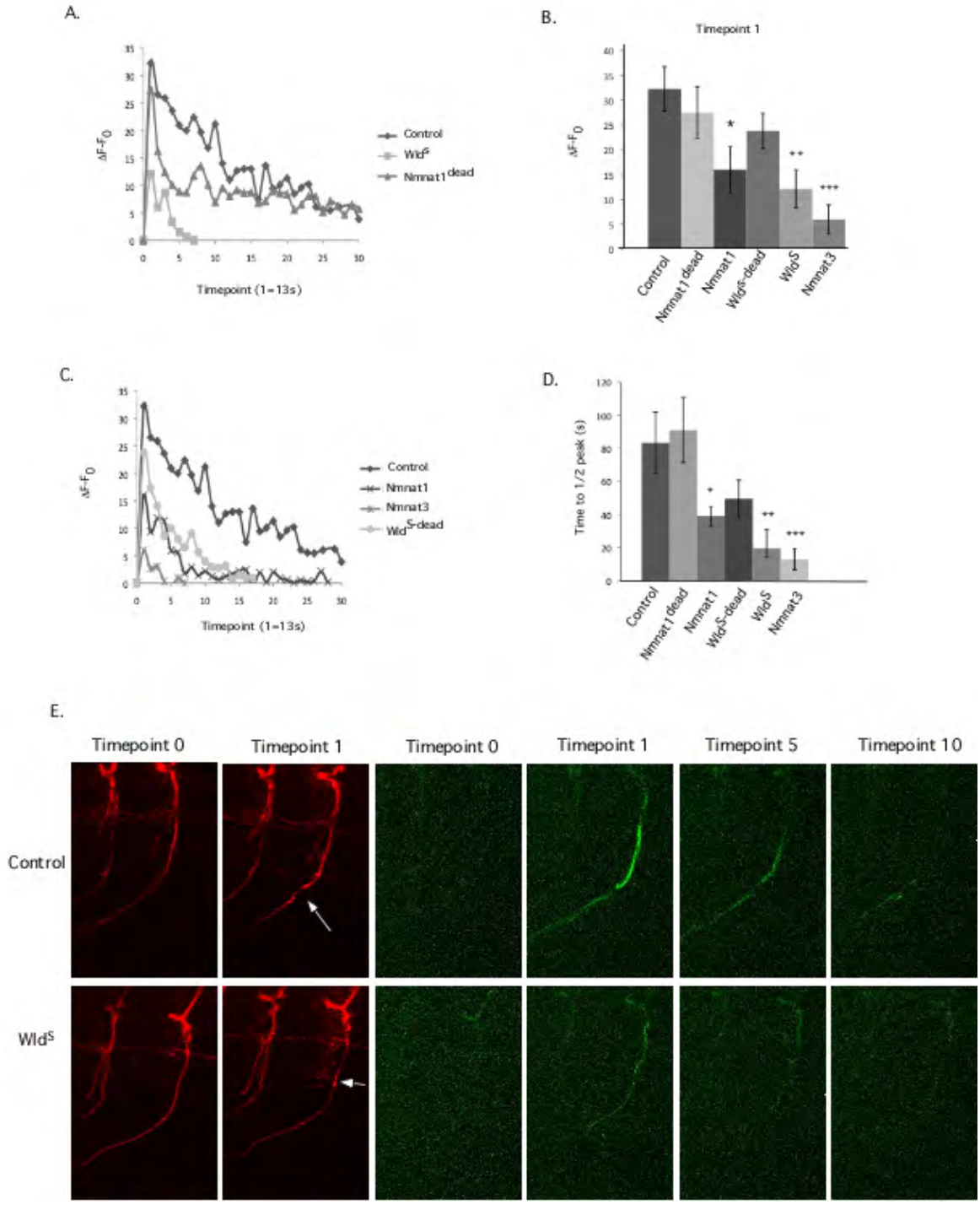
A.
ΔF-F0
Timepoint (1=13s)
Control
Wld^S
Nmnat1 dead
B.
Timepoint 1
ΔF-F0
Control
Nmnat1 dead
Nmnat1
Wld^S-dead
Wld^S
Nmnat3
C.
ΔF-F0
Timepoint (1=13s)
Control
Nmnat1
Nmnat3
Wld^S-dead
D.
Time to 1/2 peak (s)
Control
Nmnat1 dead
Nmnat1
Wld^S-dead
Wld^S
Nmnat3
E.
Timepoint 0
Timepoint 1
Timepoint 0
Timepoint 1
Timepoint 5
Timepoint 10
Control
Wld^S

**Fig. 3-4**

**Fig. 3-4. $Wld^S$ and Nmnat3 decrease the intensity and duration of gCaMP3 signal post-axotomy.** (A) Time course of gCaMP3 signal in the distal portion of the axon post axotomy in control, $Wld^S$-, and $Nmnat1^{dead}$-expressing 3$^{rd}$ instar larvae. (B) gCaMP3 signal intensity peak after laser-induced axotomy. (C) Time course of gCaMP3 signal in the distal portion of the axon post axotomy in control, Nmnat1-, Nmnat3-, and $Wld^{S\text{-}dead}$-expressing 3$^{rd}$ instar larvae. (D) Recovery time of the gCaMP3 signal to ½ its peak. (n=5, *p<.05, **p<.01, ***p<.001)

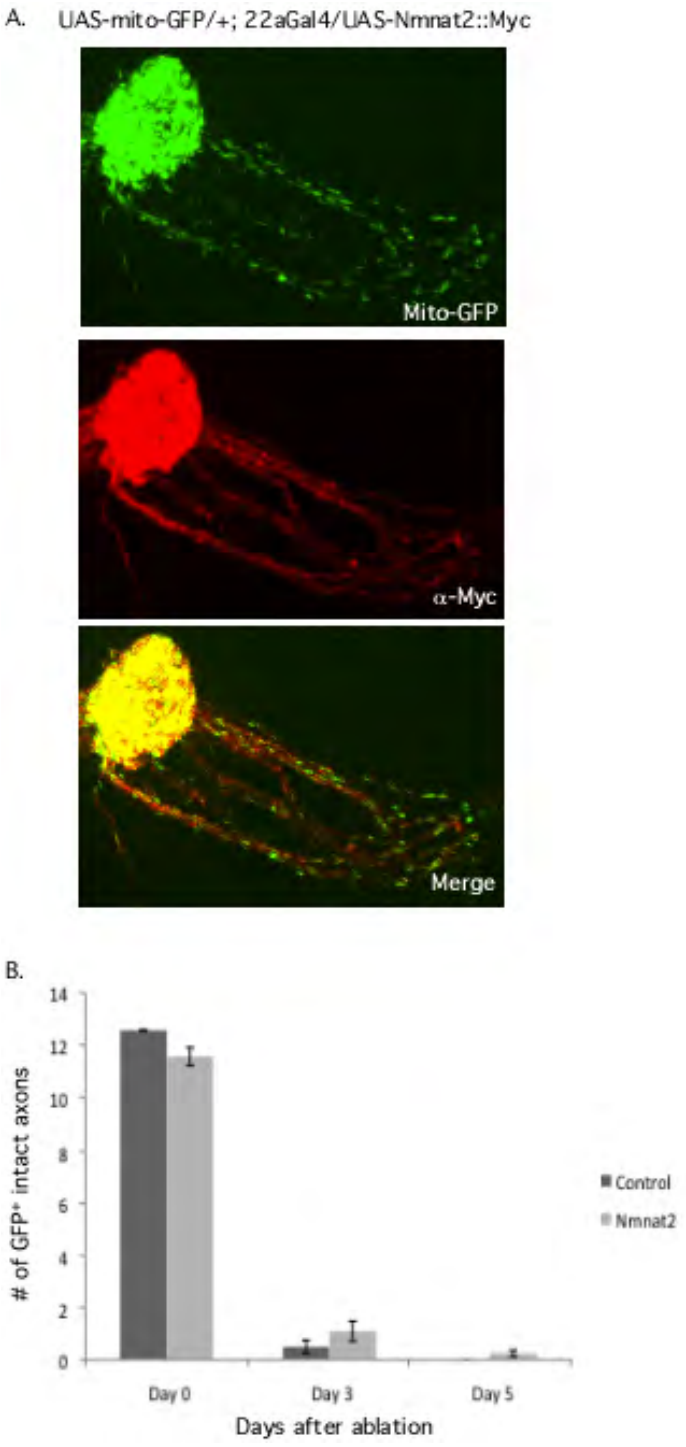
A.
UAS-mito-GFP/+; 22aGal4/UAS-Nmnat2::Myc
Mito-GFP
α-Myc
Merge
B.
# of GFP+ intact axons
14
12
10
8
6
4
2
0
Day 0
Day 3
Day 5
Days after ablation
Control
Nmnat2

**Fig. 3-S1**

**Fig. 3-S1. Nmnat2 localizes to the cytoplasm of *Drosophila* ORNs and cannot protect severed ORNs.** (A) Mito-GFP (top panel) does not colocalize with the Nmnat2 myc antibody stain (middle panel. Bottom panel shows merge. (B) Quantification of control and Nmnat2 $GFP^{+}$ intact axons at 0, 3, and 5 days after injury.

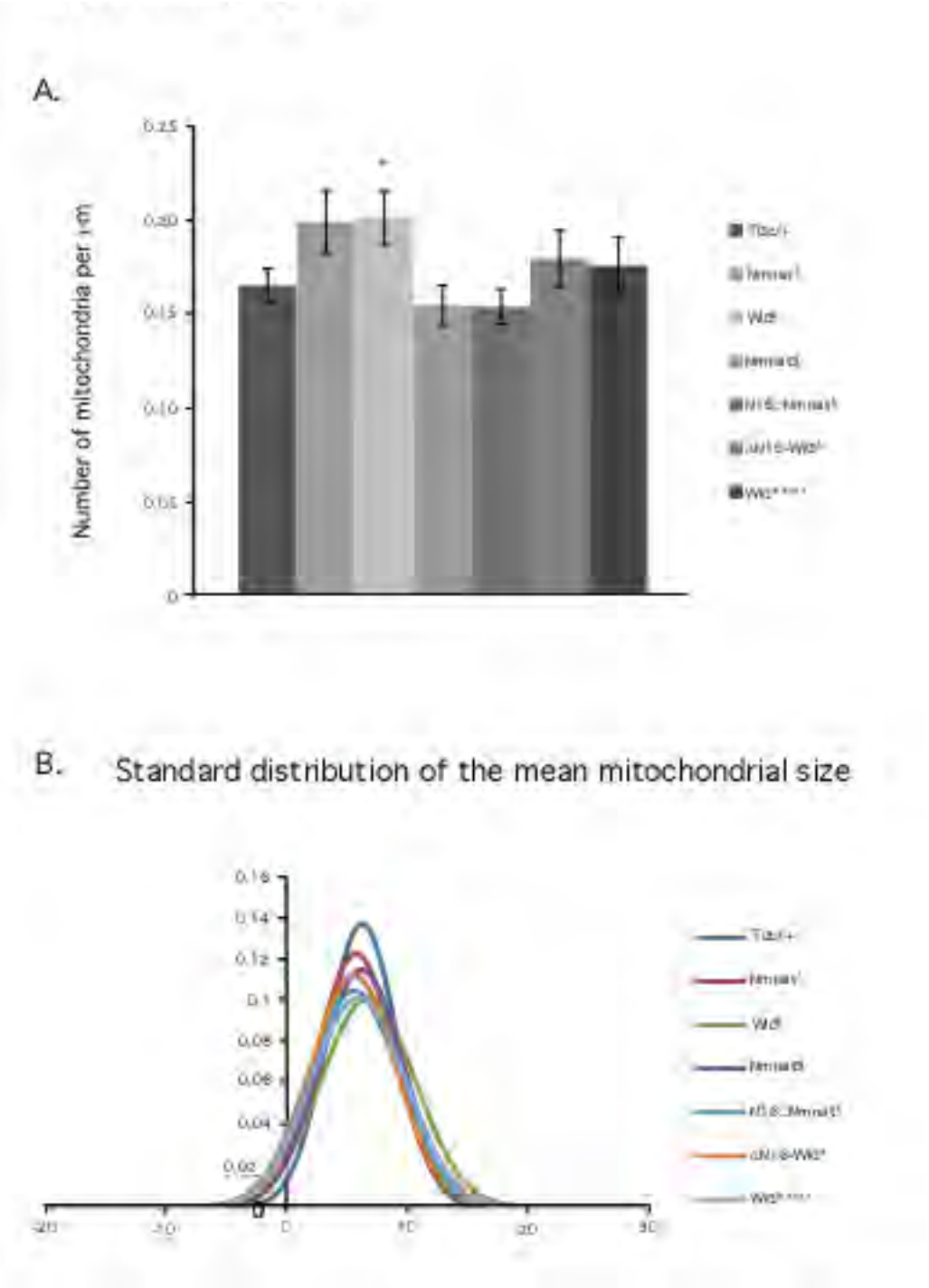
A.
Number of mitochondria per µm
0.25
0.20
0.15
0.10
0.05
0
B. Standard distribution of the mean mitochondrial size
0.16
0.14
0.12
0.1
0.08
0.06
0.04
0.02
0
-20
-10
0
10
20
30

**Fig 3-S2**

**Fig 3-S2. Number and size of mitochondria are not changed amongst genotypes.** (A) Number of mitochondria per µm. Only $Wld^S$ shows a slight increase in size compared with control. (B) Standard distribution of the mean mitochondria size. (n>10, *p<.05)

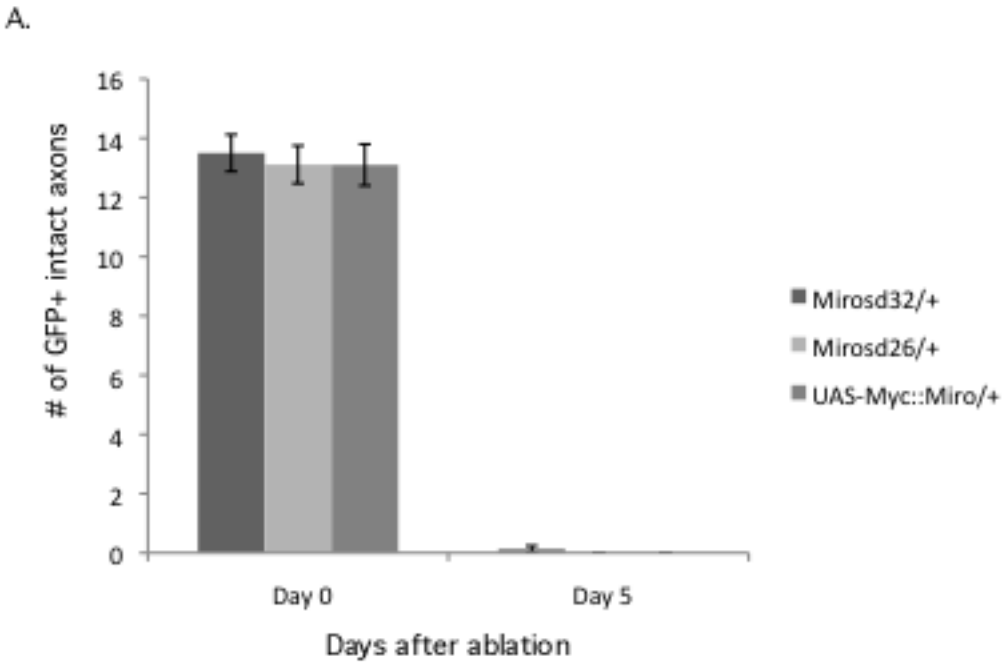
A.
16
14
12
10
8
6
4
2
0
# of GFP+ intact axons
Day 0
Day 5
Days after ablation
Mirosd32/+
Mirosd26/+
UAS-Myc::Miro/+

**Fig. 3-S3**

**Fig. 3-S3. *Miro* heterozygous alleles and Miro overexpression do not affect development or degeneration.** (A) Quantification of *miro* heterozygous alleles and Miro overexpression before and 5 days post-injury. *Miro* heterozygous alleles and Miro overexpression do not differ from controls in number of axons present before and 5 days post-axotomy.

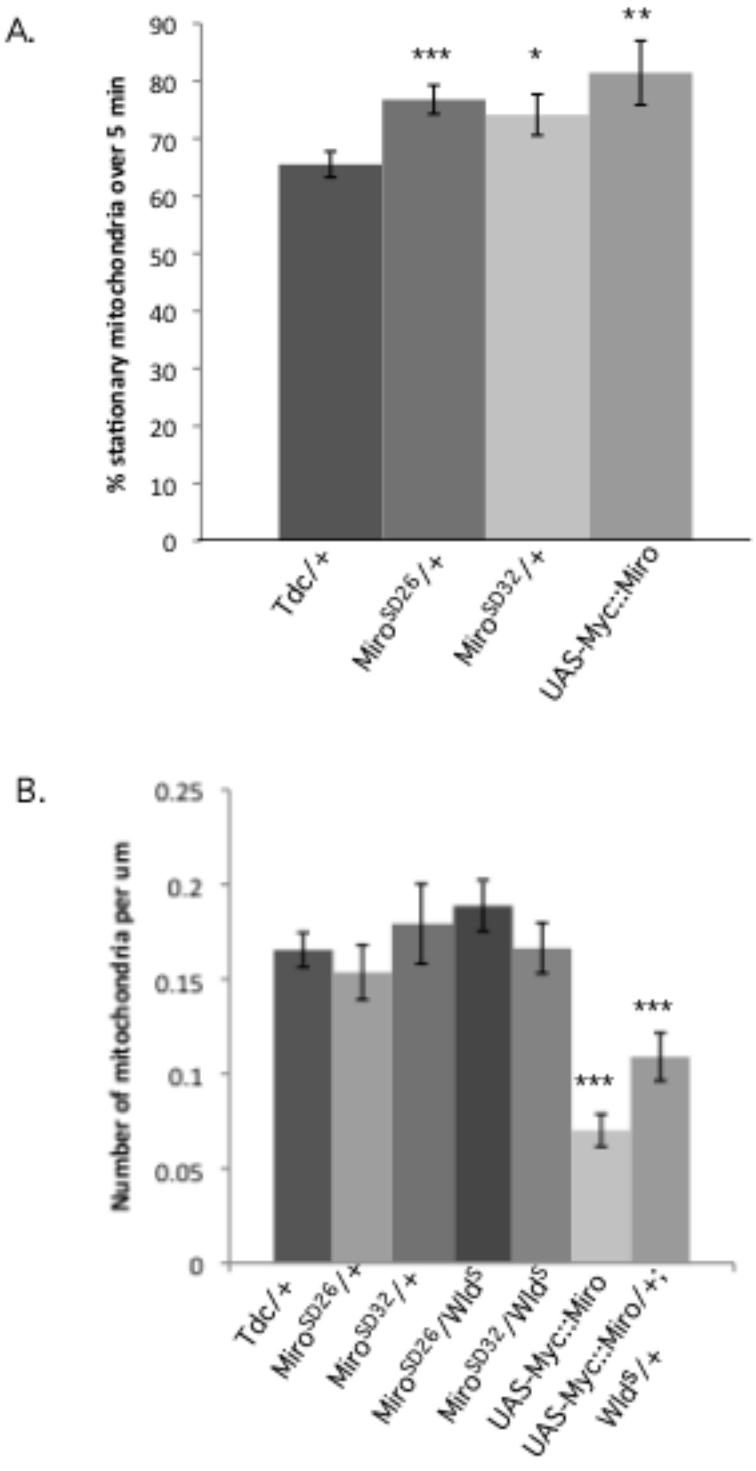
A.
% stationary mitochondria over 5 min
90
80
70
60
50
40
30
20
10
0
***
*
**
Tdc/+
Miro^SD26/+
Miro^SD32/+
UAS-Myc::Miro
B.
Number of mitochondria per um
0.25
0.2
0.15
0.1
0.05
0
***
***
Tdc/+
Miro^SD26/+
Miro^SD32/+
Miro^SD26/Wld^S
Miro^SD32/Wld^S
UAS-Myc::Miro
UAS-Myc::Miro/+; Wld^S/+

**Fig. 3-S4**

**Fig. 3-S4. *Miro* heterozygous alleles and overexpression alone increase stationary mitochondria and the overexpression decreases the number of mitochondria present.** (A) Quantification of mitochondrial movement over 5 minutes in 3$^{rd}$ instar larvae. As has been previously reported, *miro* heterozygous alleles and Miro overexpression increases the number of stationary mitochondria. (B) Number of mitochondria per μm is only changed in the Miro overexpression as has been reported. (Russo et al., 2009) (n>5, **p<.01, ***p<.001)

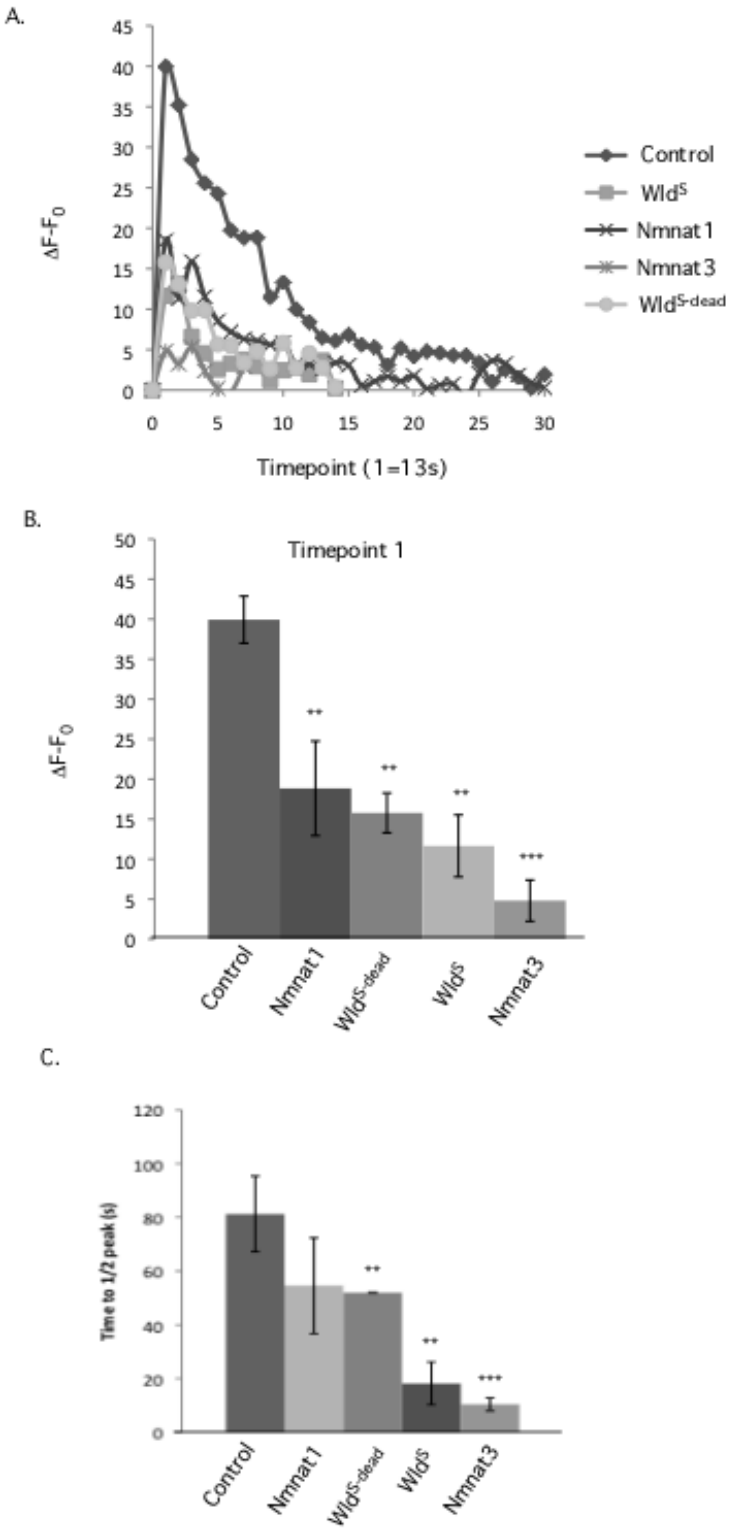
A.
ΔF-F0
Timepoint (1=13s)
Control
Wld^S
Nmnat1
Nmnat3
Wld^S-dead
B.
Timepoint 1
ΔF-F0
Control
Nmnat1
Wld^S-dead
Wld^S
Nmnat3
C.
Time to 1/2 peak (s)
Control
Nmnat1
Wld^S-dead
Wld^S
Nmnat3

**Fig 3-S5**

**Fig 3-S5. Proximal gCaMP3 signal after injury decreases in Wld$^S$ and Nmnat3.** (A) Time course of gCaMP3 signal in the proximal section of 3$^{rd}$ instar larval axons post laser-ablation. (B) Peak gCaMP3 intensity directly after axotomy. (C) Recovery time of gCaMP3 signal to ½ peak after injury.

# Chapter IV:
# A forward genetic screen to identify new genes involved in axon degeneration

## Introduction

Augustus Waller's first observation of axon degeneration in 1850 reported that after a short period of latency, an axon rapidly fragmented and was cleared from its environment (Waller, 1850). The fact that axons were able to remain intact for a latent period followed by degeneration lead researchers to believe that it was a passive process of wasting away, occurring simply due to the lack of nutrients being delivered to the severed axon. However, the discovery of the $Wld^S$ spontaneous mouse mutant began to challenge the notion that axon degeneration is a passive process. In these mice, axons can survive and function about 10-fold longer than wild-type axons, and further studies have shown the same is true in rat and *Drosophila* (Lunn et al., 1989; Adalbert et al., 2005; MacDonald et al., 2006). Because axon degeneration can be delayed, the idea emerged that Wallerian degeneration is an active process akin to apoptosis. However, the $Wld^S$ mutant is a gain-of-function mutation that protects in an overexpression manner, perhaps by enhancing normal cellular function. Therefore, this molecule still does not definitively show that axon degeneration is an active process.

To uncover genes involved in a pathway of axon degeneration, we have initiated a forward genetic screen. My part specifically was in dissecting and screening about half of the lines screened to this point. If loss of a gene prevents an axon from degenerating, that indicates there is a pathway of degeneration that can be inhibited, and Wallerian degeneration is, indeed, an active process. Here,

I describe the forward genetic screen and the classes of mutants that have been identified. I also show we have discovered the identity of one of those genes involved in Wallerian degeneration.

## Results

We generated ~3,000 ethyl methane sulfonate (EMS)-mutated lines, selecting for mutations on the 3$^{rd}$ chromosome only. The lines were set up such that if the mutation was lethal, we could use mosaic analysis with a cell repressible marker (MARCM) to get homozygous mutants in the ORNs (**Fig 4-1**; Lee and Luo, 2001). We unilaterally ablated *Drosophila* antennae so that one side served as an uninjured control, and assayed for presence of GFP+ material 7 days after ablation. During the initial screen, we retain lines that we consider potential hits, with 2 out of 3 brains from the line showing an increase in GFP+ material 7 days after ablation. We then run the potential hits through a 2$^{nd}$ screening, where we repeat the ablation to confirm the hit. Three classes of interest emerged from the screen: (1) Viable mutants with axon fragments present at 7 days after axotomy; (2) Lethal mutants with axon fragments present at 7 days after axotomy; and (3) Lethal mutants with intact axons present at 7 days after axotomy (**Fig 4-2**).

Viable mutants with axon fragments present at 7 days after axotomy represent either a delay in degeneration or a delay in the clearance of degenerated axons. Because these mutants are viable, we do not know which

cell type is responsible for the phenotype during the initial screen. To test whether the gene is neuronal or glia in nature, we make MARCM clones of the mutants within either the neurons or glia specifically. For example, if the gene is acting within the neurons, the phenotype of increased GFP+ material 7 days after ablation will remain when mutant neuronal clones are generated. Although we have several mutants within this category, we have yet to identify any of the genes.

Lethal mutations that result in fragmented GFP+ axonal material present 7 days after axotomy represent either a delay in degeneration within the neuron or a mutation in a signaling mechanism from neurons to glia, which leads to glial clearance of the debris. Because they are lethal, we know all of these mutations are within the neuron, as we use a neuronal driver to make the MARCM clones. We only have few mutants in this class, but they could possibly link the process of neuronal degeneration to clearance by glia.

The final class of mutants is lethal, with intact GFP+ axons remaining at 7 days post axotomy. This class represents mutations within the neuron that delay Wallerian degeneration. We found three very strong mutants in this class reminiscent of $Wld^{S}$ (**Fig 4-3A**). At least one of the mutants can protect axons 30 days after injury; the other mutants have not been tested at this timepoint yet. Interestingly, we found that all three of these mutants failed to complement each other for both lethality and the phenotype of intact axons after ablation, suggesting that they are all alleles of the same gene. Each mutant was also

crossed to the 3rd chromosome mini deficiency kit (Bloomington), and screened for failure to complement lethality. All 3 mutants failed to complement lethality of mini deficiencies for the same region on 3L near chromosomal location 66B5, narrowing the location of the mutation to 14 genes. Finally, I found that all three mutant phenotypes were recessive, as no GFP+ intact axons were observed when the heterozygous flies were axotomized.

EMS mutagenesis in the past has included the daunting task of finding the mutant gene after a phenotype of interest has emerged. However, with the new technology of deep sequencing, it is possible to sequence the entire *Drosophila* genome in a very short period of time. Due to our isolation of mutant 3rd chromosomes, we already knew that our genes of interest were on the 3rd chromosome. We also knew we had 3 independently isolated alleles of the gene, and that they failed to complement a small number of genes from the mini deficiency kit. Therefore, through the process of deep sequencing, we were able to find our gene of interest very quickly. Stephan Zuchner (University of Miami) compared the DNA sequences of the 3 mutant lines to an isogenized control line. He looked for short nucleotide polymorphisms in exons that were present in the same gene for all 3 mutant lines, and which would result in a non-functional protein. Because the complementation crosses had narrowed the region of interest, he concentrated his analysis to those 14 genes. All 3 alleles were found to be early stop codons in the gene Ect-4 (**Fig 4-3B**). Jeannette Osterloh will

continue to study this gene and try to find the mechanism or pathway through which Ect-4 acts to prevent axon degeneration.

## Conclusions

Through an EMS-induced forward genetic screen, we have uncovered 3 classes of mutants of interest: viables with axon fragments remaining at 7 days post axotomy, lethals with axon fragments remaining at 7 days post axotomy, and lethals with intact axons remaining at 7 days post axotomy. In the work of one screen, we now have genes which may be found in glia to regulate clearance of axons, may be in neurons to communicate to glia to clear axonal debris, and genes that suppress Wallerian degeneration in the axon. In this aspect, the screen has been very fruitful for a variety of projects on-going in the lab. In the years to come, these genes will be identified through complementation and deep sequencing, and hopefully, new genes and pathways will emerge. The most exciting mutant to emerge from the screen is Ect-4, which definitively shows that Wallerian degeneration is an active process.

Although not a lot is known about *Drosophila* Ect-4, there have been papers published on its mammalian homologue, MyD88-5 or SARM, and its *C. elegans* homologue, TIR-1. Interestingly, MyD88-5 has been found to be preferentially expressed in neurons and is localized to the outer membrane of mitochondria as well as microtubules (Kim et al., 2007). The exact mechanism of Ect-4 in Wallerian degeneration is unknown, but some clues have come from the

studies in the mouse. Kim et al. discovered that MyD88-5 binds JNK3 both *in vitro* and *in vivo* (2007). MyD88-5 promotes the relocalization of JNK3 from the cytoplasm and plasma membrane to the mitochondria (Kim et al., 2007). JNK3 has been reported to be involved in neuronal death following ischemia, making this pathway a very intriguing possibility for involvement in Wallerian degeneration as well. JNK3 is also reported to be downstream of, and activated by, CamKII in apoptosis. This draws another intriguing parallel between apoptosis and Wallerian degeneration, as CamKII is activated by $Ca^{2+}$, which is involved in both apoptosis and axon death signaling. Thus, a model could arise whereby an increase in $Ca^{2+}$ activates CamKII, which in turn activates JNK3 that is bound to MyD88-5 at the mitochondrial membrane, and leads to cell death or Wallerian degeneration through the mitochondria. In the absence of MyD88-5 (Ect-4), JNK3 cannot localize to the mitochondria and therefore, the Wallerian death pathway cannot be initiated. MyD88-5 was also shown to have an involvement in neuronal cell death following oxygen-glucose deprivation, as knockouts of MyD88-5 showed a decrease in cell death (Kim et al., 2007). It will be imperative to study whether JNK3 is involved in Wallerian degeneration and to identify components both up- and downstream of Ect-4 after axotomy.

In conclusion, our work has identified the first mutant gene that blocks Wallerian degeneration thereby classifying Wallerian degeneration as an active pathway. Further work needs to be done to identify the pathway that leads to

degeneration and all of the genes discovered will represent possible therapeutic targets for neurodegeneration.

## Materials and Methods

### Fly stocks used

The following stock were used: OR22a-Gal4 (B. Dickson, Vienna); pUAST-MCD8::GFP; FRT2A, tub-Gal80; FRT82B, tub-Gal80; ey-flp, UAS-mCD8::GFP; mini Df kit of 3$^{rd}$ chromosome (Bloomington); and FRT2X (T. Lee, Janelia Farms).

### EMS mutagenesis

Adult male *Drosophila* were starved for at least 5 hours prior to mutagenesis and kept at 25°C. About 100 males were placed in a bottle with about 25 mM EMS solution soaked into Kimwipes. To prepare the 25mM EMS, 63µL of EMS was added to 25mL of 1% sucrose, and then 5mL of this solution was added to empty bottles. Males were remained in the EMS bottle overnight, and were transferred to clean bottles with normal food the following morning. Males were allowed to clean themselves all day before being transferred to another bottle with non-EMS treated virgins.

### Injury protocol

Flies were anesthetized on $CO_2$ pads and the left 3$^{rd}$ antennal segment was removed. The right antenna was kept intact as an internal control. Flies were ablated at least 1 week post-eclosion, and dissected 7 days after ablation. Brains were then imaged with confocal microscopy.

### Confocal Imaging

Standard methods were used for dissection and fixation labeling of the *Drosophila* adult brain (Voshall et al., 2000). Brains were then mounted in 75% glycerol and viewed with either a Zeiss Imager M10 spinning disc confocal or a Axioskop2 LSM 5 Pascal point scanning confocal. Lines with a GFP+ axonal material present 7 days after axotomy in 2 out of 3 brains were kept for confirmation and analysis. For confirmation, the lines were retested for GFP+ axonal material present 7 days after axotomy, and after the phenotype was confirmed, the lines were tested for complementation and DNA was sent for deep sequencing.

**Complementation assay**

The Exelixis mini deficiency kit of chromosome 3 was used in our complementation assay. We screened for deficiencies which failed to complement the lethality of the mutant lines of interest.

**Deep sequencing**

Deep sequencing of the *Drosophila* genomes of interest were performed by Stephan Zuchner, PhD, of the University of Miami. DNA from our background isogenized strain of 22a-Gal4, UAS-MCD8::GFP/ CyO; FRT2X was compared to the DNA of our mutant strains. Dr. Zuchner then looked for single nucleotide polymorphisms in exons in the region of interest on 3L narrowed down by the complementation crosses and found mutations that led to early stop codons.

EMS fed to:

22a-Gal4, UAS-MCD8::GFP ; FRT2X
CyO FRT2X

**100 males to 150 virgins:**

22a-Gal4, UAS-MCD8::GFP ; FRT2X* X 22a-Gal4, UAS-MCD8::GFP ; Dr
CyO FRT2X CyO TM3

**Single male to 3 virgins:**

22a-Gal4, UAS-MCD8::GFP ; FRT2X* X 22a-Gal4, UAS-MCD8::GFP ; Dr
CyO TM3 CyO TM3

22a-Gal4, UAS-MCD8::GFP ; FRT2X*
CyO TM3 Self-cross to make stocks

If viable, test homozygous stock; If lethal:

22a-Gal4,UAS-MCD8::GFP;FRT2X* ey-flp,UAS-MCD8::GFP;;FRT2A,tub-Gal80
CyO TM3 X FM7 TM3

For other chromosome, use FRT82B, tub-Gal80

**Fig 4-1**

**Fig. 4-1 The cross schematic for creation of EMS-mutagenized stocks.**

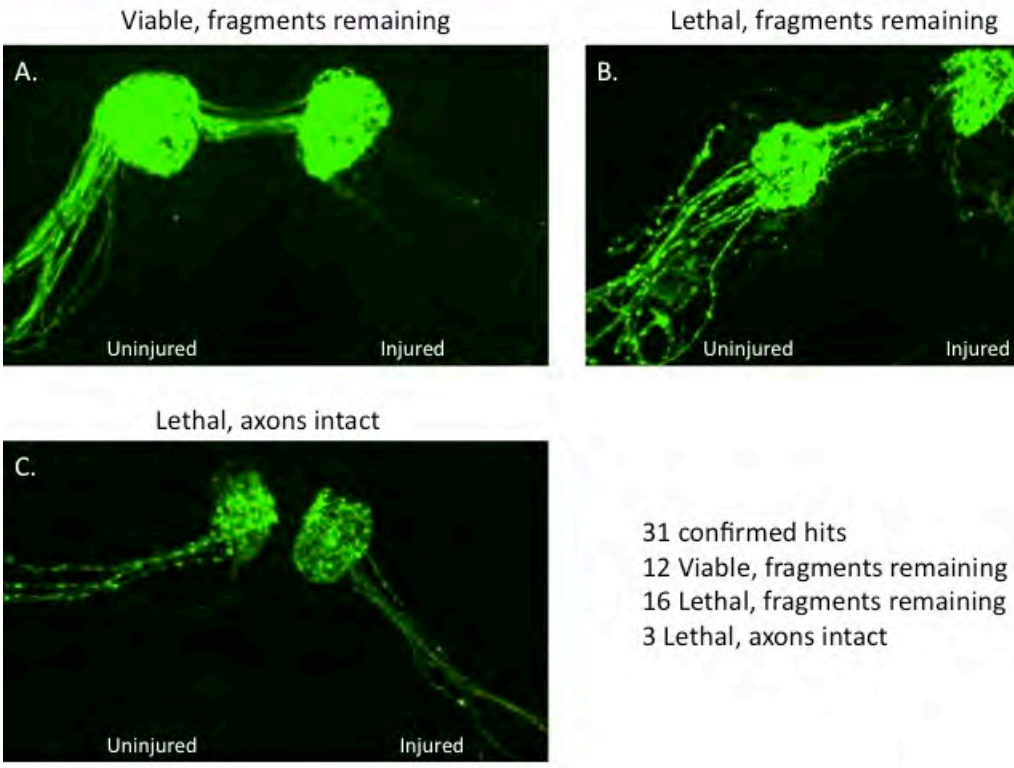
Viable, fragments remaining
A.
Uninjured
Injured
Lethal, fragments remaining
B.
Uninjured
Injured
Lethal, axons intact
C.
Uninjured
Injured
31 confirmed hits
12 Viable, fragments remaining
16 Lethal, fragments remaining
3 Lethal, axons intact

**Fig 4-2**

**Fig 4-2. Three classes of mutants of interest emerged from the screen.** (A) Representative image of a viable mutant with axon fragments remaining. (B) Representative image of a lethal mutant with axon fragments remaining. (C) Representative image of a lethal mutant with intact axons remaining, reminiscent of $Wld^S$. In all cases, the left side is uninjured and the right side is injured. Images are of 7 days post-axotomy.

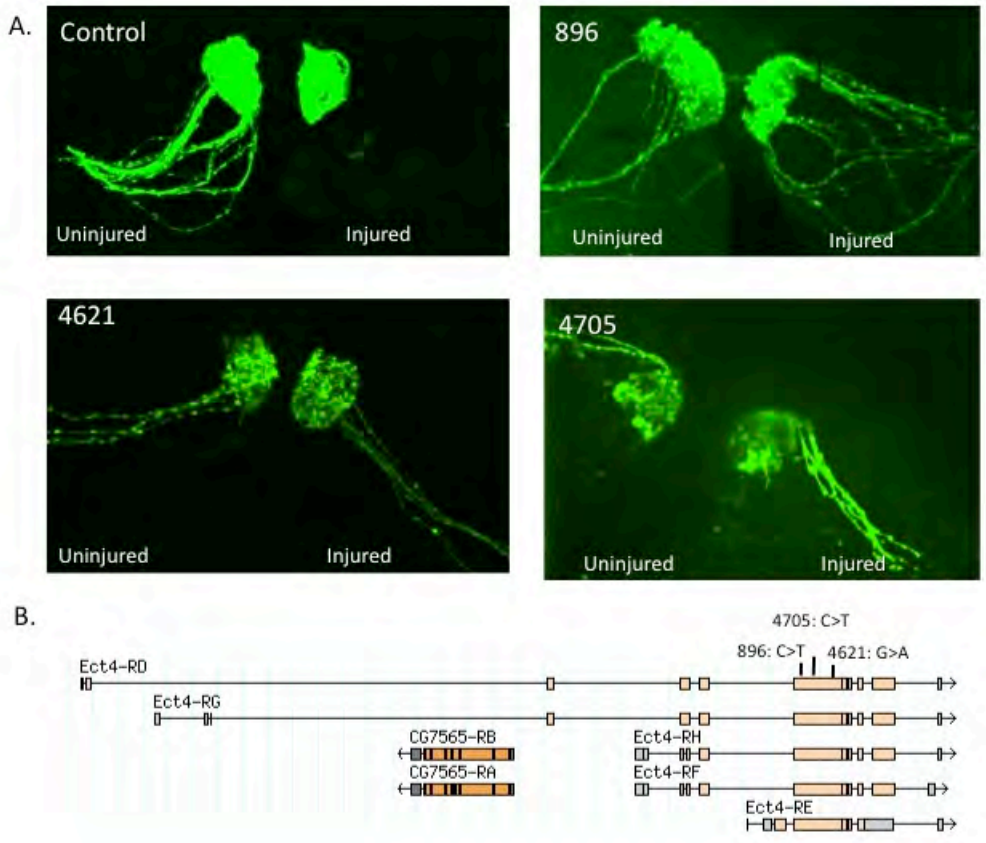
A.
Control
Uninjured
Injured
896
Uninjured
Injured
4621
Uninjured
Injured
4705
Uninjured
Injured
B.
4705: C>T
896: C>T
4621: G>A
Ect4-RD
Ect4-RG
CG7565-RB
CG7565-RA
Ect4-RH
Ect4-RF
Ect4-RE

**Fig 4-3**

**Fig 4-3. *Ect4* mutants protect axons after axotomy.** (A) Representative images of control and 3 separate alleles of *Ect4* (896, 4621, and 4705). Left side is uninjured and right side is injured, imaged 7 days post-axotomy. (B) Locations of the *Ect4* mutations in all 3 alleles. All resulted in an early stop codon in an exon shared by all *Ect4* isoforms.

# Chapter V:

# Conclusions

The work presented in this thesis has focused on: (1) the mechanisms of axon degeneration through the study of the novel fusion protein, $Wld^S$, (2) the function of $Wld^S$ within the mitochondria, and (3) the discovery of a gene involved in Wallerian degeneration. The second chapter of this thesis identified the domains of $Wld^S$ that are necessary and sufficient for protection of severed axons, highlighted a role for VCP/TER94 in $Wld^S$-mediated protection, and began to suggest that subcellular localization of Nmnat is what determines protection. The third chapter focused on a role for mitochondria in $Wld^S$-mediated axon protection, and found that mitochondria show an increase in movement before injury and a decrease in $Ca^{2+}$ post-injury in *Drosophila* larval axons. The fourth chapter in this thesis showed that Wallerian degeneration is an active process, which can be prevented by a loss of Ect-4 protein, a proposed mitochondrial protein based on its mammalian homology.

**N16 fused to Nmnat1 phenocopies $Wld^S$**

My first goal was to narrow down the domains of $Wld^S$ that contribute to the protection of severed axons. We showed for the first time, *in vivo*, that mammalian Nmnat1 can protect severed *Drosophila* axons, however, this protection is always lower than that of full-length $Wld^S$. We also found that enzymatic activity of $Wld^S$ and Nmnat1 is necessary for protective function, a finding that has been repeated in the mammalian literature as well (Conforti et al., 2009; Sasaki et al., 2009; Yahata et al., 2009). Although Nmnat1 with

enzymatic ability accounts for the majority of the axon protection seen with $Wld^S$, addition of some N-terminal portion boosts Nmnat1 protection to that of $Wld^S$ since the level of protection afforded by Nmnat1 is always lower than that of $Wld^S$.

Clues as to which portion of the N-terminus of $Wld^S$ is important for axonal protection came from the Laser et al. study that found the first 16 amino acids of $Wld^S$ bind to VCP, a molecule with several cellular functions. The authors thought that VCP's interaction with the UPS was important in regards to $Wld^S$ (2006). We found that the first 16 amino acids (N16) of $Wld^S$ are important for $Wld^S$ protective function in *Drosophila* ORNs. When we deleted the first 16 amino acids, we found that $Wld^S$ protection of severed axons was weakened. Reciprocally, when we fused N16 to Nmnat1, we found that it completely recapitulated the $Wld^S$ phenotype. Conforti et al. found that removing N16 from $Wld^S$ resulted in little to no axonal protection in the mouse, supporting our work in the fly (2009). We then tested the requirement of VCP/TER94 in axonal protection by using RNAi to knock down VCP/TER94 specifically in the olfactory neurons we assay for protection. When we expressed VCP/TER94 RNAi with $Wld^S$, we found that axonal protection after axotomy decreased, indicating that VCP/TER94 is involved with the N-terminal protective boost that N16 gives to Nmnat1. Conforti et al. found that if N16 of $Wld^S$ is replaced with a different VCP/TER94 binding site in the mouse, this molecule is able to protect as well as

normal Wld$^S$, again indicating that VCP/TER94 is important for Wld$^S$ protection (2009).

Interestingly, when we knocked down other UPS components known to form a complex with VCP/TER94, we found no effect on Wld$^S$ protection. At the time we thought that perhaps VCP/TER94 was acting through one of its many other cellular functions to boost Nmnat1 protection. However, now that we think the site of Wld$^S$ action is in the mitochondria, we believe that the purpose of VCP/TER94 binding is actually to aid in the relocalization of Nmnat1 from the nucleus to the mitochondria. To further support that there is not a role for VCP/TER94 beyond its physical interaction with Wld$^S$, Beirowski et al. has tested a Wld$^S$ in which VCP binding is weakened. This altered molecule protects as well as normal Wld$^S$ (2010). Whatever weak binding remains is likely enough to relocalize Wld$^S$ to the mitochondria, and therefore, high protective levels remain.

**Nmnat targeted to mitochondria protects as well as Wld$^S$**

Although Wld$^S$ predominantly localized to the nucleus, we wondered if its nuclear localization was necessary, or if Nmnat or Wld$^S$ targeted to other portions of the cell could protect axons after injury as well. The first clue that the nucleus is not the site of action came from over-expressing Nmnat1. We knew from our first study that the majority of Nmnat1 is expressed in *Drosophila* nuclei, and we also knew that Nmnat1 could not protect as well as Wld$^S$. So we decided to test if plasma membrane-tethered Wld$^S$, NADS (*Drosophila* NAD-synthesizing

molecule), or 2 other mammalian Nmnats (Nmnat2 and Nmnat3) could protect severed axons. Tagging $Wld^S$ to the plasma membrane with mCD8 rendered $Wld^S$ unable to protect severed axons. It is important to note that we do not know if the Nmnat1 of membrane-tethered $Wld^S$ was able to form hexamers essential for Nmnat1 function of NAD synthesis, which could account for its inability to protect. However, this result led us to believe that localization of $Wld^S$ was important for its suppression of axon degeneration. We also wanted to test if any NAD-synthesizing molecule could protect severed axons, or if there was something special about Nmnat. We drove NADS in ORNs and found that it offered no axon protection 5 days post injury. We also added the N16 domain to NADS, but found no protection offered by this molecule, indicating there is something unique about Nmnat. Therefore, we conclude that Nmnat is necessary for axon protection after injury, and that its localization is important.

From the mammalian literature, we knew that there were 3 different Nmnats. Nmnat1 is predominantly nuclear, Nmnat2 is either Golgi-associated or cytoplasmic, and Nmnat3 is mitochondrial (Sasaki et al., 2006). As stated above, Nmnat1 can protect *Drosophila* severed axons, but not as well as $Wld^S$. We find that Nmnat2 cannot protect severed axons *in vivo* 5 days post injury, though 2 studies in mammals have reported slight protection *in vitro* (Yan et al., 2009; Gilley and Coleman, 2010). It still remains an open question if Nmnat2 can protect *in vivo* in mammals. It has also been reported that Nmnat2 has a short half-life, which could account for the lack of protection seen *in vivo* in *Drosophila*

axons (Gilley and Coleman, 2010). To test if Nmnat2 protein is degraded at the 5 day timepoint thus accounting for the lack of axon protection seen, we expressed Nmnat2::myc with $Wld^S$. We found that Nmnat2::myc is still expressed in axons 5 days post-injury. This result indicates that Nmnat2 is not degraded within 5 days post-injury and thus, a shortened half-life cannot account for the lack of axon protection in *Drosophila*. We propose instead, that the lack of protection of Nmnat2 is due to its localization.

Mitochondrial localization appears to be imperative for Nmnat-mediated severed axon protection in *Drosophila*, as Nmnat3, a mitochondrial protein can protect as well as $Wld^S$. We have tested the ability of Nmnat3 to protect severed axons for as long as 50 days post-axotomy and found in all cases, Nmnat3 protects as well as $Wld^S$. Around the same time we discovered this result, $Wld^S$ was reported to localize to mitochondria and Nmnat3 was found to be the only Nmnat that could protect in the mouse when over-expressed (Yahata et al, 2009). It was also found that if $Wld^S$ is forced out of the nucleus, the level of axon protection actually increases, and cytoplasmic $Wld^S$ fractionates predominantly with mitochondria (Beirowski et al., 2009). All of this evidence points to a role in mitochondria for $Wld^S$, which has fueled our subsequent study.

**Mitochondria are more motile when neuroprotective molecules are present**

Evidence was accumulating which pointed to mitochondria as the potential site of $Wld^S$ action. Therefore, we decided to study mitochondria in a $Wld^S$-

expressing axon. We used a 3rd instar larval fillet preparation to examine mitochondria in a live animal. We found that mitochondria in Wld$^{S}$-expressing larvae are more motile than those in wild-type. What is more interesting, the amount of neuroprotection afforded by several molecules correlated perfectly with the increase in motile mitochondria. For instance, Nmnat1, ΔN16-Wld$^{S}$, and Wld$^{S\text{-}dead}$, which all show a weak protection at 5 days post axotomy, all showed a slight increase in mitochondrial movement. Molecules which show strong protection of severed axons at 5 days post injury, such as Wld$^{S}$, Nmnat3, and N16::Nmnat1, all had a great increase in mitochondrial motility. The strong correlation of mitochondrial motility and axon protection led us to postulate that mitochondrial motility is necessary for axon protection.

To test this hypothesis directly, we used heterozygous mutants of *miro*, which are known to decrease mitochondrial movement without disrupting the number of mitochondria present in the neuron (Russo et al., 2009). We first found the heterozygous mutants of *miro* were able to suppress the increase in mitochondrial motility in axons expressing Wld$^{S}$. Upon suppressing mitochondrial motility, we found that we could also suppress Wld$^{S}$ axon protection, indicating that mitochondrial motility is critical for Wld$^{S}$-mediated protection. In this study, we uncovered the first cell biological difference prior to injury in Wld$^{S}$-expressing axons, and showed that the difference in mitochondrial motility is necessary for Wld$^{S}$ function.

This finding that an increase in mitochondrial motility boosts protection of $Wld^S$ is very intriguing, as many neurological diseases report a deficit in mitochondrial trafficking. Deletion of Mfn2, a gene involved in mitochondrial fusion, is a mouse model of Charcot Marie Tooth disease 2A (CMT2A). Recently, it was reported that these mice show a decrease in mitochondrial transport, but other organelles remain unaffected (Misko et al., 2010). The decrease in mitochondrial transport seems unrelated to Mfn2's mitochondrial fusion function as another gene which affects mitochondrial function does not disrupt transport. It has also been reported that mitochondria accumulate and stop in amyloid precursor protein+ axonal swellings produced in a mouse model of Alzheimer's disease (Adalbert et al., 2008). Whether the impairment of mitochondrial trafficking is causal to Alzheimer's disease remains to be seen, however both studies highlight the importance of maintaining proper mitochondrial trafficking to sustain a healthy neuron.

**Injury-induced $Ca^{2+}$ waves are decreased in the presence of neuroprotective molecules $Wld^S$ and Nmnat3**

Discovering an increase in mitochondrial motility in $Wld^S$-expressing axons is an exciting finding, but it left the question open of why do the mitochondria move more. Moreover, why do mitochondria need to move in the first place? Axons are long structures (in some animals a length of many feet) that need a constant supply of energy to aid in synaptic transmission. The mitochondria

travel along the axon to produce ATP at hot spots of high-energy consumption. A constant delivery of mitochondria down the axon ensures that new, healthy mitochondria are able to meet the high-energy demands of the axon. The movement also ensures that the entire axon is monitored for areas of high calcium and low ATP. As mitochondria age, they becomes less able to produce high amounts of energy, and are either transported back to the cell body to be degraded, or undergo mitophagy within the axon (Cal and Sheng, 2009).

Mitochondria also have the ability to buffer large amounts of calcium. Calcium actually controls mitochondrial movement, in that as the amount of calcium increases, the number of moving mitochondria decreases (Saotome et al., 2009). Mitochondrial movement resumes once mitochondria have taken up and buffered calcium from the cytosol. We hypothesized that the amount of calcium present in the cytoplasm is reduced in $Wld^{S}$-expressing axons, which would lead to an increase in mitochondrial movement. We found that after axotomy there is a spike in calcium in the axon, as seen by an increase in gCaMP3 fluorescence. Interestingly, when we express $Wld^{S}$ or Nmnat3, we find this large increase in gCaMP3 fluorescence is greatly dampened, and the time it takes the gCaMP3 signal to return to baseline is quicker than in wild type. We also found that the weakly neuroprotective molecules, Nmnat1 and $Wld^{S\text{-}dead}$, slightly decreased the gCaMP3 signal after axotomy, correlating the amount of neuroprotection with a decrease in gCaMP3 signal after injury. These data suggest that calcium buffering in $Wld^{S}$-expressing axons is increased as the

gCaMP3 signal is decrease, but this needs to be confirmed by studying the $Ca^{2+}$ buffering capacity of mitochondria expressing $Wld^S$ through biochemical means.

How could $Wld^S$ increase the calcium buffering capacity of mitochondria? It is known that calcium buffering is controlled by negative membrane potential in mitochondria, amongst other factors (Babcock et al., 2007). It is possible that a local increase in $NAD^+$ production in the mitochondria by Nmnat1 could lead to more ATP production. ATP production maintains a negative mitochondrial membrane potential by pumping protons out of the mitochondria. Interestingly, it has been recently noted that both $Wld^S$- and Nmnat3-expressing mitochondria produce more ATP (Yahata et al., 2009), fitting in with our model (**Fig. 5-1**). With hyperpolarized mitochondria, calcium buffering is increased. If calcium buffering is increased, the amount of calcium within the cytosol is decreased, and therefore, the mitochondria exhibit increased movement. One could also imagine that an increase in movement would allow the mitochondria to cover more space faster, thereby again increasing the amount of calcium buffering that can occur. Once again, a study of mitochondrial bioenergetics of $Wld^S$-expressing mitochondria can confirm this model, and plans are in the works to collaborate with James Geddes, Ph.D. (University of Kentucky) to test our hypothesis. Our model assumes that $Ca^{2+}$ is most likely a trigger for axonal death. Although this has been shown in the case of nerve cut (Knoferle et al., 2010; Ziv and Spira, 1995; and George et al., 1995), it remains to be seen if $Ca^{2+}$ is a death signal in the case of axonal transport blockade and protein synthesis inhibition, both of

which are sensitive to $Wld^S$. It seems highly likely, as $Ca^{2+}$ increase triggers cell death in a variety of other instances, but until it is proven in other types of axonal degeneration, the proposed model may be limited to axonal cut.

**Ect-4, a mitochondria protein, is involved in Wallerian degeneration**

In the final study of this thesis, many members of the lab and I performed an EMS-based forward genetic screen. We aimed to identify mutants that could disrupt glial clearance of axons, disrupt neuron to glia signaling to clear axonal debris, and disrupt Wallerian degeneration itself. We have since confirmed mutants of all three classes, which will provide years of studies to come from the lab. What is most relevant to my work, however, is the discovery of a gene that blocks Wallerian degeneration. Previously, the only evidence that Wallerian degeneration is an active process came from the $Wld^S$ protein itself. Although $Wld^S$ has been a great tool to discover how to prevent an axon from degenerating, its nature as a gain-of-function mutation that is over-expressed to prevent axon degeneration does not address whether Wallerian degeneration is an active pathway. The discovery of Ect-4, however, definitively shows that Wallerian degeneration is an active process, as mutation of this gene blocks degeneration in *Drosophila* neurons for at least 30 days post-injury.

The mammalian homologue of *Drosophila* Ect-4 to date, MyD88-5 or SARM, offer some clues as to its function. MyD88-5 is localized to mitochondria and microtubules specifically in neurons. Part of its function seems to be in

binding JNK3 to relocalize JNK3 to the mitochondria. JNK3 and MyD88-5 have been shown to be involved excitotoxic neuronal death, and are thought to act through the mitochondria to induce cell death (Kim et al., 2007). Further studies are being done by Jeannette Osterloh in the lab to uncover the role of Ect-4 in Wallerian degeneration.

**Mitochondria and neurodegeneration**

The overall theme of this thesis is mitochondria are important in Wallerian degeneration. Whether they are the source of the death pathway or simply upstream in Wallerian degeneration remains to be seen, but certainly changing the properties of mitochondrial movement or function can affect axonal death. Many studies are showing evidence of mitochondria dysregulation in many neurological diseases. For instance, impairment in the respiratory complex I is an early change detected in sporadic and familial Parkinson's disease (Bueler, 2009). Mutations in mitofusin2 cause mitochondria transport defects that are thought to be a causal event in Charcot-Marie Tooth disease 2A (CMT2A) (Chen and Chan, 2009). In Alzheimer's disease, decreased cytochrome c oxidase activity, increased reactive oxygen species, and abnormal mitochondrial morphology have been detected (Celsi et al., 2009). Finally, in Huntington's disease, complex II, III, and IV activity is reduced. It has also been reported that mutant huntingtin can open the permeability transition pore of mitochondria, which results in the collapse of the mitochondria membrane potential, and

eventual cell death (Celsi et al., 2009). The only disease in this list that $Wld^S$ can protect against is CMT2A. Taking our model into account, the dysfuction in mitochondrial movement seen in CMT2A could be overcome with $Wld^S$. In the cases of Alzheimer's, Parkinson's, and Huntington's disease, all have dysfunctions that would result in alteration of the membrane potential, which is most likely downstream of where $Wld^S$ can act. So no matter how much $NAD^+$ is produced in the mitochondria, if the electron transport chain is dysfunctional, the membrane potential cannot be hyperpolarized.

**Looking forward in the fields of $Wld^S$ and neurodegeneration**

Although my studies have put forth a plausible mechanism for how $Wld^S$ can protect severed axons, the model still needs rigorous testing to confirm the action of $Wld^S$. The model contains two parts that we believe are important for $Wld^S$ function, both of which can be tested: (1) mitochondria motility is increased, and (2) mitochondrial $Ca^{2+}$-buffering capacity is increased. My results have already shown that the increase in mitochondrial motility is necessary for $Wld^S$-mediated axon protection. However, it remains to be tested if an increase in mitochondrial motility alone can suppress Wallerian degeneration. Although there are no known molecules in *Drosophila* that increase mitochondrial motility, there are known ways to increase mitochondria motility in mammals. Syntaphilin is a gene known to be involved in docking stationary mitochondria (MacAskill et al., 2009; Cai and Sheng, 2009). Upon knock out of syntaphilin, there is a great

increase in mitochondrial motility (Kang et al., 2008). Also, simply overexpressing Miro in mammalian axons results in an increase in mitochondrial movement (Saotome et al., 2008). Both of these models could be used to test if an increase in mitochondrial motility is sufficient for axonal protection after injury.

The second part of the $Wld^S$ model that needs to be tested is the necessity for an increase in $Ca^{2+}$ buffering capacity. First, results from James Geddes, Ph.D. will allow us to say that the biochemistry of $Wld^S$-expressing mitochondria has changed. In order to test if an increase in $Ca^{2+}$ buffering is necessary for $Wld^S$ to protect severed axons, we need a way to affect the import of $Ca^{2+}$ into the mitochondria. *LetM1* and *MICU1* are two genes that are reported to decrease the entry of $Ca^{2+}$ into mitochondria (Kirchok et al., 2004; Jiang et al., 2009; Perocchi et al, 2010). If our model is correct, the mutating either of these genes in the presence of $Wld^S$ should suppress protection of severed axons. There are a few complications that may arise from suppressing the uptake of $Ca^{2+}$ in the mitochondria. It is possible that an excess of $Ca^{2+}$ in the cytosol produced by blocking mitochondrial $Ca^{2+}$ uptake would cause spontaneous degeneration by activating calpains or other $Ca^{2+}$-sensitive molecules that may drive axon destruction. Alternatively, if $Ca^{2+}$ is needed in the mitochondria to initiate a death signal, then blocking the uptake of $Ca^{2+}$ would lead to protection of severed axons and have no effect on $Wld^S$. There is a need for a more specific test to only inhibit the action of $Wld^S$ and not affect normal cell function. However, we can test if increasing mitochondrial calcium buffering capacity can

delay Wallerian degeneration. To test this idea, addition of molecules like taurine, which increase calcium buffering capacity, to injured axons should suppress degeneration. We can also test if an increase in mitochondrial calcium after axotomy initiates mPTP by inhibiting cyclosporin A, preventing mPTP, and thereby protecting a severed axon from degenerating.

Finally, it remains to be seen if $Wld^S$ affects calcium buffering under normal circumstances, and if this has an effect on neurotransmission or another cellular function. To test if calcium dynamics are changed without axonal injury, octopamine can be applied to my 3$^{rd}$ instar larval fillet preparation with a TdcGal4 driving gCaMP3 and $Wld^S$. Additions of octopamine would stimulate Tdc neurons, thereby causing an increase in calcium within the cell. If $Wld^S$ increases calcium buffering under "physiological" conditions, then a decrease in the gCaMP3 signal would be observed when compared to control. Electrophysiology or behavioral tests could show if there is a change in neurotransmission in $Wld^S$-expressing neurons. Tests like these would be very important in deciding whether $Wld^S$ may have some therapeutic possibilities, provided a way to deliver the protein or gene was uncovered.

I have also shown in chapter 4 that we have uncovered a mutant that suppresses Wallerian degeneration. This discovery will open many doors in neurodegenerative treatment. First and foremost, it shows that Wallerian degeneration is an active process that can be prevented by inhibiting molecules. This is an exciting finding not only for the scientific community, but in terms of

creating therapeutic drugs, it is much easier to find small molecule inhibitors than to find drugs that enhance a protein or find a way to deliver molecules, like $Wld^S$, to the correct cells. Although we have only uncovered one gene involved in the Wallerian degeneration so far, there is a high possibility that more will emerge from our EMS mutagenesis screen or a candidate gene approach. It will be very important to analyze the role of Ect-4 not only in axon degeneration, but also in other cellular roles to determine if it is a viable target for drug therapies. Also, as more genes from the pathway are uncovered, more therapeutic targets will emerge.

In my thesis, I have narrowed down the important domains for $Wld^S$ function to N16 fused to enzymatically active Nmnat1. I have observed that mitochondria in $Wld^S$-expressing axons are more motile, which is the first biological change seen in $Wld^S$-expressing axons prior to injury. I further demonstrated that this change in mitochondrial trafficking is necessary for full $Wld^S$-mediated protection of axons after injury. I also observed a decrease in calcium signal after axotomy in $Wld^S$-expressing axons. Because of these results, I have proposed a model of $Wld^S$ function and hypothesized that an increase in mitochondrial calcium buffering capacity, which causes an increase in mitochondrial motility, is responsible for the ability of $Wld^S$ to protect axons after degeneration. I also helped uncover the first Wallerian degeneration loss-of-function mutant in *Drosophila* that results in preserved axons after axotomy. My data point to the importance of mitochondria in injury-induced death, and, along

with emerging data from neurodegenerative diseases detailing mitochondrial dysfunction as a major contributor to disease, highlight the importance of studying mitochondria function in health and disease. The future of the axon degeneration field should focus on therapies which can alter the mitochondria or a Wallerian degeneration pathway in such a way to save axons from degeneration.

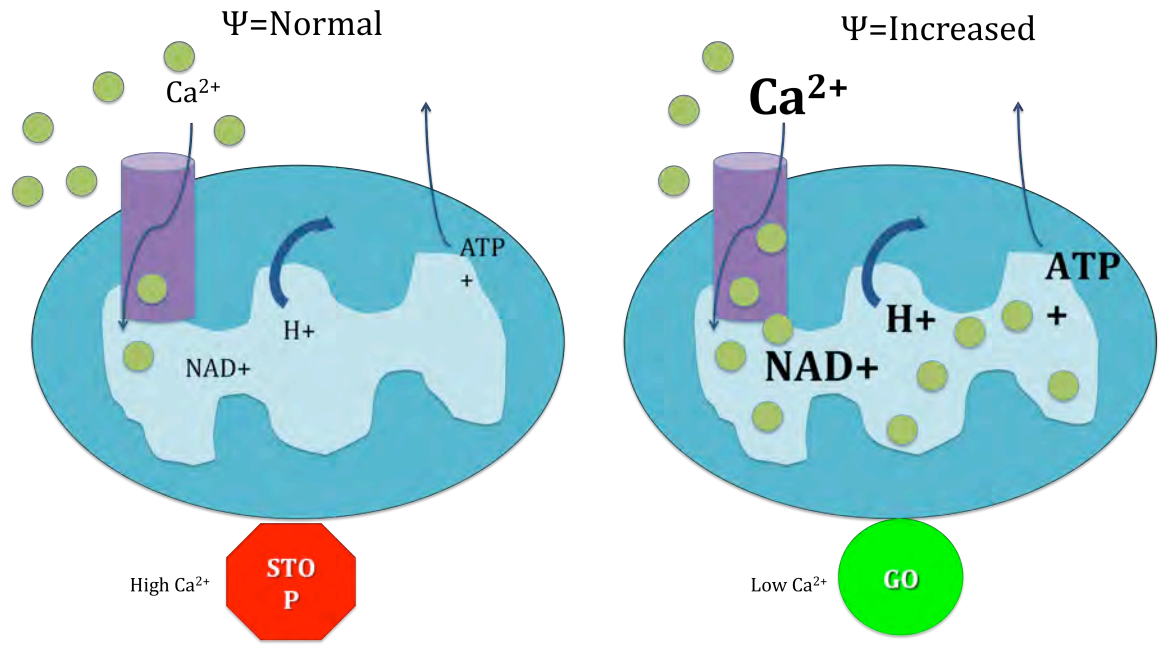
Ψ=Normal
Ca2+
ATP
+
H+
NAD+
High Ca2+
STO
P
Ψ=Increased
Ca2+
ATP
+
H+
NAD+
Low Ca2+
GO
Wild-type
Wld^S

**Fig. 5-1**

**Fig. 5-1. Model of how $Wld^S$ affects mitochondria to increase calcium buffering.** In the wild-type case, mitochondrial membrane potential is normal, therefore the calcium buffering is normal as well. Upon encountering a high amount of calcium, the mitochondria stop until the calcium is cleared from the cytosol. In the case of $Wld^S$, the mitochondrial membrane is hyperpolarized. This occurs due to the increase of $NAD^+$ activity of $Wld^S$ inside the mitochondria, which leads to an increase in proton pumping out of the mitochondria and an increase in $ATP^+$ synthesis. The hyperpolarization of the membrane leads to an increase in calcium buffering. Upon encountering a high amount of calcium, the mitochondria quickly buffer the calcium present and so are able to move.

## References

Adalbert, R., Nogradi, A., Babetto, E., Janeckova, L., Walker, S., Kerschensteiner, M., Misgeld, T., and Coleman, M. 2008. Severly dystrophic axons at amyloid plaques remain continuous and connected to viable cell bodies. Brain. *132*(2): 402-16.

Araki , T. , Y. Sasaki , and J. Milbrandt . 2004 . Increased nuclear NAD biosynthesis and SIRT1 activation prevent axonal degeneration. Science. *305*:1010–1013.

Avery, M.A., Sheehan, A.E., Kerr, K.S., Wang, J., and Freeman, M.R. 2009. $Wld^S$ requires Nmnat1 enzymatic activity and N16-VCP interactions to suppress Wallerian degeneration. J Cell Biol. *184*(4): 501-13.

Babcock, D.F., Herrington, J., Goodwin, P.C., Park, Y.B., and Hille, B. 1997. Mitochondrial participation in the intracellular $Ca^{2+}$ network. J Cell Biol. *136*(4): 833-44.

Babetto, E., Beirowski, B., Janeckova, L., Brown, R., Gilley, J., Thomson, D., Ribchester, R.R., and Coleman, M.P. 2010. Targeting Nmnat1 to axons and synapses transforms its neuroprotective potency in vivo. J Neurosci. *30*(40): 13291-304.

Beirowski, B., R. Adalbert, D. Wagner, D.S. Grumme, K. Addicks, R.R. Ribchester, and M.P. Coleman . 2005 . The progressive nature of Wallerian degeneration in wild-type and slow Wallerian degeneration (WldS) nerves. BMC Neurosci. *6*:6.

Beirowski, B., Morreale, G., Conforti, L., Mazzola, F., DiStefano, M., Wilbrey, A., Babetto, E., Janeckova, L., Magni, G., and Coleman, M.P. 2010. $Wld^S$ can delay Wallerian degeneration in mice when interaction with valosin-containing protein is weakened. Neuroscience. *166*(1): 201-11.

Bittner, G.D. 1991. Long-term survival of anucleate axons and its implications for nerve regeneration. Trends Neurosci. *14*:188–193.

Brown, M.R., Sullivan, P.G., and Geddes, J.W. 2006. Synaptic mitochondria are more susceptible to $Ca^{2+}$ overload than nonsynaptic mitochondria. J Biol Chem. *281*(17): 11658-68.

Cai, Q. and Sheng, Z.H. 2009. Mitochondrial transport and docking in axons. Exp Neurol. *218*(2): 257-67.

Carafoli, E. 2010. The fateful encounter of mitochondria with calcium: how did it happen? Biochim Biophys Acta. *1797*(6-7): 595-606.

Celsi, F., Pizzo, P., Brini, M., Leo, S., Fotino, C., Pinton, P., and Rizzuto, R. 2009. Mitochondria, calcium and cell death: a deadly triad in neurodegeneration. Biochim Biophys Acta. *1787*(5): 335-44.

Chen, H., and Chan, D.C. 2009. Mitochondrial dynamics—fusion, fission, movement, and mitophagy—in neurodegenerative diseases. Hum Mol Genet *18*(R2): R169-76.

Coleman, M. 2005. Axon degeneration mechanisms: commonality amid diversity. Nat. Rev. Neurosci. *6*:889–898.

Coleman , M.P. , and V.H. Perry. 2002 . Axon pathology in neurological disease: a neglected therapeutic target Trends Neurosci. *25*:532–537.

Conforti, L., A. Tarlton, T.G. Mack, W. Mi, E.A. Buckmaster, D. Wagner, V.H. Perry, and M.P. Coleman. 2000. A Ufd2/D4Cole1e chimeric protein and overexpression of Rbp7 in the slow Wallerian degeneration (WldS) mouse. Proc. Natl. Acad. Sci. USA. *97*:11377–11382.

Conforti, L., G. Fang, B. Beirowski, M.S. Wang, L. Sorci, S. Asress, R. Adalbert, A. Silva, K. Bridge, X.P. Huang, et al. 2007. NAD(+) and axon degeneration revisited: Nmnat1 cannot substitute for Wld(S) to delay Wallerian degeneration. Cell Death Differ. *14*:116–127.

Conforti, L., Wilbrey, A., Moreale, G., Janeckova, L., Beirowski, B., Adalbert, R., Mazzola, F., DiStefano, M., Hartley, R., Babetto, E., Smith, T., Gilley, J., Billington, R.A., Genazzani, A.A., Ribchester, R.R., Magni, G., and Coleman, M.P. 2009. $Wld^S$ protein requires Nmnat activity and a short N-terminal sequence to protect axons in mice. J Cell Biol. *184*(4): 491-500.

Couto, A., Alenius, M., and Dickson, B.J. (2005). Molecular, anatomical, and functional organization of the *Drosophila* olfactory system. Current Biology *15*, 1535-1547.

Dai, R.M., and C.C. Li. 2001. Valosin-containing protein is a multi-ubiquitin chain-targeting factor required in ubiquitin-proteasome degradation. Nat. Cell Biol. *3*:740–744.

El Idrissi, A. 2008. Taurine increases mitochondrial buffering of calcium: role in neuroprotection. Amino Acids. *34*(2): 321-8.

Ferri , A. , J.R. Sanes , M.P. Coleman , J.M. Cunningham , and A.C. Kato . 2003 . Inhibiting axon degeneration and synapse loss attenuates apoptosis and disease progression in a mouse model of motoneuron disease. Curr. Biol. *13*:669–673.

Fischer, L. R., Culver, D.G., Davis, A.A., Tennant, P., Wang, M., Coleman, M., Asress, S., Adalbert, R., Alexander, G.M., and Glass, J.D. (2005). The Wlds gene modestly prolongs survival in the SOD1G93A fALS mouse. Neurobiology of Disease. *19*: 293-300.

George, E.B., Glass, J.D., and Griffin, J.W. 1995. Axotomy-induced axonal degeneration is mediated by calcium influx through ion-specific channels. J Neurosci. *15*(10): 6445-52.

Gilley, J., and Coleman, M.P. 2010. Endogenous Nmnat2 is an essential survival factor for maintenance of healthy axons. PLoS Biol. *8*(1): e1000300.

Gillingwater, T. H., Wishart, T.M., Chen, P.E., Haley, J.E., Robertson, K., MacDonald, S.H.F., Middleton, S., Wawrowski, K., Shipston, M.J., Melmed, S., Wyllie, D.J.A., Skegel, P.A., Coleman, M.P., and Ribchester, R.R. (2006). The neuroprotective Wlds gene regulates expression of PTTG1 and erythroid differentiation regulator 1-like gene in mice and human cells. Human Molecular Genetics. *15*: 625-635.

Glass, J.D., T.M. Brushart, E.B. George, and J.W. Griffin. 1993. Prolonged

survival of transected nerve fibres in C57BL/Ola mice is an intrinsic characteristic of the axon. J. Neurocytol. *22*:311–321.

Glater, E.E., Megeath, L.J., Stowers, R.S., and Schwarz, T.L. 2006. Axonal transport of mitochondria requires milton to recruit kinesin heavy chain and is light chain independent. J Cell Biol. *173*(4): 545-57.

Gunter, T.E., Buntinas, L., Sparagna, G.C., and Gunter, K.K. 1998. The $Ca^{2+}$ transport mechanisms of mitochondria and $Ca^{2+}$ uptake from physiological type $Ca^{2+}$ transients. Biochim Biophys Acta. *1366*(1-2): 5-15.

Guo, X., Macleod, G.T., Wellington, A., Hu, F., Panchumarthi, S., Schoenfield, M., Charlton, M.P., Atwood, H.L., and Zinsmaier, K.E. 2005. The GTPase dMiro is required for axonal transport of mitochondria to Drosophila synapses. Neuron. *47*(3): 379-93.

Halawani, D., and M. Latterich. 2006. p97: the cell's molecular purgatory? Mol. Cell. *22*:713–717.

Hatakeyama, S., and K.I. Nakayama. 2003. Ubiquitylation as a quality control system for intracellular proteins. J. Biochem. *134*:1–8.

Hatakeyama, S., M. Yada, M. Matsumoto, N. Ishida, and K.I. Nakayama. 2001. U box proteins as a new family of ubiquitin-protein ligases. J. Biol. Chem. *276*:33111–33120.

Higashiyama, H., Hirose, F., Yamaguchi, M., Inoue, Y.H., Fujikake, N., Matsukage, A., and Kakizuka, A. (2002). Identification of ter94, Drosophila VCP, as a modulator of polyglutamine-induced neurodegeneration. Cell

Death and Differentiation. *9*: 264-273.

Hollenbeck, P.J., and Saxton, W.M. 2005. The axonal transport of mitochondria. J Cell Sci. *118*(Pt 23): 5411-9.

Hoopfer, E.D., T. McLaughlin, R.J. Watts, O. Schuldiner, D.D. O'Leary, and L. Luo. 2006. Wlds protection distinguishes axon degeneration following injury from naturally occurring developmental pruning. Neuron. *50*:883–895.

Hoppe, T. (2005). Multiubiquitylation by E4 enzymes: 'one size' doesn't fit all. Trends in Biochemical Sciences. *30*:183-187.

Jiang, D., Zhao, L., and Clapham, D.E. 2009. Genome-wide RNAi screen identifies Letm1 as a mitochondrial $Ca^{2+}/H^{+}$ antiporter. Science. *326*(5949): 144-7.

Kaneko-Oshikawa, C., Nakagawa, T., Yamada, M., Yoshikawa, H., Matsumoto, M., Yada, M., Hatakeyama, S., Nakayama, K., and Nakayama, K.I. 2005. Mammalian E4 is required for cardiac development and maintenance of the nervous system. Molecular and Cellular Biology. *25*: 10953-10964.

Kang, J.S., Tian, J.H., Pan, P.Y., Zald, P., Li, C., Deng, C., and Sheng, Z.H. 2008. Docking of axonal mitochondria by syntaphilin controls their mobility and affects short-term facilitation. Cell. *132*(1): 137-48.

Kim, Y., Zhou, P., Qian, L., Chuang, J.Z., Lee, J., Li, C., Iadecola, C., Nathan, C., and Ding, A. 2007. MyD88-5 links mitochondria, microtubules, and JNK3 in neurons and regulates neuronal survival. J Exp Med. *204*(9): 2063-74.

Kirichok, Y., Krapivinsky, G., and Clapham, D.E. 2004. The mitochondrial calcium uniporter is a highly selective ion channel. Nature. *427*(6972): 360-4.

Knoferle, J., Koch, J.C., Ostendorf, T., Michel, U., Planchamp, V., Vutova, P., Tonges, L., Stadelmann, C., Bruck, W., Bahr, M., and Lingor, P. 2010. Mechanisms of acute axonal degeneration in the optic nerve in vivo. Proc Natl Acad Sci. *107*(13): 6064-9.

Laser, H., L. Conforti, G. Morreale, T.G. Mack, M. Heyer, J.E. Haley, T.M. Wishart, B. Beirowski, S.A. Walker, G. Haase, et al. 2006. The slow Wallerian degeneration protein, WldS, binds directly to VCP/p97 and partially redistributes it within the nucleus. Mol. Biol. Cell. *17*:1075–1084.

Lee, T., and L. Luo. 2001. Mosaic analysis with a repressible cell marker (MARCM) for Drosophila neural development. Trends Neurosci. *24*:251–254.

Lunn , E.R. , V.H. Perry, M.C. Brown , H. Rosen , and S. Gordon . 1989. Absence of Wallerian degeneration does not hinder regeneration in peripheral nerve. Eur. J. Neurosci. *1*:27–33.

Luo , L. , and D.D. O ' Leary. 2005 . Axon retraction and degeneration in development and disease. Annu. Rev. Neurosci. *28*:127–156.

MacAskill, A.F., Rinholm, J.E., Twelvetrees, A.E., Arancibia-Carcamo, I.L., Muir,

J., Fransson, A., Apenstrom, P., Attwell, D., and Kittler, J.T. 2009. Miro1 is a calcium sensor for glutamate receptor-dependent localization of mitochondria at synapses. Neuron. *61*(4): 541-55.

MacDonald, J.M., M.G. Beach, E. Porpiglia, A.E. Sheehan, R.J. Watts, and M.R. Freeman. 2006. The Drosophila cell corpse engulfment receptor Draper mediates glial clearance of severed axons. Neuron. *50*:869–881.

Mack, T.G., M. Reiner, B. Beirowski, W. Mi, M. Emanuelli, D. Wagner, D. Thomson, T. Gillingwater, F. Court, L. Conforti, et al. 2001. Wallerian degeneration of injured axons and synapses is delayed by a Ube4b/Nmnat chimeric gene. Nat. Neurosci. *4*:1199–1206.

Mahoney, J.A., J.A. Odin, S.M. White, D. Shaffer, A. Koff, L. Casciola-Rosen, and A. Rosen. 2002. The human homologue of the yeast polyubiquitination factor Ufd2p is cleaved by caspase 6 and granzyme B during apoptosis. Biochem. J. *361*:587–595.

Matsumoto, M., Yada, M., Hatakeyama, S., Ishimoto, H., Tanimura, T., Tsuji, S., Kakizuka, A., Kitagawa, M., and Nakayama, K.I. (2004). Molecular clearance of ataxin-3 is regulated by a mammalian E4. The EMBO Journal. *23*: 659-669.

Mi, W., Beirowski, B., Gillingwater, T.H., Adalbert, R., Wagner, D., Grumme, D., Osaka, H., Conforti, L., Arnhold, S., Addicks, K., Wada, K., Ribchester, R.R., and Coleman, M.P. (2005). The slow Wallerian degeneration gene, Wlds, inhibits axonal spheroid pathology in gracile axonal dystrophy mice.

Brain. *128*: 405-416.

Misko, A., Jiang, S., Wegorzewska, I., Milbrandt, J., and Baloh, R.H. 2010. Mitofusin 2 is necessary for transport of axonal mitochondria and interacts with the Miro/Milton complex. J Neurosci. *30*(12): 4232-40.

Newman, B.L., J.R. Lundblad, Y. Chen, and S.M. Smolik. 2002. A Drosophila homologue of Sir2 modifies position-effect variegation but does not affect life span. Genetics. 16I2:1675–1685.

Perlson, E., Maday, S., Meng-meng, F., Moughamian, A., and Holzbaur, E. 2010. Retrograde axonal transport: pathways to cell death? Trends in Neuroscience. *33*(7): 335-44.

Perocchi, F., Gohil, V.M., Girgis, H.S., Bao, X.R., McCombs, J.E., Palmer, A.E., and Mootha, V.K. 2010. MICU1 encondes a mitochondrial EF hand protein required for $Ca^{2+}$ uptake. Nature. *467*(7313): 291-6.

Pilling, A.D., Horiuchi, D., Lively, C.M., and Saxton, W.M. 2006. Kinesin-1 and Dynein are the primary motors for fast axonal transport of mitochondria in Drosophila motor axons. Mol Biol Cell. *17*(4): 2057-68.

Pinter, M. , G. Jekely, R.J. Szepesi , A. Farkas ,U. Theopold , H.E. Meyer, D. Lindholm , D.R. Nassel , D. Hultmark , and P. Friedrich . 1998 . TER94, a Drosophila homolog of the membrane fusion protein CDC48/p97, is accumulated in nonproliferating cells: in the reproductive organs and in the brain of the imago. Insect Biochem. Mol. Biol. *28*:91–98.

Press, C., and J. Milbrandt. 2008. Nmnat delays axonal degeneration caused by

mitochondrial and oxidative stress. J. Neurosci. *28*:4861–4871.

Raff, M.C., A.V. Whitmore, and J.T. Finn. 2002. Axonal self-destruction and neurodegeneration. Science. *296*:868–871.

Rongvaux, A., F. Andris, R. Van Gool, and O. Leo. 2003. Reconstructing eukaryotic NAD metabolism. Bioessays. *25*:683–690.

Ruden, D.M., V. Sollars, X. Wang, D. Mori, M. Alterman, and X. Lu. 2000. Membrane fusion proteins are required for oskar mRNA localization in the Drosophila egg chamber. Dev. Biol. *218*:314–325.

Russo, G.J., Louie, K., Wellington, A., Macleod, G.T., Hu, F., Panchumarthi, S., and Zinsmaier, K.E. 2009. Drosophila Miro is required for both anterograde and retrograde axonal mitochondrial transport. J Neurosci. *29*(17): 5443-55.

Sajadi, A., Schneider, B.L., and Aebischer, P. (2004). Wlds-mediated protection of dopaminergic fibers in an animal model of Parkinson disease. Current Biology. *14*: 326-330.

Saotome, M., Saflulina, D., Szabadkai, G., Das, S., Fransson, A., Apenstrom, P., Rizzuto, R., and Hajnoczky, G. 2008. Bidirectional $Ca^{2+}$-dependent control of mitochondrial dynamics by the Miro GTPase. Proc Natl Acad Sci. *105*(52): 20728-33.

Saridakis, V., D. Christendat, M.S. Kimber, A. Dharamsi, A.M. Edwards, and E.F. Pai. 2001. Insights into ligand binding and catalysis of a central step in NAD+ synthesis: structures of Methanobacterium thermoautotrophicum

NMN adenylyltransferase complexes. J. Biol. Chem. *276*:7225–7232.

Sasaki, Y., T. Araki, and J. Milbrandt. 2006. Stimulation of nicotinamide adenine dinucleotide biosynthetic pathways delays axonal degeneration after axotomy. J. Neurosci. *26*:8484–8491.

Sasaki, Y., Vohra, B.P., Baloh, R.H., and Milbrandt, J. 2009. Transgenic mice expressing the Nmnat1 protein manifest robust delay in axonal degeneration in vivo. J Neurosci. *29*(20): 6526-34.

Sasaki, Y., Vohra, B.P., Lund, F.E., and Milbrandt, J. 2009. Nicotinamide mononucleotide adenylytransferase-mediated axonal protection requires enzymatic activity but not increased levels of neuronal nicotinamide adenine dinucleotide. J Neurosci. *29*(17): 5525-35.

Stengl, M. 1995. Pigment-dispersing hormone-immunoreactive fibers persist in crickets which remain rhythmic after bilateral transection of the optic stalks. J. Comp. Physiol. [A]. *176*:217–228.

Suda, Y., H. Tachikawa, A. Yokota, H. Nakanishi, N. Yamashita, Y. Miura, and N. Takahashi. 2003. Saccharomyces cerevisiae QNS1 codes for NAD(+) synthetase that is functionally conserved in mammals. Yeast. *20*:995–1005.

Tanaka, K., Iijima, T., Mishima, T., Suga, K., Akagawa, K., and Iwao, Y. 2009. $Ca^{2+}$ buffering capacity of mitochondria after oxygen-glucose deprivation in hippocampal neurons. Neurochem Res. *34*(2): 221-6.

Vosshall, L. B., Wong, A.M., and Axel, R. (2000). An olfactory sensory map in the

fly brain. Cell *102*, 147-159.

Waller, A. 1850. Experiments on the section of the glossopharyngeal and hypoglossal nerves of the frog, and observation of the alterations produced thereby in the structure of their primitive fibres. Philos. Trans. R. Soc. Lond. (1776–1886). *140*:423–429.

Wang, J., Q. Zhai, Y. Chen, E. Lin, W. Gu, M.W. McBurney, and Z. He. 2005. A local mechanism mediates NAD-dependent protection of axon degeneration. J. Cell Biol. *170*:349–355.

Wang, M. S., Davis, A.A., Culver, D.G, and Glass, J.D. (2002). Wlds mice are resistant to paclitaxel (Taxol) neuropathy. Annals of Neurology *52*, 442-447.

Wang, M., Y. Wu, D.G. Culver, and J.D. Glass. 2001. The gene for slow Wallerian degeneration (Wld(s)) is also protective against vincristine neuropathy. Neurobiol. Dis. *8*:155–161.

Wang, X., and Schwarz, T. 2009. The mechanism of $Ca^{2+}$-dependent regulation of kinesin-mediated mitochondrial motility. Cell. *136*(1): 163-74.

Watts, R.J., E.D. Hoopfer, and L. Luo. 2003. Axon pruning during Drosophila metamorphosis: evidence for local degeneration and requirement of the ubiquitin-proteasome system. Neuron. *38*:871–885.

Yahata, N., Yuasa, S., and Araki, T. 2009. Nicotinamide mononucleotide adenylytransferase expression in mitochondrial matrix delays Wallerian degeneration. J Neurosci. *29*(19): 6276-84.

Yan, T., Feng, Y., Zheng, J., Ge, X., Zhang, Y., Wu, D., Zhao, J., and Zhai, Q. 2010. Nmnat2 delays axon degeneration in superior cervical ganglia dependent on its NAD synthesis activity. Neurochem Int. *56*(1): 101-6.

Zhai, Q., J. Wang, A. Kim, Q. Liu, R. Watts, E. Hoopfer, T. Mitchison, L. Luo, and Z. He. 2003. Involvement of the ubiquitin-proteasome system in the early stages of Wallerian degeneration. Neuron. *39*:217–225.

Zhai, R.G., Y. Cao, P.R. Hiesinger, Y. Zhou, S.Q. Mehta, K.L. Schulze, P. Verstreken, and H.J. Bellen. 2006. Drosophila NMNAT maintains neural integrity independent of its NAD synthesis activity. PLoS Biol. *4*:e416.

Zhai, R.G., F. Zhang, P.R. Hiesinger, Y. Cao, C.M. Haueter, and H.J. Bellen. 2008. NAD synthase NMNAT acts as a chaperone to protect against neuro- degeneration. Nature. *452*:887–891.

Ziv, N.E., and Spira, M.E. 1995. Axotomy induces a transient and localized elevation of the free intracellular calcium concentration to the millimolar range. J Neurophysiol. *74*(6): 2625-37.